



Bio-acceptable 0D and 1D ZnO nanostructures for cancer diagnostics and treatment

Brandon Ortiz-Casas ^{1,2,†}, Andrés Galdámez-Martínez ^{3,†}, Jorge Gutiérrez-Flores ^{3,†},
Andrés Baca Ibañez ^{1,†}, Pritam Kumar Panda ^{4,†}, Guillermo Santana ³,
Horacio Astudillo de la Vega ¹, Mrutyunjay Suar ^{5,6}, Citlaly Gutiérrez Rodelo ^{1,*},
Ajeet Kaushik ⁷, Yogendra Kumar Mishra ^{8,*}, Ateet Dutt ^{3,*}

¹ Healthcare Business and Computer Technology and Nanopharmacia Diagnostica, Tlaxcala No. 146/705, Col. Roma Sur, Cuauhtémoc, Cuidad de México C.P. 06760, Mexico

² Department of Engineering Science, University of Oxford, Parks Road, Oxford OX1 3PJ, United Kingdom

³ Instituto de Investigaciones en Materiales, Universidad Nacional Autónoma de México, Coyoacan, México City C.P. 04510, Mexico

⁴ Condensed Matter Theory Group, Materials Theory Division, Department of Physics and Astronomy, Uppsala University, Box 516, 75120 Uppsala, Sweden

⁵ School of Biotechnology, Kalinga Institute of Industrial Technology (KIIT), Deemed to be University, Bhubaneswar, Odisha, India

⁶ KIIT-Technology Business Incubator (KIIT-TBI), Kalinga Institute of Industrial Technology (KIIT), Deemed to be University, Bhubaneswar, Odisha, India

⁷ NanoBioTech Laboratory, Health System Engineering, Department of Environmental Engineering, Florida Polytechnic University, 4700 Research Way, Lakeland, Florida 33805, United States

⁸ Smart Materials, NanoSYD, Mads Clausen Institute, University of Southern Denmark, Alsion 2, 6400, Sønderborg, Denmark

As bioapplications of 0D and 1D zinc oxide (ZnO) seem a recent development, they have brought many exciting proposals showing exquisite signs as sensors and assay platforms offering biomolecular selectivity and sensitivity for cancer diagnosis and treatment. Cancer researchers are looking for diagnostic and molecular instruments to identify the cancer-causing agents and subtle molecular shifts. The inclusion of high-performance ZnO materials due to their intrinsic properties such as viability, bio-acceptability, high isoelectric point, tunable morphology, etc., is promising for targeted detection and treatment processes. More specifically, ZnO nanowires (NWs) have offered the opportunity to yield new types of approaches against targeted cancer in contrast to their 0D counterparts. The ability of ZnO NW sensors to identify the molecular features (i.e., biomarker) of cancer and their integration portability has the potential to revolutionize cancer diagnosis and patient health monitoring timely and efficiently. Despite being robust, tunable properties based on surface chemistry and eco-friendly, scalable opportunities are yet to be explored. This review considers captivating research advances to identify and understand fundamental properties and examine various biosensing approaches and nanomedicine (via performing targeted drug delivery or therapeutic) aspects utilizing them while paying attention to different size regimes of ZnO NWs. The high-performance role of 0D and 1D ZnO as biosensors, capture devices, cell imaging complexes, or treatment is addressed on the bases of the controlled functions such as enhanced adsorption, reactivity, surface chemistry, cytotoxicity, and biocompatibility in various biological systems and models. With a

* Corresponding authors.

E-mail addresses: Gutiérrez Rodelo, C. (citlalygutierrezrodelo@gmail.com), Kumar Mishra, Y. (mishra@mci.sdu.dk), Dutt, A. (adutt@iim.unam.mx).

† Authors contributed equally.

comparative viewpoint, 0D and 1D ZnO nanostructures are going to emerge as breakthrough candidates for diagnostics and treatment of cancer effectively and efficiently.

Keywords: Zinc oxide; 0D and 1D nanostructures; Cytotoxicity and biocompatibility; Cancer nanotechnology; Cancer management

Trends in cancer nanotechnology

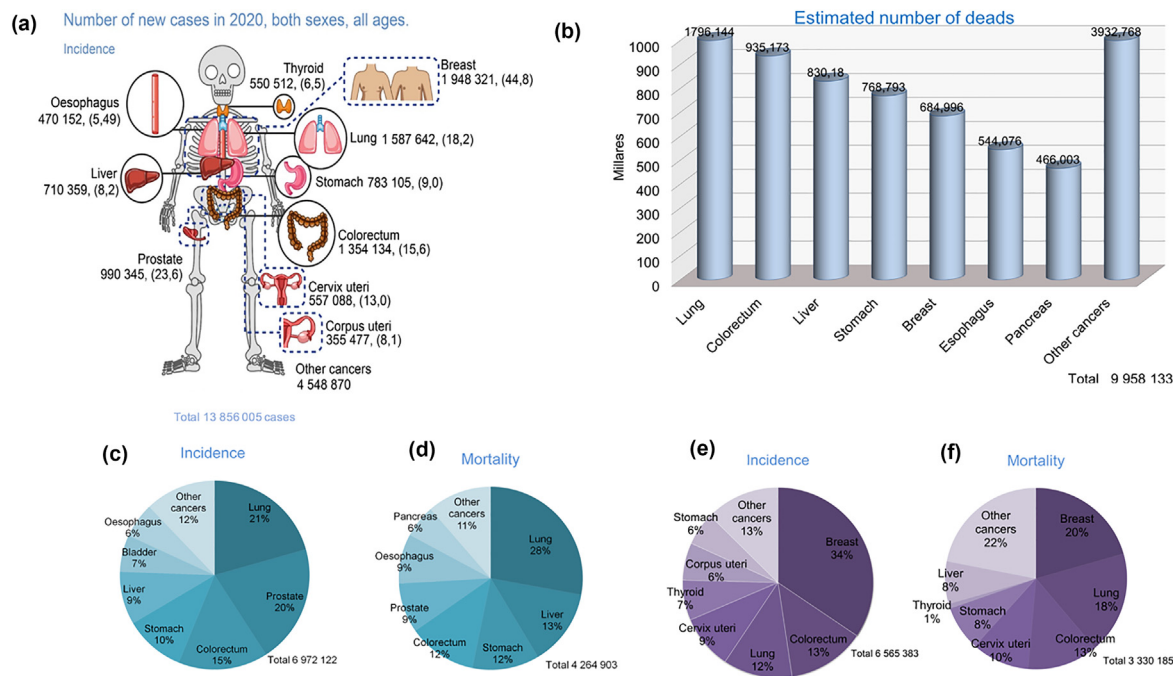
Cancer is classified as a disease emerged and characterized due to uncontrolled growth and proliferation of abnormal cells [1]; other terms are malignant tumors and neoplasms [2]. According to the international standard for the classification of oncology diseases, cancers are classified based on tissue types in the following six categories carcinoma, sarcoma, myeloma, leukemia, lymphoma, or mixed [3]. Presently, cancer is the second leading reason for global deaths and represents one of the critical public health concerns worldwide [4]. An update of the worldwide cancer burden (incidence and deaths) based on the International Agency for Research on Cancer (IARC) and GLOBOCAN 2020 reports is summarized in Fig. 1 (a and b) [4,5]. The different kinds of cancer and their mortality rates by gender are illustrated in Fig. 1 (c-f) [6]. As an estimate, until 2020, around 19.3 million new cancer cases (18.1 million excluding nonmelanoma skin cancer) and 10.0 million cancer deaths (9.9 million excluding nonmelanoma skin cancer) have been reported [7].

Although the causes of cancers are not entirely understood, but numerous factors are known to increase the existence of the disease. It has been described that roughly one-third of cancer deaths are due to infectious agents, behavioral aspects, and dietary risks; for example, tobacco use is responsible for approximately 22% of cancer deaths [2]. Cancer-causing infections, such as hepatitis and human papillomavirus (HPV), are responsible for up to 25% of cases in low- and middle-income countries. Other factors (not less important) are inherited genetic mutations [1]. In this matter, the diagnosis of cancer predisposition syndromes can usually be confirmed with molecular genetic testing of patients based on clinical, pathologic, or family history indicators [8]. Several procedures and drugs are in practice to treat and manage cancer depending on the type, cancer stage, and treatment goals. Therefore, oncologists perform surgery, radiation therapy, lasers, and cryoablation for local therapy on specific tumors or relieve symptoms in a particular area (skin cancer, breast cancer, and prostate cancer). Another investigated procedure is systemic therapy, including drug administration, hormone therapy, chemotherapy, targeted therapy, and stem cell or bone marrow transplant (for example, lung cancer, leukemia, and metastatic breast cancer). An emerging approach is precision medicine; the concept refers to a method based on individual variability in genes, environment, and lifestyle for each person and is supported by the components of the tumor microenvironment (TME) at the cellular and molecular levels (endothelial cells, angiogenic vessels, and other cellular environments) [9]. At present, the targeted therapy is compelling and a new method for cancer treatment. Under this category, numerous novel drugs have been approved as of now, including anti-mutation targeting drugs like the EGFR T790M targeting (osimertinib), drugs with multiple targets like the EGFR/HER2 (neratini), and drug combinations like (encorafenib/binimetinib and

dabrafenib/trametinib) [10]. The contemporary modalities for cancer treatment include RNA interference (RNAi) and antisense techniques, hereditary control of apoptotic and tumor-attacking pathways treatment, anti-angiogenic therapy, and oncolytic viral therapy [11]. Some of the complications in cancer cure optimization are as follows: (1) response of the patient to immunotherapy, (2) present tomography approaches cannot distinguish benign lesions from malignant lesions, (3) the uncovering of cancer in the initial phase has been hindered by the intrinsic limits of conventional cancer diagnostic methods, and (4) late-stage presentation and out-of-the-way analysis/treatment of cancer are ubiquitous.

To investigate and optimize an efficient diagnostics and treatment of higher efficacy, sincere efforts are made by researchers since 1980 to explore nanoscale materials. An early-stage detection system is critical for the efficient treatment and monitoring of cancer. Although unfortunately, there have been several shortcomings with traditional cancer detection approaches. Nanotechnology has emerged as a very sensitive, accurate, and standardized technique for identifying extracellular cancer biomarkers and cancer cells [12]. Over the past decade, there have been tremendous developments in cancer detection technologies focused on nanotechnology and miniaturized electronics i.e., the internet of medical things (IoMT). Several nanoparticles (NPs)-based assays demonstrated substantial progress in selectivity and sensitivity compared with the available cancer diagnostics in the laboratory. This may lead to the creation of more successful therapies for many cancers since a limited number of nanotechnology-based cancer detection systems have progressed to the level of clinical trials.

Nanotechnology offers great potential to advance cancer detection and treatment, eventually contributing to an increased cancer patient survival rate. To date, nanotechnology proposes a novel and highly valuable offering as a vital role in cancer theragnostic, integrating therapy and diagnosis [13]. Numerous NPs are currently part of ongoing research orients towards investigating cancer disease detection and its effective treatment, for instance: liposomes, chitosan, micelles, nanoshells, 0D, 1D, and 2D nanomaterials, paramagnetic nanoparticles (PMNPs), quantum dots (QDs), magnetic nanoparticles (MNPs), etc. [14–18]. Among them, metal oxides such as titanium oxide (TiO_2), copper oxide (CuO), iron oxide (Fe_3O_4), and zinc oxide (ZnO) have received a substantial amount of attention in nanoscience due to their relative ease of nano-structuring and the wide variety of possible optical, electrical, magnetic, and morphological properties [19]. For cancer detection, NPs are being employed to capture cancer biomarkers, such as cancer-associated proteins, circulating tumor DNA and tumor cells, and exosomes, because nanomaterials surfaces can be compactly coated with antibodies, small molecules, peptides, aptamers, and other moieties. Due to the large surface area, NPs are also pledging candidates for a

**FIGURE 1**

Estimated new cancer cases and mortality worldwide in 2020. (a) New patients, both sexes, all ages. (b) Mortality of both sexes, all ages. (c) new patients, male, of all ages. (d) Mortality, male, all ages. (e) new cases, female, all ages. (f) Mortality female, all ages. Source: GLOBOCAN: International Agency for Research on Cancer 2020.

delivery system that can efficiently transport target antigens into dendritic cells (DCs) and serve as imaging contrast agents [20]. Other emerging systems are biomimetic NPs involving biological and synthetic materials; for instance, the cancer cell membrane coating nanoparticles. They comprise of a NP core in a cancer cell plasma membrane coating that can carry tumor-specific receptors and antigens for cancer targeting with therapeutic or imaging applications [21]. One more advancement on the nanometric scale is nano surgery because of its immense prominence in removing residual micrometastases/single cancer cells that remain in organs after macro surgery and represent a considerable threat for later lethal cancer recurrence [22].

Therefore, to combat targeted cancer, collaboration among experts is currently required for effective disease control, a crucial action to scale up inhibition, initial recognition diagnosis, treatment, and care services are also essential. Distant metastasis of the tumor is regarded as the main reason for death in cancer patients, and for that reason, an initial detection to plan subsequent treatment is one of the principal goals [23,24]. About an early detection system in cancer prognosis, our review specifically shifted gears from traditional methods to nanotechnology-based techniques describing why the implementation of nanotechnologies in cancers has an added and recommended advantage. This study projects an overview of recent progress toward the *in-vivo* application of different nanomaterials in cancer detection via a selective sensing approach. Additionally, careful analysis of 1D ZnO NWs and a comparison of their properties with respect to 0D NPs is discussed. Besides, molecular aspects, intrinsic properties, biocompatibility, toxicity mechanism, and environmental factors of both 0D and 1D ZnO nanomaterials for biosensing and treatment are also reviewed. These

emerging innovations or methods may not be immediately applicable to clinical oncology; nonetheless, they are of great scientific interest and may be helpful in the treatment of other diseases.

Tailoring the interface of cancer-therapies and nanostructures

Nano-systems based various devices and formulations have already been authorized by The United States Food and Drug Administration (FDA), for example, liposome-based systems, the Cathepsin B-sensitive nanoprobe for metastasis detection, and the folate-functionalized superparamagnetic iron oxide NPs, for liver cancer treatment [15,25]. In this direction, a drug-delivery system (i.e., nanomedicine) developed against targeted cancer rely on complemented passive and active targeting [26–28]. Meanwhile, it has been shown that NPs and their functionalized systems can be taken up by tumor site due to the advantage of size, which enhanced permeability and retention (EPR) effect. This is one of the laying foundations currently under investigation in anticancer therapy optimization and development [29]. Once the NPs-ligand enters the tumor microenvironment via the EPR effect, the ligands cell-specific binding will further enhance retention on the cell membrane or stimulate cell internalization and intracellular retention. This effect is related to cancer tissue anatomy differences compared to normal tissue (angiogenesis, endothelial cells, and extravasation). Applying NPs as anticancer agents has shown improvements compared to conventional techniques because of their ability to target specific locations in the body, reducing the overall amount of drug use, diminished side effects, and decreasing drug concentrations at nontarget sites.

Magnetic and thermal therapeutic features of NPs along with phototherapeutic could help to fight cancer via different therapies such as photodynamic therapy (PDT), photothermal therapy (PTT), and magnetic hyperthermia (MH) [30,31]. The PDT uses photosensitizing agents to produce toxic reactive oxygen species (ROS), leading to cancer cell death [30,32]. Whereas the PTT uses light irradiation to heat cancer cells, leading to thermal ablation with subsequent death of the malignant cells (Fig. 2 [33]). Phototherapeutic treatments are still an experimental process but a promising cancer treatment option. It is mediated mainly by metallic and magnetic NPs like Au, Ag, Cu, CNTs, and graphene [34,35], and these materials can be stimulated by either light (near-infrared, NIR) or magnetism with minimal tissue absorption. The advantages of NIR stimulation comprise excellent tissue penetration, minimal treatment cycles, lowers the procedure of macroscopic implants. Their size is ideal for crossing biological barriers, and the procedure generally produces beneficial heat as close as possible to the injury site [36]. Evidence indicates that tissue heating with magnetic NPs may further enhance immune function to benefit cancer treatment [37]. At present, the most common design of nanostructures for photothermia (PT) are nanorods (NRs), NWs, nanoshells, and nanostars [38]. Magnetic iron oxide NPs have demonstrated potential in preclinical strategies for PTT and PDT therapies, as well as HT. The only approved thermal nanomedicine is with magnetic iron oxide NPs [39]. The FDA-approved applications of iron oxide NPs include cancer diagnosis, cancer HT, and iron deficiency anemia (parental iron oxide NPs) [40]. The clinical success of injectable iron feats the interaction between NPs and the innate immune system [39]. These NPs have already been approved for human use as MRI contrast agents and have already reached the clinical practice to treat solid tumors [39,41]. One of the most studied treatments in bone cancer complications involves the blend of surgery with HT, PTT, and the utilization of NPs [42]. The use of magnetic NPs is beneficial because of the decrease in cytostatic activity and, subsequently, decreased systemic toxicity [43]. Likewise, for central nervous system (CNS) disorders, NPs containing metals (Ag, Cu, Al) have shown less neurotoxicity, better drug targeting, and rapid renal clearance [15,44].

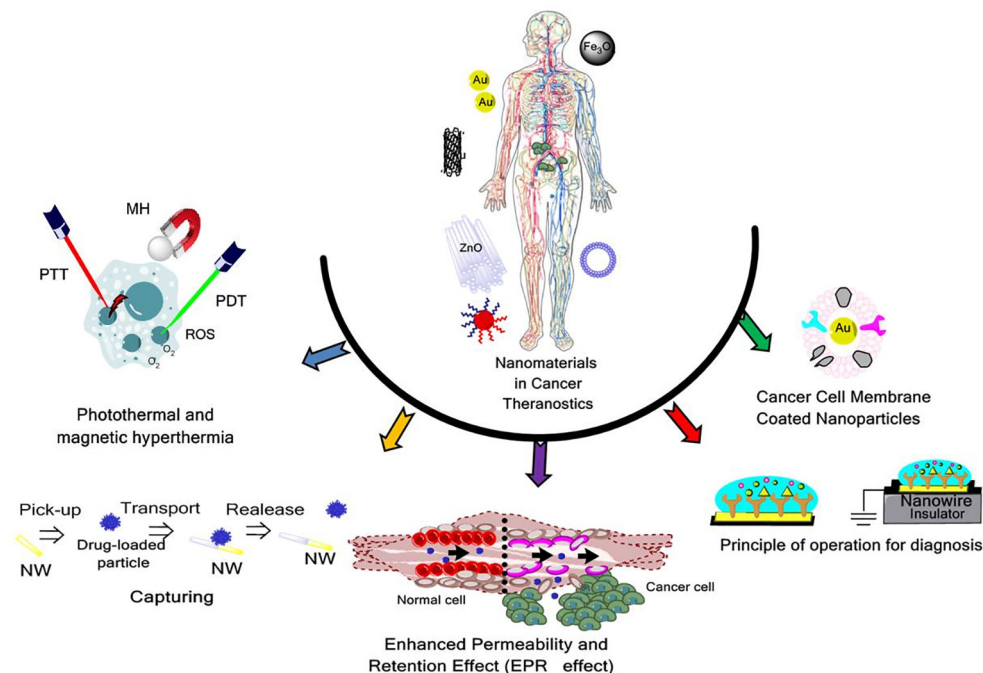
On the other hand, NWs-based sensors impact cancer diagnosis, and precision medicine offering high sensitivity [45]. Biosensors based on NWs can be electrochemical, piezoelectric, optical, and field-effect transistors (FET) biosensors [46]. The semiconductors NWs composed of Si, SnO₂, and ZnO are very useful to develop FET biosensors of desired properties [47]. The detection foundation of an NW sensor could involve an electrical or a memristor signal and the interaction of sensed biological molecules such as enzymes, antibodies, DNA, RNA, proteins, or drugs [48]. The sensitivity, limit of detection (LoD), and signal-to-noise ratio are key performance metrics of these devices. The current biomedical applications for 1D magnetic NWs are magnetic separation, magnetic HT, and magnetic resonance imaging (MRI). The main benefits related to NWs are the electrical interaction between nanomaterials and cells, their low cytotoxicity, biocompatibility, shape anisotropy, and cellular internalization. The research proposes that ZnO NWs could penetrate the cellular membrane, influencing cytotoxicity and inducing cellular apop-

tosis of cancer cells [49]. Among all the nanomaterials mentioned above, ZnO nanostructures due to high iso-electric point (9.5 useful for high affinity with biomolecules) and surface functionalized features (useful as a viable surface, DDS, and stimuli-responsive enhanced properties) show promising application and efficacy in cancer therapy because of highly selective nature and potency towards cancer cells. The following section implicates the unique properties of ZnO nanostructured materials in various applications, including the intrinsic properties related to the cytotoxicity mechanism.

Horizons of 0D and 1D ZnO nanostructures

The ZnO nanostructures exhibit a broad spectrum of useful properties such as high isoelectric point, stability, high exciton binding energy, effective electron transport, non-toxicity, piezoelectric and pyroelectric behaviors. For this reason, ZnO nanostructures have proven to be a promising platform for addressing challenges found in energy scavenging, photocatalysis, biosensing, and theragnostic applications [50–60]. Among the semiconducting metal oxides, ZnO has significant advantages for biomedical [61,62], gas sensing [63–66], chemical [67,68], biosensing [69], photocatalyst [70,71], and other biological purposes due to its good biocompatibility, chemical stability, biodegradability, and biosafety [72] along with its excellent optical [73], electrical [74] and piezoelectric [75] and pyroelectricity [76] properties. Also, ZnO is a significant, low-cost, highly abundant, soluble, and non-toxic semiconductor. It has a wide direct band gap of 3.37 eV [77] and a considerable excitonic binding energy of 60 meV [78] that makes it a transparent and highly sensitive transductor [79]. The compound has a hexagonal wurtzite structure under pressure and temperature ambient conditions, in which each one of the O²⁻ ions are tetrahedrally coordinated to four Zn²⁺ ions and vice versa. Zn²⁺ is a divalent metal cation that works as a human metabolite, cofactor, and an indispensable trace element for adults (8.25 mg of Zn²⁺ are required for an average person per day [72]), controlling more than 300 metabolic functions [80].

The unit cell of the wurtzite structure belongs to the P63mc space group and C_{6v}⁴ class and a c/a ratio of 1.6 for the ideal lattice. However, due to the defects or strain in the system and the presence of foreign elements (intended or not doping/impurities), the experimental value of this ratio usually ranges from 1.593 to 1.604 when measured by X-ray diffraction [81]. The spatial distribution of the interpenetrated Zn²⁺ and O²⁻ tetrahedrons results from the sp³ hybridization of the bonding orbitals and generates a matrix of alternating bilayers of zinc (Zn) atoms and oxygen (O) atoms. This type of coordination is strongly related to the highly polar character of the Zn-O bond. The electronegativity difference between the Zn and O atoms causes the bond to have a character between a covalent and an ionic bond [82]. This also produces polarization along the c axis of the hexagonal structure. The alternation between positive charges Zn²⁺ and negative charges O²⁻ generates two characteristic faces of opposite polarity oriented in the c direction. The positive side (0001) of Zn ions and the negative side (000⁻1) of O ions. On the other hand, the faces with the same number of positive and negative charges have a non-polar character, the most common

**FIGURE 2**

Role of nanotechnology in cancer theranostics. Left top (blue arrow), Therapeutics Techniques: Photothermal Therapy (PTT) uses light irradiation to heat malignant cells, Magnetic Hyperthermia (MH) uses heating magnetic nanoparticles, and Photodynamic therapy (PDT) uses photosensitizing agents to produce toxic Reactive Oxygen Species (ROS). Orange arrow: Nanowire (NW) drug capturing proposed operation principle: NW picks up the drug-loaded particle, transports it to the target cancer cells, and then releases the drug. Wiley & Sons. Copyright © 2010 WILEY-VCH Verlag GmbH & Co. KGaA, Weinheim [33]. Purple arrow: Foundation for anticancer therapy, the Enhanced Permeability and Retention Effect (EPR effect) in normal and cancer cells. Red arrow, the principle of operation of a nanowire sensor (FET type nanowire sensors exhibit changes in conductance (source) upon signal transduction in response to the interaction of immobilized antibody (target) with a soluble antigen (receptor). Green arrow- Biomimetic NPs, cancer cell membrane coated NPs (CCMCNPs) for cancer theranostics.

being $(11\bar{2}0)$ and $(10\bar{1}0)$, both oriented on the a -axis [83]. This polar/nonpolar character of different crystal faces is responsible for the piezoelectric and spontaneous polarization properties. It is also a deciding factor in crystalline growth [84], defect generation, and biological functionalization. Selective polarity opens the possibility of a broad spectrum of chemical reactions in the nanostructure surface, and this originates from the need for additional positive or negative charges required in the polar faces [85].

Many works have reported the direct immobilization of diverse biomolecules on the surface of ZnO nanostructures by electrostatic interaction between the surface of the semiconductor and the biological analyte [86–88]. It has also been found that the morphology of nanostructure defines the number of adsorption sites and protein adsorption dynamics [89–91]. As mentioned before, ZnO has characteristic optoelectronic properties that make it a promising candidate for optical biomedical applications [92]. Additionally, as mentioned above, it exhibits a wide family of nanostructures such as nanoparticles NPs [93], 1D NWs [94], nanotubes (NTs) [95], nanorods (NRs) [96], thin films [97], nanorings [98], nanobelts [99], nanohelix [100], nanoflowers [101], nanocages [102] among others. These can be employed as biodegradable and biocompatible nanoplates for cancer detection and treatment applications such as magnetic resonance [103], optical [72], and microwave imaging [104], as well as optical [69] and electrochemical [84] biosensors.

The numerous physicochemical properties of ZnO nanostructured materials, along with their low toxicity, have motivated the study of their performance in biological applications such as biosensing, antimicrobial agents, DDS, bioimaging, gene therapy, tissue regeneration, and anticancer treatment [105]. The ZnO nanostructures are a less toxic and cheaper alternative than conventional QDs used for selective drug delivery. Proper surface modification of ZnO NPs allows selective endocytosis to target cells, where the drug release can be controlled by changing the pH of the system and temperature [106]. This is based on the chemical stability of the ZnO under general physiological pH conditions (7.4), while under acid conditions (<5.5), the nanostructures tend to dissolve rapidly in Zn²⁺ ions, which have also exhibited cytotoxicity towards carcinogenic/tumor cells [107]. Furthermore, in addition to the mentioned biomedical applications, a considerable effort has been made to implement nanostructured ZnO platforms as systems that increase epithelial tissue regeneration for wound healing. According to Martínez-Carmona et al., [108], Zn deficiencies complicate the wound healing process. Consequently, many researchers seek to implement nanostructured ZnO in different topical products taking advantage of the antibacterial and healing properties of the material [109–111]. Finally, multiple ZnO nanostructures have been used to prevent DNA degradation in gene therapy applications [112]. The most reported techniques to improve efficiency include encapsulation, functionalization, and entrapping of the

employed ZnO nanostructures in the target cells. One interesting phenomenon investigated by Moon et al., [113] illustrated the fabrication of chips deposited with ZnO thin films and characterized their anticancer activity by releasing Zn ions in a ZnO deposition cycle-dependent manner, independent of conductivity. ZnO chips facilitate cell death due to the ability of Zn to cause oxidative stress and downregulate protein levels of anti-apoptotic molecules such as IAPs, claspin, p-p53, and HIF-1 α in Raji cells. The IC₅₀ of ZnO for the first time was quantitatively measured as 121.5 loops. Unfortunately, ZnO NPs at a specific concentrations have shown liver, intestine, and lung chemical poisoning in healthy mice [114]. They assumed that the combination of ZnO-based patches, topical and systemic treatments for melanoma might have additive effects or synergistic effects on melanoma [115]. ZnO per se can also be used as a coating for implants to inhibit bacterial adhesion and encourage osteoblast growth [116]. The designers of potential biomedical materials need to understand the cytotoxicity of ZnO-related materials. ZnO nanostructures possess a completely new cytotoxic behavior with great potential and are exploitable for developing new efficacious therapeutic strategies. Apart from the above-discussed biomedical properties, in detection techniques, ZnO nanostructured biosensors stand out to be effective in disease monitoring which has been discussed in the next section as a multifunctional entity. ZnO nanostructures operation is based on the generation of an analytical signal (optical or electrical) product of the interaction between the analyte to be detected (e.g., infectious diseases, enzymes, antibodies, proteins, specific types of cells) and the nanostructured probe [117]. They offer several advantages over conventional analytical bulk platforms, such as high selectivity and high detection thresholds. Furthermore, the ease of obtaining ZnO nanostructures of the desired morphology and structural defects allows precise control over the immobilization of a targeted bio-active molecule and absorption processes to the surface of the transducer. As a result, ZnO nanosystems can be a high-quality bio-selective layer. In addition to its application in biological analyte sensing platforms, ZnO nanostructures have also been used as DDS for cancer treatment and other chronic diseases [107,118,119].

The synthesis and growth mechanisms of ZnO nanostructures also play a vital role in various physical, chemical, and biological applications. There are many physical and chemical growth methods for the obtention of ZnO nanostructures. For instance, the biological synthesis of NPs (also referred to in the literature as green synthesis) has proved to be an effective and cost-beneficial alternative to the more polluting chemical and physical growth approaches [120]. Even when the synthesis of NPs through plant extracts was initially implemented for the obtention of metal NPs, their application for the obtention of 0-D ZnO nanostructures has been widely spread recently [121]. The process described in multiple articles can be summarized as follows: 1) the plant extract obtention by boiling the rinsed plant parts (e.g., flowers, leaves, roots, fruits, etc.) into water or alcohol, 2) the extract is then mixed with various Zn based salts (e.g., zinc nitrate, zinc acetate [122]) and is kept at a controlled temperature and pH without adding extra chemical reagents, 3) a centrifugation process is then used to separate the obtained ZnO NPs from the rest of the solution. Furthermore, the microorganisms such

as bacteria and fungi have been used to synthesize NPs to mimic the decomposing role of these creatures in nature [123–141].

Considering 1D nanostructures, they are obtained by promoting the crystallization of solid-state structures along one direction. Several ZnO nanostructure morphologies can be achieved with the use of techniques such as sol-gel method [142], hydrothermal [143], solvothermal growth [144], thermal evaporation [145], chemical vapor deposition (CVD) [146], molecular beam epitaxy (MBE) [147], metal-organic vapor-phase epitaxy (MOVPE) [148] and template techniques. Each of these methods has a consistent set of relevant parameters that control the morphological characteristics of the synthesized 1D nanostructure [133]. A schematic of different growth techniques for 1D ZnO nanostructures has been illustrated in Fig. 3.

The ZnO acts as a brilliant emitter compound; for instance, ZnO tetrapods (ZnO-T) have been used for various biological applications due to their good biocompatibility, low toxicity, and innocuity towards healthy cells. The ZnO-T has been used in all the previously mentioned biological applications from wound healing, DNA delivery, drug transport, antibacterial/antivirus [149], anti-cancerous agents, and tactile sensors for skill implants [149]. ZnO-T has proven to be a key nanostructure within the extended family of ZnO nanostructured materials due to the precise control over their mechanical, optical, electrical, and chemical properties compared to other 3D nanostructures systems [150]. In broad terms, a ZnO-T is formed by four 1D ZnO nanostructures (NWs or NRs) interconnected by a common center so that the other ends coincide with the vertices of a tetrahedron. Therefore, the high surface and high chemical reactivity features of 1D ZnO nanostructures are inherited from ZnO-T. These 3D nanostructures spatial arrangement allows the obtention of highly porous matrices where accumulation is significantly reduced. The surface is considered even more available compared to conventional nanorod systems. However, as is the case with other ZnO nanostructures, mass production is one of the most pressing challenges for the practical application of these materials. In this matter, relatively simple strategies with a high yield of the ZnO-T production, such as the flame transport synthesis (FTS) technique, offer a suitable solution for incorporating these structures in multiple theranostics applications [149,150].

Multitarget and multifunctional properties of 0D and 1D ZnO nanostructures

ZnO NPs (0D) have been widely employed as anticancer activity agents by inducing cancer cell apoptosis in different human cancers due to their capacity to generate ROS [151] and Zn ions release [152]. However, the indistinct cytotoxicity (to even healthy body cells) in ZnO NPs from a range of 4–20 nm must be minimized by further surface engineering to improve cancer cell selectivity [153]. Also, ZnO NPs offer transformation of cancer treatment by combining the drug delivery to specific cells with the characteristic imaging visualization modalities attributed to the NPs [154]. Another successful implementation of ZnO nanostructures is presented in both the work of Punnoose et al., [153] and Wang et al., [155], where ZnO NPs and nanosheets were employed for fluorescence and dual MRI/fluorescence imaging. As mentioned earlier, many authors report

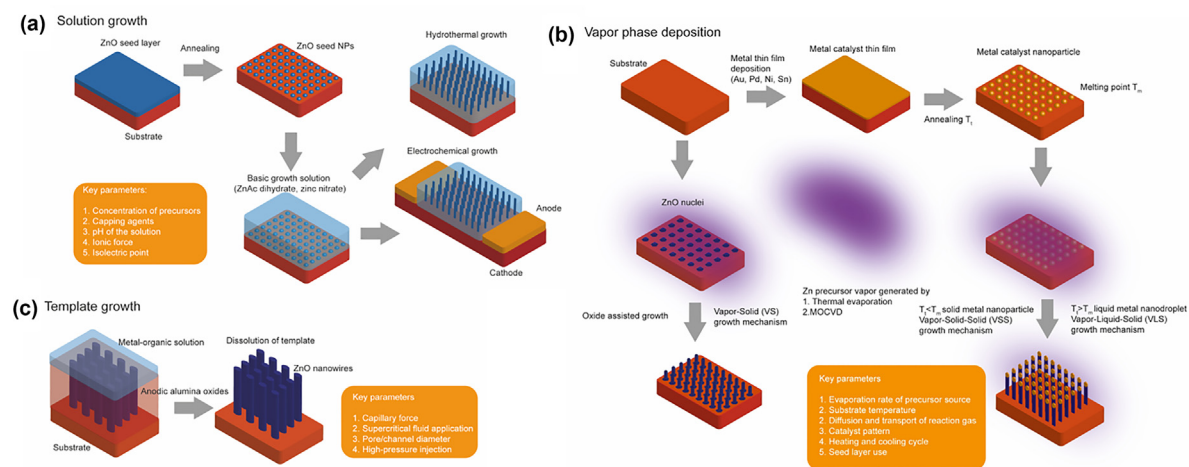


FIGURE 3

Schematics of the different ZnO NW growth techniques reported by various authors [134-137]. (a) Solution growth techniques: The growth of the nanostructures results from the crystallization of hydrolyzed Zn precursor salts in a basic solution. Common mechanisms to enhance anisotropic crystallization include hydrothermal [138], electrodeposition [139], epitaxial [136], and the use of different capping agents [140], templates [141], and seed layers[125]. (b) Vapor phase deposition techniques: the precursor elements of the desired nanowire are carried in a gas phase to the substrates surface, where the formation reactions occur. The nucleation process can be surface induced by thin oxide layers deposition around the semiconductor core [126,127] or by a metal catalytic metal nanoparticle [128,129,133,135]. (c) Template growth techniques: Metal-organic solutions containing the precursors are used to fill cylindrical holes templates (anodic alumina oxides, track-etched polycarbonate, nanochannel glass [130,131]) followed by subsequent thermolysis or electrolysis process to obtain the nanowires structure [132].

the use of different morphologies of ZnO nanostructures in cancer-related research.

However, 1D ZnO nanostructures such as NRs and NWs have a substantial advantage over nanoparticle systems in terms of the electrical and chemical surface properties, so they are at the vanguard of nanoscience and nanotechnology. A 1D nanostructure is characterized by having radial dimensions below 100 nm and a few microns longitudinal dimensions. They usually have mono or polycrystalline structures depending on the employed synthesis technique and highly anisotropic properties due to rapid growth in a preferential direction. Depending on the geometrical shape of the cross-section of the structure, they can be divided into squares, hexagonal, or cylindrical shapes. Synergistically this works with the spatial distribution of nanostructures, causing better entrapment of the optical signals to increase the platforms messages in optical biosensing. In the work of Huang et al., [156], a localized surface plasmon resonance (LSPR)-based sensor was used to diagnose prostate cancer. With the implementation of a ZnO NWs array with Au NPs on their surface, they reported an enhancement of 404% compared to a simple 2D Au NPs layer.

Another type of ZnO NW-based biosensors that many researchers have currently developed is electrochemical and field-effect transistors (NWFET) [79,156-161], Fig. 4 a and b). These systems transduce the charge of molecules attached to the ZnO structures surface into an electrical signal that can be measured by taking advantage of the high electronic mobility within the NW [162]. Optical and electrical based ZnO biosensing platforms offer precise/rapid response, selectivity, high sensitivity, and inexpensive biological detection alternatives implemented in cancer detection devices [163]. A standard comparison between 0D and 1D nanosystems properties is the effective confinement (below 100 nm), which will influence the

electron mobility of the material. In the case of ZnO NPs, electron mobility is low due to the high presence of surface defects and grain boundaries. While, in NWs or NRs, the electronic transport in the axial direction of the structure is highly efficient [164]. For this reason, ZnO NWs are incorporated into electrochemical biosensing platforms as they have an advantage over ZnO NPs due to the large surface area to volume ratio and the isoelectric point, which helps them to sense diverse biological analytes.

Size and morphology control over the ZnO NWs, their sharpness, and robustness are among the main requirements to avoid and prevent cell/tissue damage making it a viable candidate for *in vivo* biomedical applications. For instance, in the work of Hong et al., [72], a positron emission tomography of mice is reported by using ZnO/⁶⁴Cu NWs as an optical agent. The NWs conjugate was later peptide-functionalized (NW-PEG-DOTA) to improve biocompatibility and reduce cellular toxicity. In Fig. 4 c), the nontargeted composite accumulation in the mouse's liver can be observed. As mentioned before, ZnO NWs-based optical biosensors have attracted attention due to their fast response, selectivity, and low detection thresholds. An LSPR biosensor for the early detection of prostate cancer based on ZnO NWs is presented by H.-M. M. Kim et al., [165]. In this system, ZnO NWs were grown on top of an optical fiber to increment the sensing area and improve the capturing of optical signals. After that, Au NPs were attached to the ZnO matrix. The NWs based results showed an increment in the density of Au NPs per unit plane where the analyte could easily reach the surface of the noble metal [72,161,166,167].

The ZnO also stands out as a direct and inverse piezoelectric semiconducting compound. In other words, it can be both polarized by mechanical deformation or by the effect of an external electric field. As mentioned before, the ZnO piezoelectric proper-

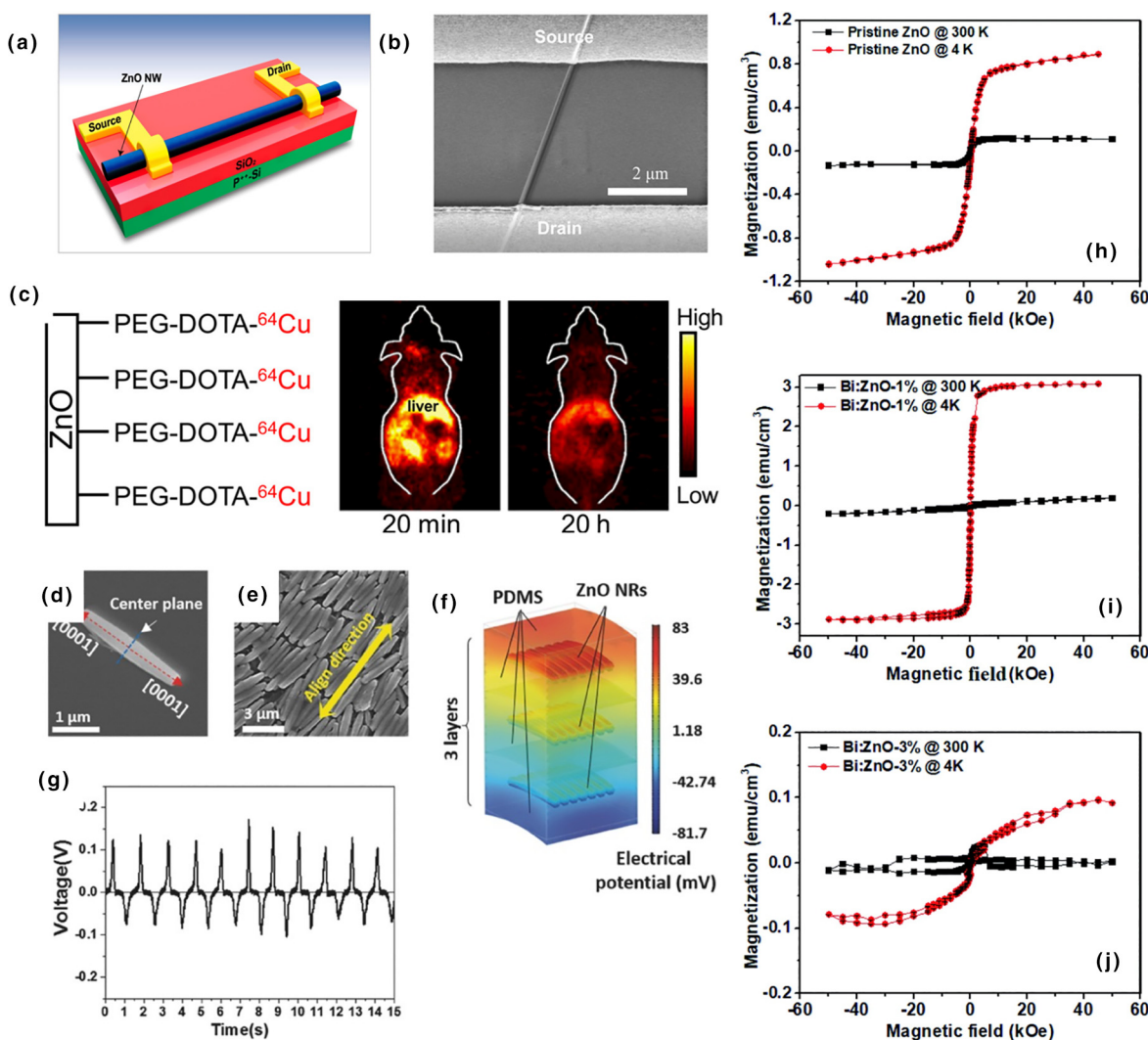


FIGURE 4

Properties of ZnO NWs as biosensors. (a) Diagram and (b) micrograph of ZnO NWFET with back gate device, Copyright 2020 MDPI [161]. (c) Positron emission tomography (PET) of mice using ZnO NWs-peptide-⁶⁴Cu conjugates as an optical agent, Copyright 2011 ACS Publications [72]. (d–g) ZnO-based thermosensitive, stretchable, and piezoelectric substrate (TSPS). (d) Wet chemical synthesized ZnO NR, (e) Monolayer of aligned ZnO NRs obtained by unidirectional rubbing process, (f) Calculated piezoelectric potential of the three layers of ZnO NRs sheets embedded in PDMS, (g) Generated piezoelectric response, Copyright 2017 Wiley [166]. (h–j) Superconducting quantum interference measurements of (h) pristine ZnO NWs, (i) 1%, and (j) 3% Bi doping at 300 and 4 K, Copyright 2020 Royal Society of Chemistry [167].

ties arise from the non-centrosymmetric lattice of tetrahedrally coordinated Zn²⁺ and O²⁻ ions [168]. Temperature, load frequency, and crystallinity are among the parameters that affect the piezoelectric response of material [169]. In 1D ZnO nanostructures, nanometric scales also alter the piezoelectric phenomena, making it different from bulk systems. Ghosh et al., [170] illustrated that wurtzite ZnO NRs prepared by the Sol-gel method exhibit a piezoelectric charge constant d₃₃ of 44.33 pm/V, which is almost 4.5 times the piezoelectric response measured in a ZnO single crystal [171]. In highly anisotropic ZnO nanostructures, such as NTs and NWs, a dependence of the piezoelectric constant as a function of the diameter of the structure has also been observed [172,173]. Furthermore, multiple works report the obtention of ZnO NWs on economic substrates to develop flexible piezoelectric nanodevices [174,175]. In biomedicine, ZnO-based nanocomposites (multiphase solid material) have been used to developed piezoelectric responsive tissue scaffolds and

wound healing patches. These systems operate by producing an adequate electric field that can boost cell proliferation and viability [166,176–178]. In the work of Yoon et al., [166], the implementation of a ZnO piezoelectric substrate to provide mechanical and electric stimulation to enhance myogenic differentiation is further presented. For the substrate fabrication, three layers of aligned ZnO NRs were embedded in PDMS, as shown in Fig. 4 d–g). These devices could be applied for muscle regeneration therapies, whereas their piezoelectric properties have also been used to reduce the growth of cancer cells [179].

The magnetic behavior of ZnO NWs is yet another essential property for their biomedical application. During the last decade, magnetic NWs have been used in drug delivery, magnetic HT, MRI contrast, and magnetic separator applications [180]. The origin of ferromagnetism in pristine ZnO is still a matter of debate, and therefore, many theoretical and experimental works have been dedicated to study the source of magnetism in ZnO nano-

tructures [181–185]. In the theoretical work of Wang et al., [186], the effect of intrinsic point defects in the ZnO NW lattice (i.e., V_O and V_{Zn}) over the magnetic properties of the structure is presented. No significant change was observed in the NWs magnetic properties when the V_O concentration was increased to 6.35%. However, the magnetic moment of the studied supercell was strongly influenced by the concentration of V_{Zn} . Therefore, it was suggested that the magnetism of ZnO NWs comes from the unpaired 2p orbitals of the O atoms in the vicinity of the Zn vacancy and not from the 3d orbitals of the Zn atoms. Complete control on the defect level to modulate the final properties of these nanostructures is still a topic of debate [70]. This is a reason why scientists doped ZnO with transition metals such as Mn, Co, Fe, Ni, Cu [187–191] as well as rare-earth ions such as Dy, Gd, and Er [192–194]. Such systems, where small concentrations of trivalent or pentavalent external cations or anions are inserted in a metal oxide matrix, are commonly known as diluted magnetic semiconducting materials (DMS). Kazmi et al., [167] reported the magnetic properties of hydrothermally prepared bismuth-doped ZnO NWs. The incorporation of Bi anions at a 1% concentration into the semiconductor lattice significantly enhanced the systems ferromagnetic saturation when interacting with small magnetic fields (magnetic saturation at 300 K). This is attributed to the p-p coupling interaction between the Bi and Zn orbitals. However, as shown in Fig. 4 h–j), the further increase in the Bi doping concentration crushes the magnetic response due to the formation of Bi_3O_3 crystals, whose appearance was corroborated by XPS measurements.

Heterogeneous photocatalysis is recognized as one of the most promising approaches to enhance the properties of ZnO for biomedical applications, as discussed above. An investigation of the photocatalytic activity of nanostructured ZnO films by Canon et al., [195] showed the effect of morphology on the photocatalytic activity at different scales, e.g., the role of the thickness of thin films and surface area (aligned vs. random orientation). As the thickness of fabricated thin films is reduced to the nanoscale, the photocatalysts region is increased. However, structural properties and morphology are significant as they play a key role in how light can interact with the photocatalyst. The photocatalytic process is broadly defined as enhancing the reaction rate by the presence of a semiconductor (i.e., photocatalyst) and light without participating directly in the reaction. It begins with the electron-hole pair generation by the absorption of photons with an energy higher than that of the semiconductor bandgap. After the charge carriers are generated, these can either recombine in radiative and non-radiative processes or produce active species such as hydroxyl ($\cdot OH$) or superoxide (O_2^-) radicals. These highly reactive radicals have multiple reductions and oxidation reactions on the photocatalyst surface, converting harmful and polluting residues to innocuous or mineralized products. For this purpose, many semiconducting compounds have been used in photocatalytic applications; for instance, Cu_2O [196], CdS [197], F_2O_3 [198], WO_3 [199], $g-C_3N_4$ [199], and TiO_2 and ZnO [200]. However, novel and simpler techniques to obtain ZnO nanostructures with improved optical and electric properties are always required, and a lot of investigation is carried out for their mass production [195,201]. The 0D and 1D ZnO

nanostructures have been widely used in photocatalytic applications due to their ease of crystallization, anisotropic growth, and chemical stability [202]. Even when the magnitude of the ZnO bandgap is such that its photoexcitation requires UV radiation, the positions of its valence band ($VB=+2.7$ V) and conduction ($CB = -0.33$ V) with respect to the standard hydrogen electrode (NHE) are suitable for the significant degradation of numerous organic pollutants like dyes (methyl red, malachite green, acid yellow, etc.) [203] and antibiotics (cephalexin, ciprofloxacin, amoxicillin, tetracycline, etc.) [204–206]. Many strategies are also executed to enhance the photocatalytic performance of the ZnO nanostructures in the visible region [207]. Among the most reported non-metal/metal doping [70,208,209], semiconductor coupling (n-n and n-p heterojunctions) [210], sensitization (using organic dyes or carbon nanostructures), and noble metal deposition [211] stand out.

Perspectives of 0D and 1D ZnO nanostructures in biomedical engineering

ZnO has been vastly explored in recent years for its use in cancer applications or active drugs, with the surplus advantage of its controlled fabrication into different morphologies, as mentioned above [212]. The chemical surface of ZnO NPs permits the functionalization of biochemical species and targets the cancer cells, and as various studies have shown, ZnO NP photoactivation conjugated to tumor ligands might help the targeted destruction of cancer cells [213]. It has been proved that diverse ZnO-based composites as nanomotors for drug delivery; among them are Pt-Au-Pt-Ni-Ag-ZnO [214] and Au-Ni-Au-AgPAu [33]. Also, for cancer theranostics, researchers have tested *in vitro* Gd-doped ZnO QDs and magnetic core–shell Fe_3O_4 -ZnO [215,216], and it is demonstrated that ZnO NPs can be lethal to cancer cells [217,218]. ZnO NPs, as mentioned earlier, induce ROS generation, which can lead to cell death when the antioxidative capacity of the cell is exceeded [219]. Several studies have suggested an increase *in vitro* cytotoxicity with nanoparticle ZnO for several types of cancers, including glioma, breast, bone, colon, leukemias, and lymphomas [218,220]. Likewise, it has been shown that ZnO/Au nanocomposites have selectivity for the killing of leukemic T cells while affording normal immune cells [221]. A summary of different nanomaterials and their implementation for detection/treatment for different types of cancers has been shown in Table 1 [222–249].

1D nanostructures of multiple semiconducting compounds have been developed for the efficient recognition of both Deoxyribonucleic acid (DNA) and ribonucleic acid (RNA) chains [46,47,250]. ZnO NR-based cancer biomarker assays have been developed to detect ultra-low levels of telomerase activity for cancer identification and assessment [154,251]. ZnO NRs demonstrated suppression of growth and proliferation in human breast cancer cells (MCF-7) *in vitro*, suggesting that this may be a potent and selective formula concentration-dependent in treating cancer cells [252].

The ZnO nanostructures present a high isoelectric point of 9.5 [253], appropriate for forming a stable bioselective layer for lower isoelectric point materials (such as proteins) by the electrostatic interactions. It is also broadly accepted that morphology and the NWs structural properties lay a vital role in the function-

TABLE 1

Summary of different nanomaterials for cancer applications.

Nanomaterial	Morphology	Tumor Imaging/Treatment	[Ref]
Organic Polymer	NPs	Inhibit the growth of MDA-MB-231 tumor <i>in vivo</i>	[222]
	Poly (lactic-co-glycolic acid) NPs	Leukemia K562 cells	[223]
	7-pep HD micelles	MDR tumors-loaded	[234]
	DOX-ERLP	Liver cancer H22 cells	[243]
	Lipid-coated zinc phosphate hybrid NPs	Tumor immunotherapy	[244]
	NPs	Breast cancer cells	[560]
	NPs	Breast cancer cells	[561]
Liposomes	Liposome (pHCT74-lipo) loaded with doxorubicin	Prostate carcinoma cells	[562]
	Material in general	Imaging and treatment	[245]
	Material in general	Imaging and treatment	[246]
	NPs	MCF-7 cells	[247]
Dendrimers	NPs	Colorectal cancer	[246]
	Liposome (pHCT74-lipo) loaded with doxorubicin	Breast cancer	[247]
	Material in general	Fluorescence imaging and targeted therapies of breast cancer	[248]
	Material in general	Computerized tomography (CT) imaging and therapies of prostate cancer.	[249]
Inorganic Gold	NPs	Prostate cancer	[224]
	Nanoclusters	miR-21 inhibitor	[225]
	NPs bioconjugate	Antioncogene p53/ hepatoma HepG2 and HEK293 cell lines	[225]
	Neuropilin-1-targeted gold NPs	Glioma cell line	[226]
	NPs	NIH3T6.7	[227]
	Gold nanorods (Au@HSN-PGEA, AHPs)	LNCaP prostate cancer cells.	[563]
	Au NPs dendrimers entrapped modified with cyclodextrin (Au@DENPs-β-CD)	Human epithelial mouth carcinoma	[228]
Iron oxide NPs	Magnetism-engineered iron oxide (MEIO) NPs	Colorectal cancer diagnosis and photodynamic therapy	[229]
	Streptavidin-labeled iron oxide NPs	Lymphatic endothelial cells	[230]
	PEG-SPIO	Breast cancer cells	[231]
	Fe ₂ O ₃ NPs	Circulating tumor cells (CTCs)	[232]
	Fe ₃ O ₄ @KCTS)	Immunocompromised NOD/SCID mice MDA-MB-231 breast cancer cells	[233]
	polymeric iron oxide NPs	MCF-7 cells	[235]
	NPs	Magnetic-enhanced tumor-targeting MRI	[236]
Silica	Fe ₃ O ₄ @Arabic acid@DOX	improved antitumor activity on both HepG2 and HeLa cells.	[237]
	DOX/ Fe ₃ O ₄ -alginate chitosan microsphere	Efficacy of pancreatic cancer	[238]
	NPs	Cancer theranostics	[239]
	DOX-loaded functional MSNs	Cancer imaging	[240]
	NPs	MCF-7 and MDA-MB-231 breast cancer cells	[241]
	Mesoporous silica	Cancer imaging	[242]
	Mesoporous silica	4T1 breast cancer cells	[242]
Carbon	Se@Au@mSiO ₂ DOX	Cancer theranostics	[239]
	Chitosan- carbon dots hybrid nanogel (CCHNs)		
	Mesoporous NPs		
	Mesoporous		

alization process. Also, the surface of the nanostructures can enhance the generation of ROS to work as an anticancer and antibacterial material [151]. However, one of the shortcomings is that the ZnO surface can slowly dissolve in both acidic (tumor cells) and robust essential solutions [254] which has been covered in the subsequent sections in detail (toxicity aspects). As the central subject of this review is a general outline of ZnO NWs properties and applications, the reader is recommended to consult the reviews made by Vandebriel et al., [255], Liu et al., [256] and Król et al., [257] for a more complete and detailed view of the toxicity of ZnO nanocomposites.

Toxicity phenomena in 0D and 1D ZnO nanostructures: concerns and effects

A compounds toxicity is the possible harmful effects that the substance might have on a given organism under specific condi-

tions. For *in vivo* applications, it is essential that the nanomaterial of interest presents biocompatibility and that its synthesis methodology generates the least number of hazardous traces. Literature reports that the nanocomposites allotropic and polymorphic structures may or may not significantly impact their toxicity. Therefore, it is necessary to highlight that the toxic properties of NPs depend on their: (1) size [258–262], (2) morphology [263–266], (3) exposure dose [258,267–271], among other factors. It is always advisable to study the toxicity of the final product since its properties can change [272].

For ZnO nanometric structures, their toxicity has been mainly correlated to their solubility and the released amount of Zn²⁺ ions when the ZnO NPs are captured [273–275]. For these NPs, the main routes of exposure are oral, respiratory, dermal (only if the stratum corneum is damaged [272]), intraperitoneal and intravenous routes [255,256], of which the three first are the most common. Once inside the body, the main organs in which

NPs are distributed and deposited are the lungs, spleen, liver, and kidneys [256,276–278]. However, few studies have shown that some NPs could cross the blood–brain barrier (BBB) due to their size, inducing neuronal damage [269,279,280]. Additionally, it has also been shown that ZnO nano-compounds can also affect cells of the immune system [153,281–283]. An illustration of the possible cytotoxicity of ZnO NPs has been shown in Fig. 5 a).

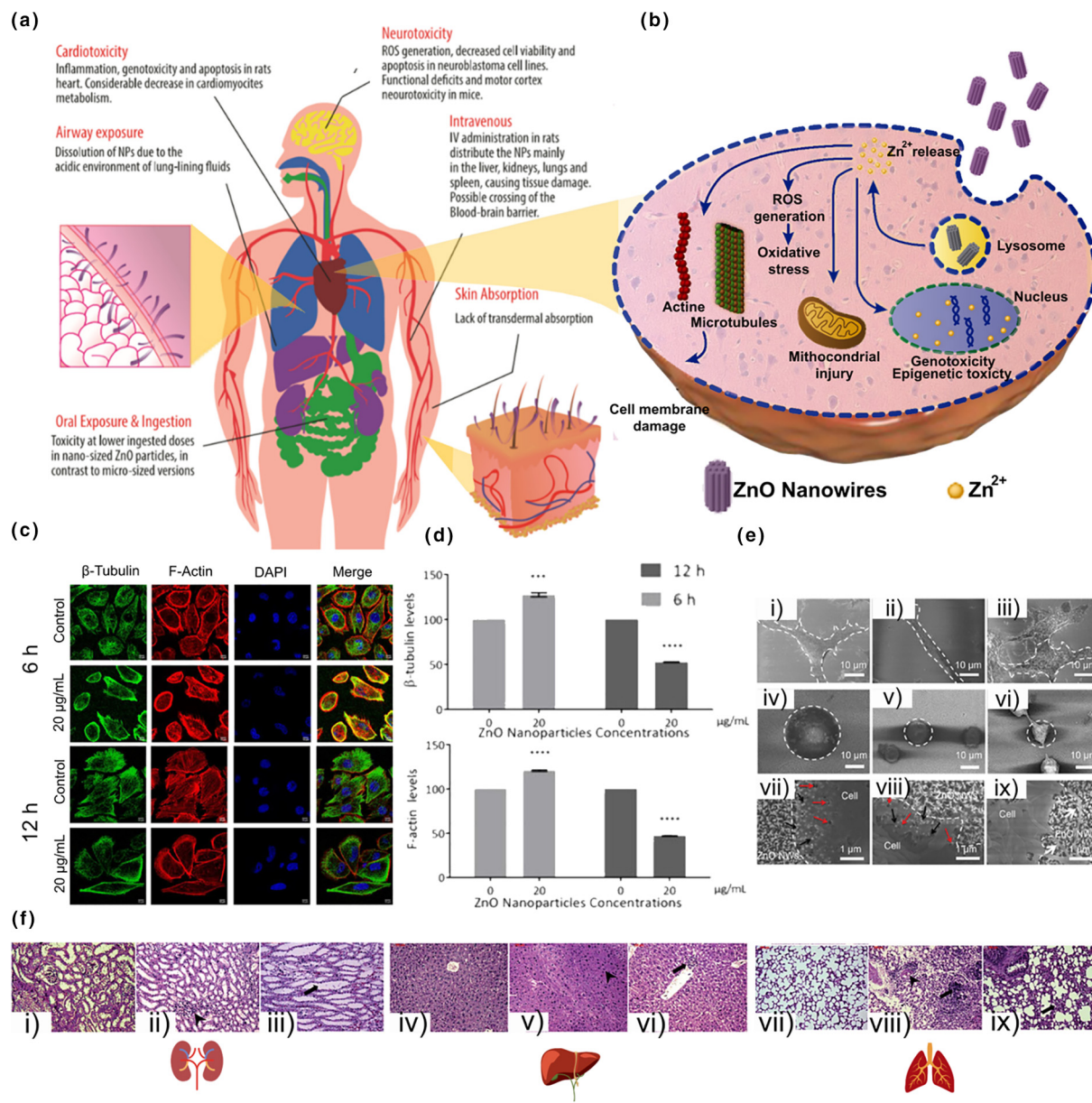
After the ZnO NPs are captured by cells, a wide variety of toxicological effects can be triggered, ranging from cellular damage (cytotoxicity) to genetic material (epigenetic toxicity). To better understand and summarize the key points of how this damage occurs, crucial steps are illustrated in Fig. 5 b), showing how the NPs are taken up by the cells and subsequently could further damage them. The critical concerns for ZnO NPs once inside the cells are that NPs are endocytosed by the cells [284], which leads to the formation of lysosomes [274], and their acidic pH causes the generation of Zn²⁺ ions [285,286]. Subsequently, the Zn²⁺ ions alter the polymerization/depolymerization of tubulin and actin, which compromises the production of microtubules and actin microfilaments, damaging the cytoskeleton and, therefore, cell viability [287]. Likewise, the Zn²⁺ ions released in the cytosol cause the generation of ROS. This process (oxidative stress) is related to the Zn^{2+/Zn⁺ redox potential of some amino acids, which leads to the generation of hydrogen peroxide (H₂O₂) and hydroxyl radicals ('OH) [284]. ROS causes damage to the mitochondrial membrane, altering its function, which can further increase ROS production and, therefore, can lead to cell death [288–291]. Additionally, oxidative stress induces damage to the nuclear membrane and provokes DNA fragmentation [292–295] (Genotoxicity).}

It has been shown that the oxidative stress associated with the ZnO NPs can cause significant alterations in DNA methylation (epigenetic toxicity), leading to the overexpression of some genes [296]. The latter is related to the development of many types of cancer. In particular ZnO NPs, a significant amount of research has been directed to discuss their toxicological properties. For example, airway exposure to ZnO nano-compounds has been shown to cause significant toxicity due to dissolution of the NPs in the acidic environment created by lung-lining fluids and inside the phagosomes, after they are phagocytized; causing inflammatory responses, changes in genetic expression, necrosis, and the generation of ROS [297,298]. In contrast, oral exposure shows a possible relationship between particle size and cytotoxicity, in which nanometric particles show higher cytotoxicity than microparticles in rats [299]. Regarding neurotoxicity, based on a study in neuroblastoma cells, Liu *et al.* found that ZnO nanocomposites can generate ROS, decreasing cell viability and leading to possible apoptosis based on the NPs size and concentration [300]. Moreover, Yaqub *et al.*, discovered that ZnO NPs induced functional deficits and motor cortex neuron toxicity in mice [301]. Additionally, there is considerable evidence suggesting diverse cardiotoxic effects from ZnO NPs. The team of Abdel Baky *et al.*, found that ZnO NPs, even in low concentration, increased the serum quantity of associated cardiac biomarkers to inflammation and myocardial infarction in rats and increased damage to genetic material and apoptosis in heart tissue [302]. Feris *et al.*, observed that ZnO NPs induced toxicity in a cell-

specific and proliferation-dependent manner employing ROS generation since activated and cancerous T-cells were more susceptible to ZnO NPs than healthy T-cells [217]. Regarding the effect of NPs on spermatogenesis, Pinho *et al.* used the GC-1 cell line as a model for monitoring morphological changes in the cytoskeleton and nucleoskeleton and intracellular levels of ROS and phosphorylation of γ-H2AX to assess DNA damage. The team observed changes in morphology and protein levels depending on the dose and time of exposure to ZnO NPs [303], Fig. 5 c–e). Furthermore, Tae-Keun Hong's team studied both the effects of ZnO NPs *in vitro* (using RAW 264.7 murine macrophages) and *in vivo* (with ICR mice). Histological analyzes of the latter showed mild to severe pathological inflammation in target organs, (Fig. 5 f) [268].

In the case of ZnO-T, Papavassopoulos *et al.*, discovered that the cytotoxicity of these nano-compounds was a function of their size and morphology. Further, the ZnO-T's toxicity was via direct contact with cells due to Zn²⁺ ions release [275]. Compared with other forms of exposure, ZnO NPs do not present appreciable toxicity in dermal exposures because of a lack of transdermal absorption, which points to its safe use in creams and sunscreens [304,305]. A more detailed discussion about the exposure of ZnO nanostructures on ecological factors has been presented in subsequent sections. In contrast with NPs, ZnO NWs toxicity information is more limited. Notwithstanding, solubility and pH-dependent toxicity (dependent on the level of internalized material into the cells) have also been found for this type of nanostructures [285,306]. Li *et al.*, showed ZnO NWs high biocompatibility with concentrations below 100 µg/mL in Hela and L-929 cell lines after performing MTT assays(3-(4,5-di methylthiazol-2-yl)-2,5-diphenyltetrazolium bromide) [105]. Although the micrographs showed an apparent process of broken NWs phagocytosis by Hela cells, most of the NW matrix is maintained externally as a support substrate [105]. On the other hand, Muller *et al.*, discovered that ZnO NWs toxicity was due to the intracellular release of Zn²⁺ (when the NWs are dissolved in the lysosomes) in a way similar to spherical NPs [285]. Contrasting with those works, Ning *et al.*; proposed with their research that extracellular 1D ZnO structures can cause cytotoxicity and apoptosis due to the penetration of NWs into the cancer cell membrane. Added to that, they attribute this phenomenon to electrostatic interactions between the positive-charged NWs and the predominantly negative-charged surface of cancer cells [307]. In this direction, Wang *et al.*, investigated the cytotoxicity of ZnO NWs in excitable neural and cardiac cells using the MTT assay, finding a considerable inhibitory effect in the cells metabolism compared to other substrates for cell culturing [306].

As discussed above, it is evident that ZnO NWs can cause toxicity mostly when the nanostructures are highly phagocytosed due to the high concentrations of Zn²⁺ ions generated after their dissolution [308]. However, the NWs appear to have considerable biocompatibility when maintained extracellularly, offering a wide range of uses for both *in vitro* and *in vivo* applications. For example, Cui *et al.*, created a Polydimethylsiloxane (PDMS) microchip covered with ZnO NWs, showing better biocompatibility compared to hydrophobic PDMS alone [309]. Therefore, beyond the overall risk that NWs pose to healthy cells and tis-

**FIGURE 5**

Routes of exposure and organ-specific toxic effects of ZnO nanostructures studied *in vitro* and *in vivo* in humans and animals. (a) ZnO nanostructures have been shown to cause toxic effects after inhalation (Blue) and ingestion (Green). Nonetheless, it is not generally capable of being absorbed via the skin (Pink). Moreover, upon reaching the bloodstream, either by ingestion or intravenously (Light red), the ZnO biodistribution is mainly seen in the liver, lungs, kidneys, and spleen (Violet and Blue). The most studied organ-specific effects are their cardiotoxic (Dark Red) and neurotoxic effects (Yellow), where many diverse molecular, biochemical, and tissue damage mechanisms occur. (b) A general overview of the ZnO NWs cytotoxicity. In the first place, ZnO NWs are endocytosed by the cells, leading to lysosomes forming and, later, to releasing Zn²⁺ ions, which alters the polymerization/depolymerization of tubulin and actin, compromising the cytoskeleton and the cell viability. Furthermore, Zn²⁺ ions drive the formation of ROS and, therefore, oxidative stress, which can cause injuries in the mitochondria and nuclear membrane. Finally, ZnO NWs can damage the DNA by its fragmentation and, besides, cause significant alterations in DNA methylation (epigenetic toxicity). (c) Effect of ZnO NPs in the cytoskeleton structure and nuclear morphology of GC-1 spg cells, observed via immunocytochemistry. Cells were incubated for 6 and 12 h with ZnO NPs concentrations of 0 (control) and 20 µg/mL. Images of β-tubulin, F-Actin, and nuclear DNA. Copyright 2020 MPDI [303]. (d) Relative fluorescence intensity quantification of β-tubulin and F-Actin protein levels. (c and d) Copyright 2020 MPDI [303]. (e) Effect of ZnO NPs layers & ZnO NWs arrays in the cellular morphology of HepG2 (i, iv, vii), Ca ski (ii, v, viii) & MCF-7 (iii, vi, ix) cell lines. Cell culture in the ZnO NP layer. (i–iii) and ZnO arrays (iv–vi). Partial enlarged details of iv–vi (vii–ix). White broken lines represent the outline of cell membranes. Black arrows show mechanical damage in the membrane, and the red arrows show defects in the cytomembrane. Copyright 2014 John Wiley & Sons [307]. (f) Histological changes of the kidney (i–iii), liver (iv–vi), and lung (vii–ix) after oral treatment of ZnO NPs in male ICR mice after two weeks of treatment. Respective controls (i, iv, vii). ZnO NPs gastrointestinal administration at 100 µg/mL (ii, v, viii). ZnO NPs intraperitoneal administration at 100 µg/mL (iii, vi, ix). Mild interstitial inflammation (ii). Focal interstitial edema & inflammation (iii). The early apoptotic change was observed by nuclear pyknosis (v). Focal inflammation in the central vein area (vi). Patchy and moderate-severe interstitial inflammation and destruction of alveolar wall & hyaline membrane (viii). Moderate interstitial inflammation (ix). Copyright 2013 Royal Society of Chemistry [268].

sues, a better understanding of ZnO NWs cytotoxicity will be critical in developing innovative strategies for implementing new cancer therapies, Fig. 5 [268,303,307].

One of determining factors for ZnO nanostructures toxicity is the ease of solubility [310]; this has already been proved *in vitro* [311] and *in vivo* [312]. In human monocyte macrophages (HMMs), the effects of toxicity are shown to be determined by the release of Zn²⁺ from the ZnO NW [285]. The studies carried out by Ho et al., [313] and Oberdörster et al., [314] proved that both mass and surface area might be used as a metric for ZnO NPs toxicity. As the nanostructures become smaller and more reactive, the cell uptake increases due to the high surface-to-volume ratio [315]. When ZnO NP are being dissolved, the ROS levels in human cells change [316] and ROS generation can also be triggered when ZnO is exposed to different kinds of excitation environments, such as UV light [317,318]. Ma et al., showed the importance of UV radiation in ZnO toxicity, especially when higher hierarchy organisms are involved in aquatic conditions [319]. The outcomes of these reports confirm that the consequences of ROS production showed oxidative stress, lipid peroxidation, Zn ion release, breakdown of the cell membrane, impairment of mitochondrial functions, and DNA damage [153,320,321]. Many experiments suggest combining ZnO with other polymers and different kinds of dressings like hydrogel [322,323], gelatin/ointments [324], or electrospinning mats [325] for improving its properties [326]. A pivotal factor that affects ROS levels is the coating of ZnO nanostructures [327], and it has been demonstrated that the composition of NP is vital for toxicity. Hsiao et al., proved that a protein coating could diminish cytotoxicity and result in a faster cell growth rate [328]. When the nanostructures core is covered with an impermeable shell and a well-passivated surface, the *in vitro* cytotoxicity can be lowered even on the most sensitive cell lines [329]. The shape of the nanostructure is also a crucial factor in toxicity, and it has been found that the toxicity of spherical ZnO nanostructures is less than that of 1D-shaped ZnO nanostructures [264,328].

As mentioned before, ZnO NPs have been a successful candidate in nanomedicine as they can destroy both prokaryotic and eukaryotic cells, which implies they hold the inherent capacity to kill cells, and this finding has alarmed us to the use of these NPs in the human body; this can be applied in diagnostics as well as helpful in the therapeutic way [330,331]. These results compelled many scientists to glance over NPs behavior to determine whether there is a human health danger connected with the usage of these NPs [332]. Incorporated in a certain concentration, Zn is one of the main trace elements present in the human body [333]. The Zn concentration in the cells increases from normal levels with the application of ZnO NPs and the intracellular release of Zn ions, contributing to the excess of Zn-mediated protein production. This influences several critical cellular processes, including replicating DNA, repairing damage to the DNA, apoptosis, oxidative stress, electron transport chain, homeostasis, etc. In host protection against cancer initiation and growth, the Zn is the co-factor of over 300 mammalian enzymes and plays a vital role in the host defense mechanism [331]. The tumor suppressor p53 gene and caspase enzyme allow cells periodically to search and avoid cancer. A DNA repair system can repair the altered

DNA if the cell indicates malignancy of some type. If this process cannot restore the DNA, the cell is exposed to 'programmed cell death' ('apoptosis') to stop the altered cell division, which can then grow in a subsequent cancer cell. Zn is active in all these cancer-protection mechanisms in one direction or another [334]. Although apoptosis induction precise mechanism is not clear, mutation or DNA disruption seems to play a vital role in activating the p53 gene leading to apoptosis [335]. The unique p53 domain for DNA binding comprises a dynamic Zn-stabilized tertiary structure and is an essential part of maintaining p53 tumor suppressor activity.

Several Zn channels regulate the inherent and free metal concentration, providing a critical equilibrium between life and cell mortality. While low Zn concentrations may trigger cancer to begin and grow, higher Zn levels have a deleterious impact on health. Excess Zn beyond the homeostasis systems ability will result in a breakdown of the plasma membrane transporting system, resulting in cell death [336]. Low intracellular Zn has been noted to trigger oxidative DNA injury, disturb p53, and disrupt DNA repair in rat glioma cell lines. In patients with kidney, breast, gastrointestinal, and gynecoid malignancy, serum Cu/Zn levels have also been found to be improved. Furthermore, the concentration of Zn in esophageal cancer has been slightly smaller than usual tissue. Similarly, data shows that Zn aggregation is a critical factor in the growth and advancement of prostate cancer, often defined by the downregulation of ZIP 1, a Zn transport protein at a low level in malignant prostate cells. These research results indicate a drop in Zn volume or altered Zn in cancer cells [337]. Proteins that rely on Zn have abnormal activities that cause high levels of oxidative stress and cell death. Using antioxidants and ROS quenchers to mitigate ZnO NPs cytotoxicity did not substantially reduce cytotoxicity. This indicates that ROS may not be the primary cytotoxicity pathway for ZnO NPs, but instead the cytotoxic answer. ROS are also produced in the process of ROS-mediated cytotoxicity, but the fundamental cause may be due to the ZnO cytotoxicity. The mechanism of cytotoxicity of ZnO NPs is assumed to increase the protein activity disequilibrium because of the elevated dissolution of free Zn ions in the cell [338]. Bogdan et al., suggested that by ultraviolet (UV) radiation or ultrasound (US) wave, nanoparticles of ZnO NPs induce ROS-mediated cell apoptosis, autophagy, or necrosis [339]. An increase in ROS level in the cytoplasm results in Trx oxidation and ASK1 activation. ASK1 can phosphorylate the ERK, JNK, p38, or Fas death ligands, thereby facilitating apoptosis. The ERKs promote cell apoptosis by disrupting the AKT kinase that regulates the NF-κB-mediated synthesis of Bcl-2 and Bcl-xL proteins. Oxidative damages to mitochondrion affect ΔΨm and ATP level, accompanied by the release of cytochrome (Cyt. c) to the cytosol. The Cyt.c binding with Apaf-1 activates the caspase-dependent apoptosis. The increase in ROS level in the nucleus contributes to the activation of mutated ataxia-telangiectasia (MTA) and ataxia telangiectasia and kinases that induce p53 mediated apoptosis and increase the DNA double-beam split marker (μH2AX). ROS-induced endoplasmic reticulum stress causes increased levels of Beclin-1 and decreased level of mTOR. All these pathways contribute to autophagy in cells. By oxidative stress, plasma membrane calcium ATPase is downregulated by the decrease of ATP level and the rise

of Ca^{2+} level, resulting in cell necrosis. Cells may become dysfunctional and cancer-prone to Zn deficiencies, as it is an essential factor for malignancy production and growth, proposing that the treatment and therapy of multiple cancer may also be effective by Zn-mediated cancer chemoprevention.

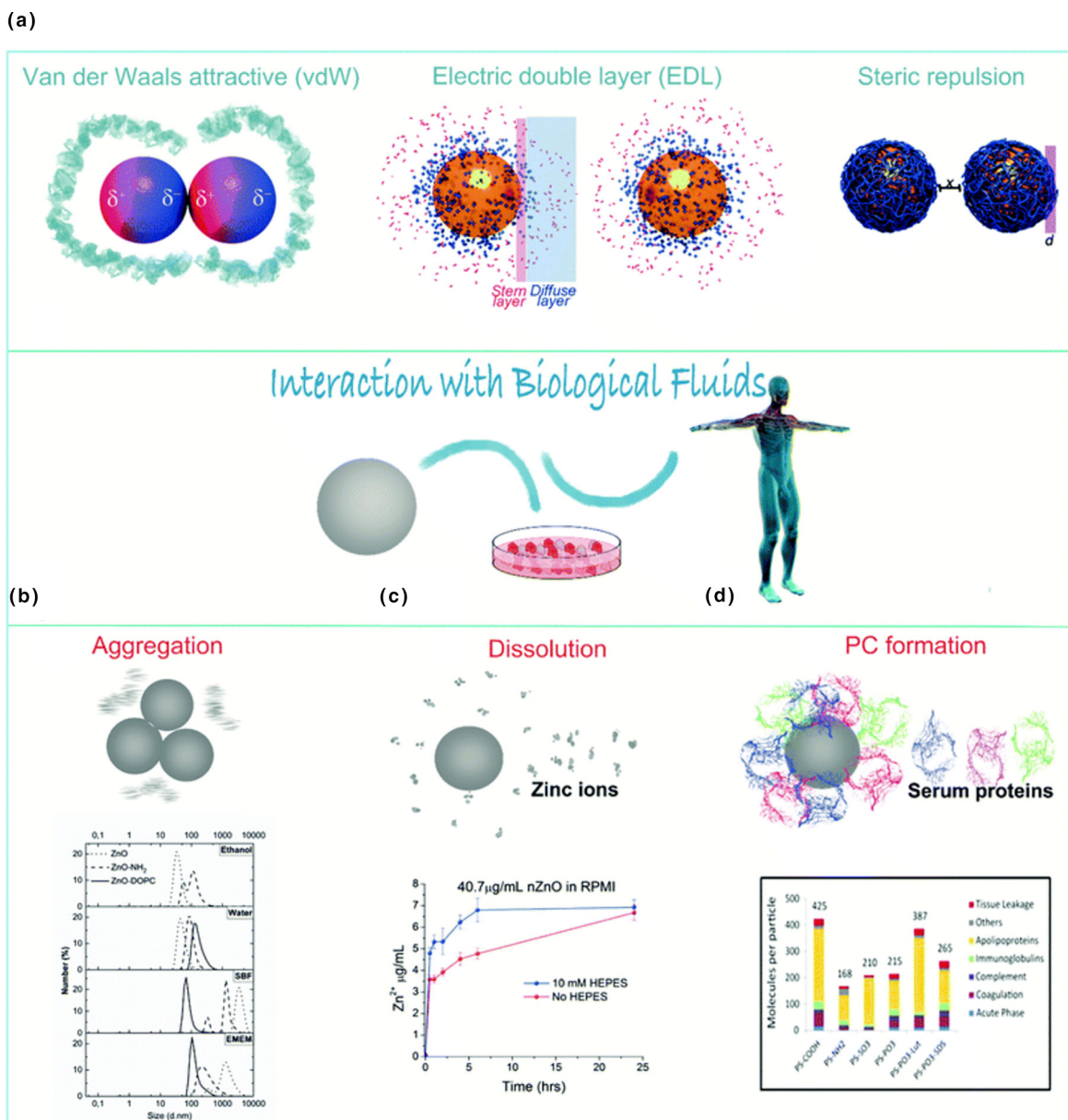
Mechanistic insights of molecular mechanism at nano-bio interface

Learning how the NPs interact with cellular membranes will improve our knowledge of the processes by which these particles function. Comprehensive nano-bio interaction studies based on bioinformatics, *in vivo*, *in vitro* have been illustrated in previous studies for various nanoparticles [340–359]. Nano-bio interface is a complex physicochemical interaction between the surface of NPs and the surface of biological elements, which deals with the thermodynamic and kinetic exchanges [360]. Besides the interaction between NPs, another vital aspect of their functionality is the interaction between themselves. Interactions influenced the agglomeration of NPs in media, which were composed of electrostatic force, Van der Waals force, solvation, and hydrophobic and depletion powers [361]. Understanding this interaction is essential for the accurate dispersal of nanoparticles with a minimal concentration in the media. The attractive force is the van der Waals, and the repulsive force is the electrostatic force. Van der Waals forces are caused by changes in the dipole moment of the electron, which induces an electron-induced dipole moment in the neighboring atoms. This effect emerges from the movement of the subatomic particles. The multiple forces have an important role in the structural and adhesive interaction of NPs on the cell surface and their passive absorption inside the cell. It would be strongly affected by the cell surface molecular receptor and the scale of the NPs relative to ligands. This process can contribute to increased cytotoxicity, and it can be found anywhere inside the cell, including the external membrane, cytoplasm, lipid vesicles (lipid vesicles), mitochondria, nuclear membrane, nucleus, DNA, etc.

Biomedical scientists should know what happens to ZnO NPs while present in the bloodstream, and this review could provide necessary information related to the effect of ZnO nanostructured materials in the human body and the environment. Cell culture media may be used for *in vitro* environments, precisely adapted for specific cell lines or forms (serum, antibiotics, additional amino acids, growth factors). In both *in vitro* and *in vivo* models, ZnO NPs are processed by the cells long before they join the bloodstream. The interactions of NPs with biological fluids alter physicochemical properties, which is the basis to determine the behavior. In Derjaguin, Landau, Verwey, and Overbeek (DLVO) theory, NP stability is regulated by the equilibrium between intermolecular and surface forces [362]. The attractive and repulsive forces are addressed because of Van der Waals forces and the electrostatic double layer forming around particles in solution. These forces dictate the transition to NP behavior. Besides, this behavior is not only dependent on the particle properties but is also highly affected by the atmosphere in which it is submerged. The biological media used for *in vitro* experiments are also made to imitate the blood chemistry. There are also complex structures made up of amino acids, ionic salts, and proteins, which would theoretically interfere with the NP surface. The

behavior of ZnO NPs in some popular culture media was analyzed in some articles that report the above three aspects: ZnO NP aggregation, dissolution of ZnO NPs, and formation of some protein films called protein corona Fig. 6 a–d)[362–365]. Three of these phenomena often co-exist in biological functions and help to drive the NPs biological reaction.

Ramani et al., reported the understanding of the nano-bio interface focused on RNA-based therapeutics developed using ZnO NPs [366]. They have explored the RNA nano-bio interface of poly I:C [367], its mononucleotides, and homopolymers with ZnO NP by UV, fluorescence, and Fourier transform Infrared (FTIR) spectroscopies, which resulted in greater interaction affinity towards RNA-ZnO NP. The outcomes of this research reported an important step in the interpretation of pIC-ZnO complexes with respect to the nano-bio-RNA interface. Excess sodium ions raise the payload of RNA on the NP and have a greater affinity for stable complex creation. Modified Stern-Volmer equations showed higher inosine binding constants than ZnO NP for cytidine, indicating pIC RNA interaction through purine nucleotides. The potential application of multi-functional NPs for the biomedical field demonstrated that it is essential to consider the relationship between inorganic and biological NPs at the atomic level. Saha et al., studied the nano-bio interface of DNA with ZnO NWs using the Density Functional Theory (DFT) approach to elucidate the interaction mechanism [368]. The study provided great insights to the interaction sites where ZnO preferred to bind through the top site of the nucleobases or with the ring atom having a lone pair in relative ring N atom and those for Uracil and thymine, e.g., NH site. From a thorough geometry inspection, they have observed that in ZnO NWs, all surface Zn atoms are surrounded by 3O atoms and vice-versa (as three Zn atoms surround surface O atom). The surface Zn–O bonding length ranges between \AA 1.86 and 1.99, while the core Zn–O bonding lengths are like 1.97 \AA for an optimized NW (not including base molecules) (close to bulk value). The local structure of the ZnO NW is subtly blurred as the base molecules are adsorbed on the ZnO NW surface. In that case, the Zn–O bond lengths are extended by a smaller quantity (1.90 to 2.01 \AA) in the adsorbed NW schemes, and core connections remain virtually unchanged. The Zn–O interactions are primarily ionic, and charge transfer occurs from Zn to more electronegative O atoms. An accurate and careful study of the nanomaterial-based interaction mechanism could make this potential real in cancer diagnosis and treatments. For instance, as of now, to the best of our knowledge, there is almost no report based on the nano-bioinformatics approach using ZnO NWs or NPs in anticancer activities, but the ROS and apoptosis mechanisms have been elucidated using *in silico* approach in bacteria [341,346], zebrafish [340,345,352,359] and human cell lines [343,344]. Therefore, an extensive study exploring ZnO nanostructures interaction (nano-bioinformatics approach) needs to be investigated in the future to describe the mechanistic molecular interaction that drives the properties exerted by these nanostructures. Although the scientific path is long and full of difficulties, the aim is to shorten the distance and reduce the challenges that research studies can face, thus helping nanoscientists to choose the right paths.

**FIGURE 6**

Scheme of the NP interaction with biological fluids. (a) depicts the interaction mechanism of the colloidal NPs in solution. (b) ZnO NP aggregation and dynamic light scattering measurements of different ZnO NP formulations in ethanol, water, simulated biological fluid (SBF), and Minimal Essential Eagle's medium (EMEM). (c) Scheme of ZnO NP dissolution and ICP of the amount of free Zn ions from ZnO present in RPMI-1640 media with and without 10 mM HEPES over 24 h. (d) LC-MS analysis of the corona proteins. Reproduced with permission from Royal Society of Chemistry ref [330]. Copyright 2020 Royal Society of Chemistry [330].

Environmental risks and benefits of ZnO nanostructures: public health concerns

Considering public health concerns associated with 0D and 1D ZnO nanostructures, their potential environmental risks should be fully understood for their global adoption and further clinical application. The toxicity that emerges from these interaction factors can be studied by exploring them independently and correlating them with existing tests to understand the phenomenon better. One crucial point that should be kept in consideration is that the toxicity of ZnO is a multivariable event. This aspect is also depending on the type of cell, selected based on the study model and targeted biomedical application, the ambient (pH,

salinity, UV presence, enzymes, etc.), the kind of ZnO nanostructure, the concentration of ZnO, duration of exposure, and cascading effects accounting for the presence of ZnO. The type of cell is vital in toxicity since this will determine if they have the mechanisms to deal with the oxidative stress or if their cell membrane will be permeable to ZnO nanostructures. The environmental conditions can influence how the cell and ZnO nanostructures behave, thus affecting permeability, oxidative stress, and bioaccumulation for the cell while also affecting solubility and stability of the ZnO nanostructure that finally will influence the toxicity. The multivariable toxicity of ZnO is an example of different thinking (chemistry into medicine), "The

dose makes the venom." By testing how ZnO affects plants (or algae), invertebrates (crustaceans), and vertebrates (fish) in acute toxicity, chronic exposure, bioaccumulation, and development will give us guidelines about the proper usage of ZnO, Fig. 7. A review of ZnO nanostructures and their toxicity on different ecological chains has been summarized in Table 2 [316,369–374].

Effect of ZnO nanoparticles on toxicity

It is crucial to keep an eye on how plants and especially horticultural species, react to different ZnO concentrations. Singh et al., demonstrated that the use of wastewater containing ZnO is feasible up to a concentration of 1000 mg/L when a reduction of total weight was noted (Table 2) [374]. *Zea mays* and *Spinach oleracea* also exhibited reduction height by 29% and total weight by 27%, respectively. The toxicity of ZnO nanostructures differs not only within a targeted species but also in different development stages and in specialized cells. Table 2 shows that the damage to fertilization done to each gamete of *Scaphichinus mirabilis* differs significantly in terms of the concentration of ZnO and Zn²⁺. Similarly, Hanley et al., showed that ZnO NPs induced high division due to toxicity [143]. An earlier research demonstrated long-term ZnO-NPs exposure to innate immunity resulting in the decreased survival of *Caenorhabditis elegans* when exposed to a *Pseudomonas aeruginosa* PA14 infection (Table 2) [375]. Besides, another investigation reported that pH is a significant factor in the toxicity of NPs as it is related to the dissolution and change in concentration of Zn²⁺ from 7.46×10^{-6} M at pH = 9 to 5.0×10^{-4} M at pH = 7 [376]. Likewise, the saltwater influence was also compared to deionized water, resulting in accelerated dissolution rates in seawater. Further, a study demonstrated that Dulbecco's modified Eagle's medium could dissolve 34 mg/L and, in contrast, for water, 7.18–7.40 mg/L of Zn [377]. This shows that the pH and ionic force of the medium affects Zn solubility. Moreover, it has been found that at greater temperatures and salinity, ZnO NPs formed larger aggregations and released less Zn²⁺; for example, the ZnO toxicity to *Thalassiosira pseudonana* was observed to be less toxic at 25 °C than at 10 °C [378]. Fig. 8 a and b shows that cell viability outcomes do not decrease at the concentration ranging from 0 and 0.1 mM of ZnO nanostructures [315].

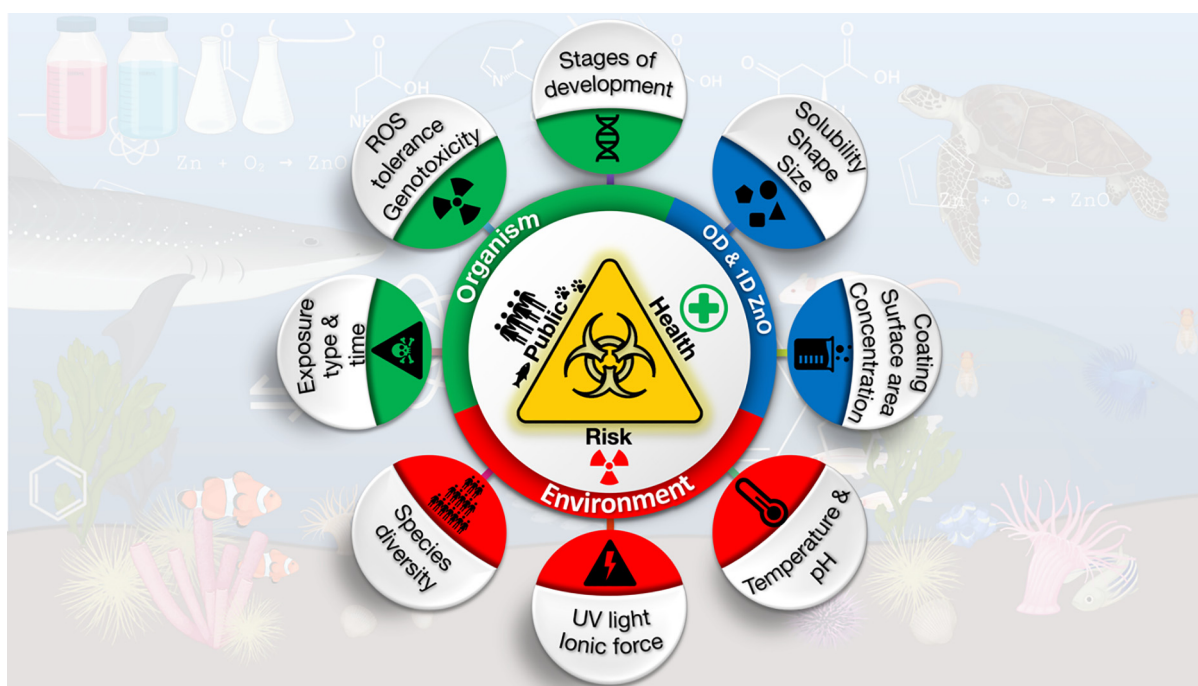
Acute toxicity hazards and risk minimization factors

The use of ZnO nanostructures in tissues has demonstrated practical applications aiming at biocompatibility or providing potentialized properties for oncology. Some examples are scaffolding to tissue, antimicrobial activity, cell growth, proliferation, differentiation, and wound healing applications. This comes from the development of new engineered nanostructures with a certain functional group and/or coating of the core–shell structures. The after-mentioned are obtained through biosynthesis methods [329,379,380]. New approaches of synthesizing ZnO nanostructures keeping in mind toxicity properties are called "safety by design" methods [329]. Using biopolymers like poly(ε-caprolactone) (PCL) has plenty of advantages, such as biocompatibility and biodegradability, when combined with ZnO for tissue-engineering applications [381]. They are already approved by the FDA and are used in clinical applications [177]. Gastrointestinal absorption could become the main point of entry for

ZnO NP in the future. The previous research mimicked the gastrointestinal route, demonstrating that ZnO NPs were slightly soluble (0.6 mg/mL) under acidic conditions. It was also noted that with phosphate ions, NP dissolution was less than 1% [382]. In this direction, ZnO distribution was examined after Intra-gastrointestinal administration, resulting in the liver and duodenum having the highest concentrations of ZnO NP, followed by the kidneys and the brain for last the lungs did not present ZnO NP. In contrast, Baek et al., found similar results except for the difference in disintegration-altering concentration in plasma [277]. In both studies, the NPs primary excretion from the body was via feces with a small urine discharge. In relation to the high concentration of ZnO NP in the liver, a study found damage to mice hepatocytes by reducing important vital factors such as kidney index and the degradation of the filtering functions [114].

Dermal exposure has been the most studied out of any tissue in the human body because of ZnO use in sun creams. As the EURO NANODERM project showed, ZnO NPs are considered safe for cutaneal application. Most studies showed no penetration of ZnO NP beyond the *stratum corneum* (SC) [305,383]. Even when there is damage to the skin, like burns caused by UV exposure [384] or if the skin is being occluded [385]. The ZnO NPs are not persistent in the skin and are almost entirely removed from the SC with tape and proper washing. A few challenges regarding keratinocytes and their decreased mitochondrial activity, loss of normal cell morphology, and cell-cycle distribution disturbances were exhibited [343]. Besides, a higher urinary 8-hydroxy-2-deoxyguanosine (8-OHdG) level with the application of nanocosmetics leading to ROS generation in the urine was also observed [386]. Some histological changes have been noted in different studies after a dose of 1000 mg/kg (ZnO NPs) for 90 days Fig. 8 (c and d) [387]. The use of ZnO nanostructures for wound dressing showed several promising potentials. Different optimized systems of ZnO and biopolymers result in antibacterial activity with reference to *Staphylococcus aureus* [388], *Escherichia coli* [218], *Pseudomonas aeruginosa*, and *Bacillus subtilis*. These developed systems exhibited remarkable antioxidant properties and faster healing of subcutaneous diabetes-induced rabbits [389]. The observed histological examinations revealed a greater cell adhesion, re-epithelialization, and collagen production by the ZnO-bio composite system [388]. It is observed that an Ag-ZnO NP nanocomposite in a gel form demonstrated wound healing ability in adult male Albino Wistar rats after ten days of administration [324].

Considering inhalation as a case, the respiratory tissue should be susceptible to exposure to ZnO NP. A detailed research demonstrated the exposure of different sizes of ZnO NPs (35 and 250 nm) [313]. Different concentrations, 2.4 to 45.2 mg / m³, terminated in increased lung inflammation and injury, increased white blood cell count in peripheral blood, and higher presence of 8-OHdG. In this direction, another research demonstrated that when human bronchoalveolar carcinoma-derived cells were exposed to ZnO, ROS species were created [284]. This resulted in intracellular oxidative stress, lipid peroxidation, cell membrane leakage, and oxidative DNA damage. Similar results were shown by Sahu et al., [390] with a different cell line, the human lung epithelial cell line (L132). Moreover, damage in

**FIGURE 7**

A correlation of public health issues of ZnO NPs. Environmental risks and benefits of ZnO nanostructures, public health concerns, Intrinsic properties of ZnO NP for toxicity, Effect of ZnO NPs toxicity on different organisms, properties of the environment on the ZnO cytotoxicity, and biocompatibility.

TABLE 2
Exposed species to different types of ZnO nanostructures and their relationship with toxicity.

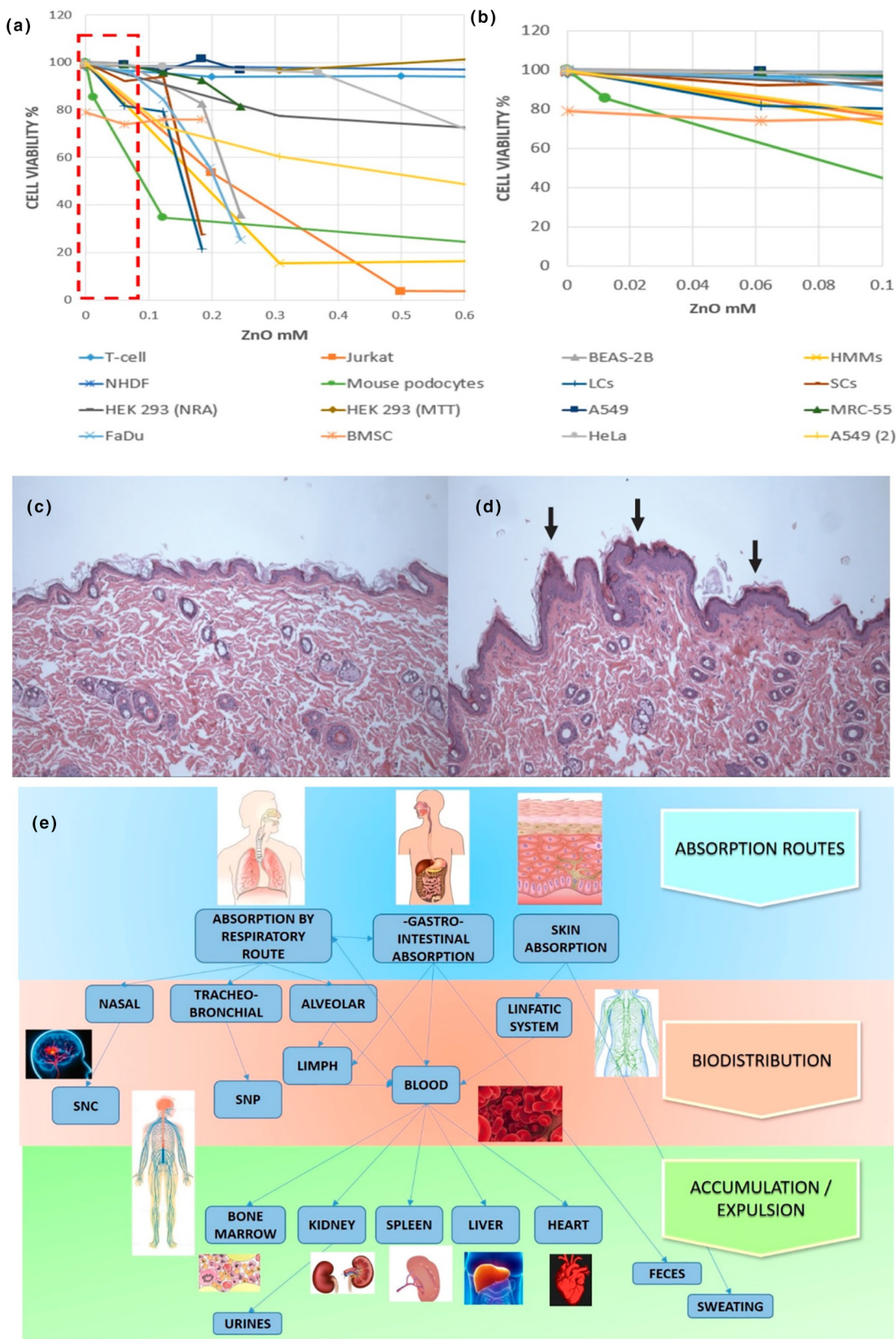
Species	Type	Concentration	ZnO Size	Toxicity Measurement	Result to Control	[Ref]
Caenorhabditis elegans	NP	0.32 mg/L	<25 nm	Percent Mortality	~ 60 %	[369]
Caenorhabditis elegans	NP	2 mg/L	<100 nm	Percent Mortality	~ 40 %	[369]
Scaphchinus mirabilis	NP	490 ± 6 µg/L	<50 nm	Fertilizing capacity of sperm	50 %	[370]
Scaphchinus mirabilis	NP	29 ± 4 µg/L	<50 nm	Fertilizing capacity of larvae	50 %	[370]
Scaphchinus mirabilis	Zn ²⁺	6526 ± 99 µg/L		Fertilizing capacity of sperm	50 %	[370]
Scaphchinus mirabilis	Zn ²⁺	67 ± 12 µg/L		Fertilizing capacity of larvae	50 %	[370]
Zea mays	NP	3200 mg/kg	90 ± 10 nm	Plant Height decreased	29%	[371]
Caenorhabditis elegans	NP	0.05 mg/L	~0.9 nm	Body bends	17 %	[372]
Drosophila melanogaster	NP	24 mM	106.55 ± 64.79 nm	%DNA in tail (Comet Assay)	18.39 + 1.49	[373]
Spinach oleracea	NP	1000 mg/L	<100 nm)	Reduction in total weight	27 %	[374]
Lolium perenne	NP	50 mg/L	19 ± 7 nm	Biomass	76 %	[316]
Lolium perenne	Zn ²⁺	50 mg/L		Biomass	68 %	[316]

the lungs due to ZnO NP interaction [114] has been reported, like inflammation, severe hyperemia in alveoli, and edema. In contrast, Morimoto et al., indicated that rats exposed to ZnO NP (35 nm) with different quantities such as 2 and 10 mg/m³ showed no persistent inflammation of the lung for four weeks, indicating less toxicity of well-dispersed ZnO NPs [391].

In a research performed by Liu et al., cytotoxicity of ZnO NP for SHSY5Y cells, with apoptosis and cytoskeleton changes was found [371]. Similar results were found in the same cell line with the addition of genotoxicity, including micronuclei production, H2AX phosphorylation, and DNA damage [269]. Besides, genotoxicity was also reported, and it is also noticed that NPs may cause a deficit in normal motor functions [392]. Histopathological investigations revealed significantly increased motor cortex nuclear size, probably resulting from neuroinflammation/neuronal damage [393]. The outcomes of hippocampal proteins-

based studies showed an increment in inflammatory markers, neurotoxicity was shown to cause long-term memory impairment and spatial cognition problems when excitable cells were exposed to ZnO NWs [394]. In contrast, ZnO NWs tested with PC12 cell line, suitable for neuronal cell modeling, concluded that a well-developed neurite network was formed when exposed under the right conditions. The same experiments contrasting results were shown for the H9C2 line used for muscle cell modeling, resulting in a negative differentiation of myotubes [395].

The toxicity of ZnO NP has been found on testicular mouse cells, where the apoptosis process is likely correlated with DNA damage caused by an increase in ROS and associated with loss of mitochondrial membrane. Besides, the injection of ZnO NPs in male mice caused structural alterations in the seminiferous epithelium and caused sperm abnormalities [294]. Equally, studies with human peripheral blood lymphocytes (HPBL) and NPs/

**FIGURE 8**

Study of ZnO NPs toxicity in organisms. (a) and (b) Summary of cell viability with different ZnO concentrations. Copyright 2019 MDPI [315]. Histopathological changes in the skin after treatment with ZnO NPs. (c) Control group and (d) 1,000 mg/kg group. Copyrights Dove Medical Press 2014 [387]. (e) ZnO nanostructures absorption, distribution, and accumulation or expulsion in the human body Copyright 2019 MDPI.

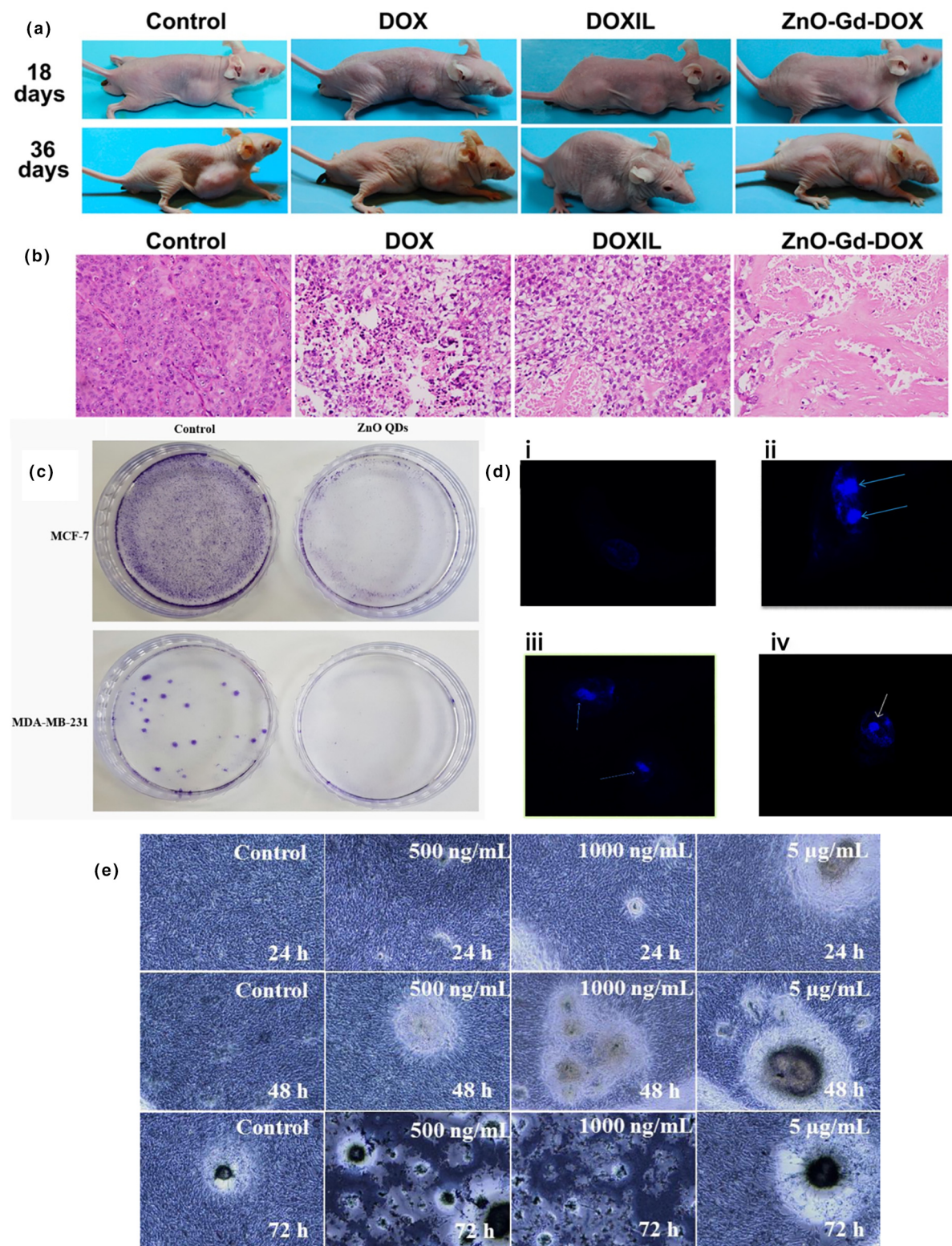
NRs showed the capacity of ROS generation [396] and displayed cytotoxicity as size and shape-dependent [306]. In another report, ZnO nanoflowers generation resulted in sufficient osteoblast growth with higher DNA content, ALP activity, and adhesion strength [395]. Similar results were found by Li et al., where ZnO/Poly(vinylidene fluoride) showed antimicrobial activity and increased osteoblast density on the piezo-excited scaffolds [397]. The ZnO nanostructures osteointegration processes and antibacterial properties make them promising materials in harsh applications as dental implants and materials [398]. Augustine et al., demonstrated that a highly branched capillary network of blood vessels is formed when a Poly (vinylidene fluoride-trifluoroethylene)/ ZnO nanocomposite tissue is being utilized in Windsor rats [177]. Also, the piezoelectric properties of the nanocomposite resulted in a better cellular response. A ZnO nanostructures interaction mechanisms with the organism (SNC: the central nervous system; SNP: the peripheral nervous system is shown in Fig. 8 (e) [315]. ZnO toxicity on the environment or organisms is case-specific and further needs a lot of investigation for its implementation in different sectors such as cancer theranostics.

Nano-enabled oncology therapeutics based on 0D and 1D ZnO nanostructures

Along with efficient bioimaging agent, ZnO nanostructures have been investigated for several other remarkable beneficial effects which can be useful for developing potential therapeutic. Significant antioxidant [399–403], anti-inflammatory [399,403–406], and antibacterial [400,402,407–415] activities in ZnO nanostructures have been studied, but their biomedical applications needed to be explored more. In this direction, ZnO nanomaterials have emerged as a potential nano platform to perform targeted drug delivery to develop nanomedicine of higher efficacy [404,416–419]. For example, ZnO-based nano-therapeutics has shown efficacy in treating diabetes and its complications [420–422]. Furthermore, the ZnO intrinsic anti-cancer, anti-tumor, and anti-angiogenic activities at the nanoscale have also been studied in detail [401,402,406,423–428], making it a big point of interest for the development of different cancer therapies. Moreover, there are various reports projecting ZnO nanostructures for cancer treatment. For example, Barick et al. developed mesoporous spherical ZnO nano-assemblies, and explored their potential use on doxorubicin release anthracycline, a widely used drug in chemotherapy [429]. In this direction, Yasser Selim et al., developed green chemistry-assisted ZnO NPs using *Deverra tortuosa* extract. The specificity of these NPs was studied *in vitro* using the appropriate cancer cell lines A549 and WI38 and the non-cancerous WI38 lung fibroblast cell line. As outcomes, this system exhibited specific and significant helpful cytotoxicity against cancer cell growth [430]. However, a common factor exploited to use ZnO NPs in cancer treatment is the associated environment with cancer cells, such as the acid pH [431–433] (which favors the Zn²⁺ ions release [434]) and the cellular membranes negative charge [435,436] (that promotes the interaction and capture of charged nanoparticles [437]), making more selective the possible application of ZnO NPs in the oncology area, as discussed earlier. For example, Fig. 9 (a, b) shows BxPC-3 tumor-

bearing after 18 and 36 days and H&E staining of tumor slices after 36 days under different treatments, respectively [434,438–440,20,441–443]. In both cases, Sn-Gf-DOX NPs achieved better results than other therapies [438]. Roshini et al., demonstrated that the ZnO quantum dots diminished the cell viability and inhibited the proliferation of MCF-7 and metastatic MDA-MB-231 breast cancer cells, Fig. 9 (c) [434]. Paino et al., analyzed the behavior of ZnO nanoflowers structures against L929 (normal) and HeLa (cancer) cells, observing certain selective cytotoxicity in HeLa cells; one route by which these nano-compounds exerted their toxic effect was via apoptosis, leading to the formation of condensed nuclei, as demonstrated in Fig. 9 (d) [439]. Wahab et al., utilized the ZnO NRs as possible anticancer agents, studying their cytotoxicity effects in C₂C₁₂ myoblast cancer cells, finding that their toxicity depend on the dose, exposure time, and the form of the ZnO NRs, decreasing the cell growth and viability, as shown in Fig. 9 (e) [440]. Additionally, it was observed that these nanostructures could alter the gene expression (caspases 3 and 7) and increase cell apoptosis [440].

Based on the previous reports on 0D nanostructures [213,416], the use of 1D ZnO nanostructures can be discreetly explored for oncological applications. The role of different ZnO-based nanostructures for potential cancer therapies is summarized in Table 3 [20,419,430,444–469]. Yuan et al., explored polyelectrolyte nanotubes to formulate a DDS where a charged array of ZnO NWs was utilized. Although this system does not use ZnO NWs directly, but it demonstrates ZnO useful for oncological treatments [470]. In this direction, the use of piezoelectricity with ZnO NWs and NRs is projected desirable, owing to recent applications of piezoelectric nanomaterials for developing stimulation responsive therapeutic approaches [471,472]. Such systems-based 1D ZnO nanostructures have been useful for cell differentiation, tissue regeneration, and wound healing [166,176]. Besides, ZnO NWs based gene delivery and cell transformation have been demonstrated earlier [473]. Even though this could be a cornerstone in developing new gene therapy technologies, more concrete evidence is needed for their clinical use. As shown in Fig. 10, Zhang et al., investigated a strategy of combined ZnO NRs with anti-cancer drug daunorubicin (DNR) in photodynamic therapy (PDT) in human hepatocarcinoma SMMC- 7721 cells. They have shown that ZnO NRs could increase the intracellular concentration of DNR and enhance its potential anti-tumor efficiency. Fig. 10 (a) depicts the cell treatment procedures, e.g., (a) SMMC-7721 cells were treated with free DNR; (b) ZnO NRs were loaded with DNR for the drug delivery system, and the corresponding fluorescence intensity curves are presented in Fig. 10 (b). The photodynamic activity of ZnO NRs also increased the cancer cell injury through ROS production, which is illustrated in Fig. 10 (c) [441]. Li et al., explored the bio-application of ZnO NPs in PDT, combining the nano ZnO with DNR as exhibited in Fig. 10 (d). Various optimized concentrations of ZnO NPs were administered into the DNR drug system [442], which decreased electrical impedance with respect to SMMC-7721 cells. Similarly, Li et al., demonstrated that the PDT process improves the cytotoxicity of ZnO NPs, Fig. 10 (e). Moreover, this activity was upgraded with the addition of DNR. Later, Wang et al., proved that ZnO NPs could be used as nanocarriers, synergizing the anticancer activity [443].

**FIGURE 9**

Therapeutic studies based on 0D and 1D ZnO nanostructures. (a) and (b) show images of BxPC-3 tumor-bearing after 18 and 36 days and H&E staining of tumor slices after 36 days under different treatments, respectively. In both cases, Sn-Gd-DOX NPs achieved better results than other therapies [438]. Copyright 2016 ACS Publication group. (c), ZnO QDs showed the diminishment in the cell viability and inhibited the proliferation of MCF-7 and metastatic MDA-MB-231 breast cancer cells [434]. Copyright 2017 Elsevier. (d) The behavior of ZnO nanoflowers against L929 (normal) and HeLa (cancer) cells, observing certain selective cytotoxicity in HeLa cells; one route by which these nano-compounds exerted their toxic effect was via apoptosis, leading to the formation of condensed nuclei, as observed in i-iv [439]. Copyright 2016 ACS. (e) ZnO NRs as possible anticancer agents and their cytotoxicity effects in C2C12 myoblast cancer cells, demonstrating that their toxicity depended on the dose, exposure time, and the form of the ZnO NRs, decreasing the cell growth and viability [440] Copyright 2020 Elsevier.

TABLE 3**List of recent advances in the creation of ZnO-based nanostructures for the development of potential cancer therapies.**

Potential Therapy	ZnO-based Nanostructure	[Ref]
Tumor targeting & drug delivery approaches	Chitosan/ZnO NPs Polyglycerol-grafted, RGD peptide-conjugated ZnO NPs ZnO NPs loaded via a mesoporous silica nanolayer and coated onto gold nanostars ZnO nanocrystals inside extracellular vesicles ZnO/Quercetin nanocomposite ZnO-doped graphene oxide nanocomposite Human serum albumin/ZnO NPs Lipid-coated ZnO NPs Folate & PEG ZnO NPs Iron oxide/ZnO NPs Folic acid-modified ZnO nanosheet Berberine/ZnO NPs Lipid-coated ZnO NPs YAG:Pr / ZnO/Protoporphyrin nanocomposite Yb/Tm/ZnO semiconductor NPs Upconversion NPs/Mesoporous silica/ZnO nanodots nanostructure Au nanorod core/ZnO shell NPs Zn/ZnO NPs conjugated with chlorine e6 Ternary modified ZnO nanocomposite Fe ₃ O ₄ core/ZnO shell NPs ZnO NPs with polyinosinic-cytidilic acid RNA complexes Mesoporous silica/ZnO doped nanospheres Radially grown ZnO NWs on poly-L-lactide microfibers	[463] [419] [464] [465] [466] [467] [468] [469] [444] [445] [446] [447] [448] [449] [450] [451] [452] [453] [454] [20] [461] [20] [455] [430] [456] [457] [458] [459] [460] [462]
Phototherapeutic approaches	ZnO/Protoporphyrin nanocomposite Yb/Tm/ZnO semiconductor NPs Upconversion NPs/Mesoporous silica/ZnO nanodots nanostructure Au nanorod core/ZnO shell NPs Zn/ZnO NPs conjugated with chlorine e6 Ternary modified ZnO nanocomposite Fe ₃ O ₄ core/ZnO shell NPs ZnO NPs with polyinosinic-cytidilic acid RNA complexes Mesoporous silica/ZnO doped nanospheres Radially grown ZnO NWs on poly-L-lactide microfibers	[450] [451] [452] [453] [454] [20] [461] [20] [455]
Immunotherapeutic approaches	ZnO NPs from Deverra tortuosa extract ZnO NPs from Capparis zeylanica extract ZnO NPs from Rheum rhabonticum waste ZnO NPs from Pandanus odorifer extract ZnO NPs from Carob extract ZnO NPs from Anabaena cylindrica extract ZnO NPs from Mussaenda frondosa extract	[430] [456] [457] [458] [459] [460] [462]
Green synthesis approaches	ZnO NPs from Deverra tortuosa extract ZnO NPs from Capparis zeylanica extract ZnO NPs from Rheum rhabonticum waste ZnO NPs from Pandanus odorifer extract ZnO NPs from Carob extract ZnO NPs from Anabaena cylindrica extract ZnO NPs from Mussaenda frondosa extract	[430] [456] [457] [458] [459] [460] [462]

Furthermore, these NPs could target cancer cells, macrophages, and cancer stem cells, aiming, therefore, both cancer cells and their tumor microenvironment (see Fig. 10 f).

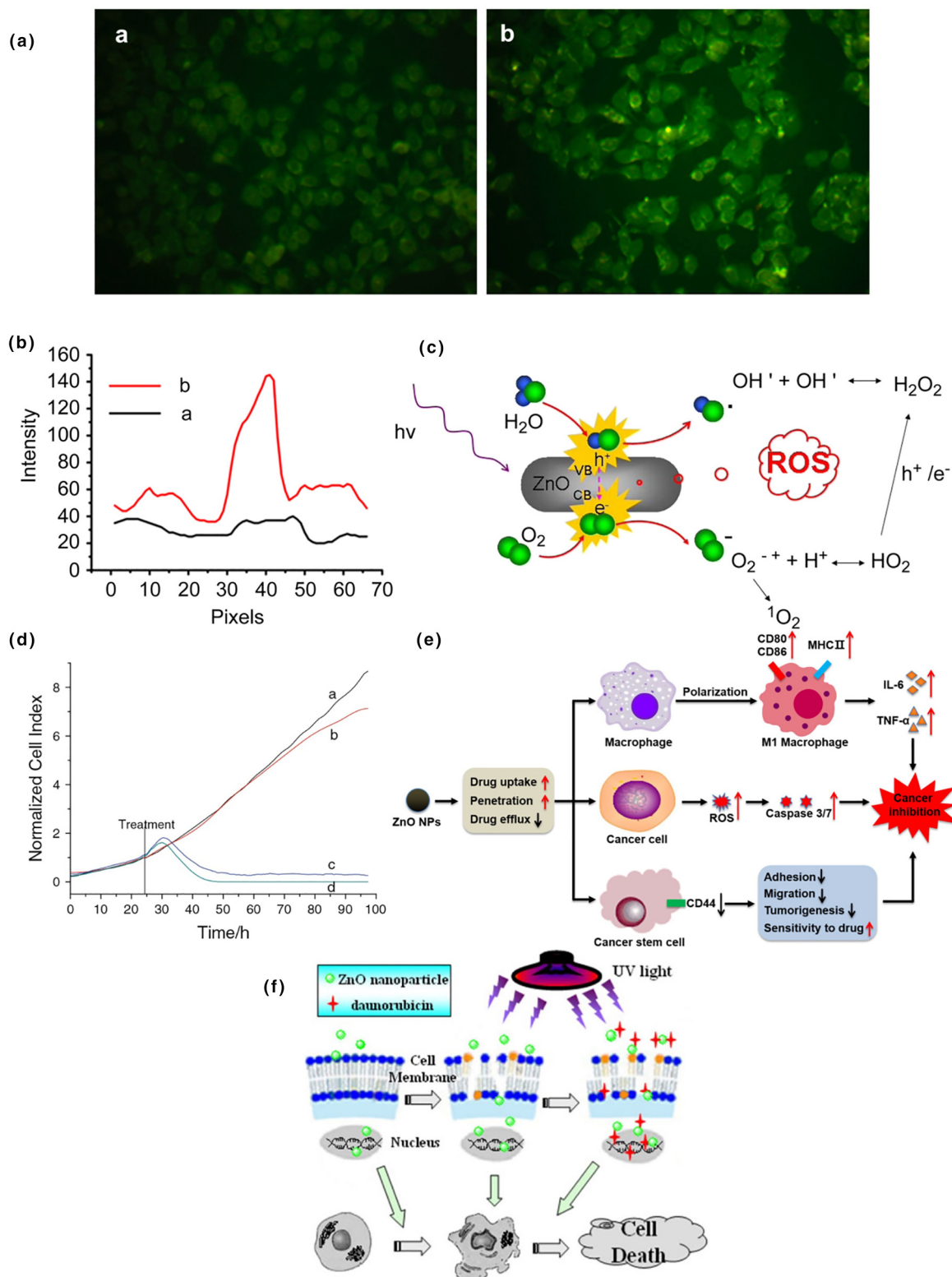
Nano-enabled ZnO nanowires-based cancer diagnosis and monitoring

The unique properties found in the 1D nanomaterials project them superior for various applications due to their flexibility to create an interesting myriad of sensors and molecular systems useful for disease diagnostic, monitoring, and efficacy assessment [474–481]. Their typical surface-to-volume and aspect ratios are useful to improve specific optical, electrocatalytic, and electronic properties. These properties can be tuned and controlled in the interfacial interactions with cells, potential biomarkers, and other range of relevant biomolecules [482,483]. In this direction, 1D nanosystems have been employed to investigate the possible adoption of a targeted diagnostics application [474–481]. Gao et al., projected the potential of silicon NWs for transistor-based biosensors applied to point-of-care cancer diagnostics applications. In this work, Si NWs supported tunneling field-effect transistors detected CYFRA 21-1 (a specific tumor marker in primary lung cancer) at a low concentration as 0.5 fg/mL [484]. These outcomes proposed silicon-based 1D materials in cancer diagnosis, allowing the creation of other array systems capable of multiplex detection of tumor biomarkers [485,486].

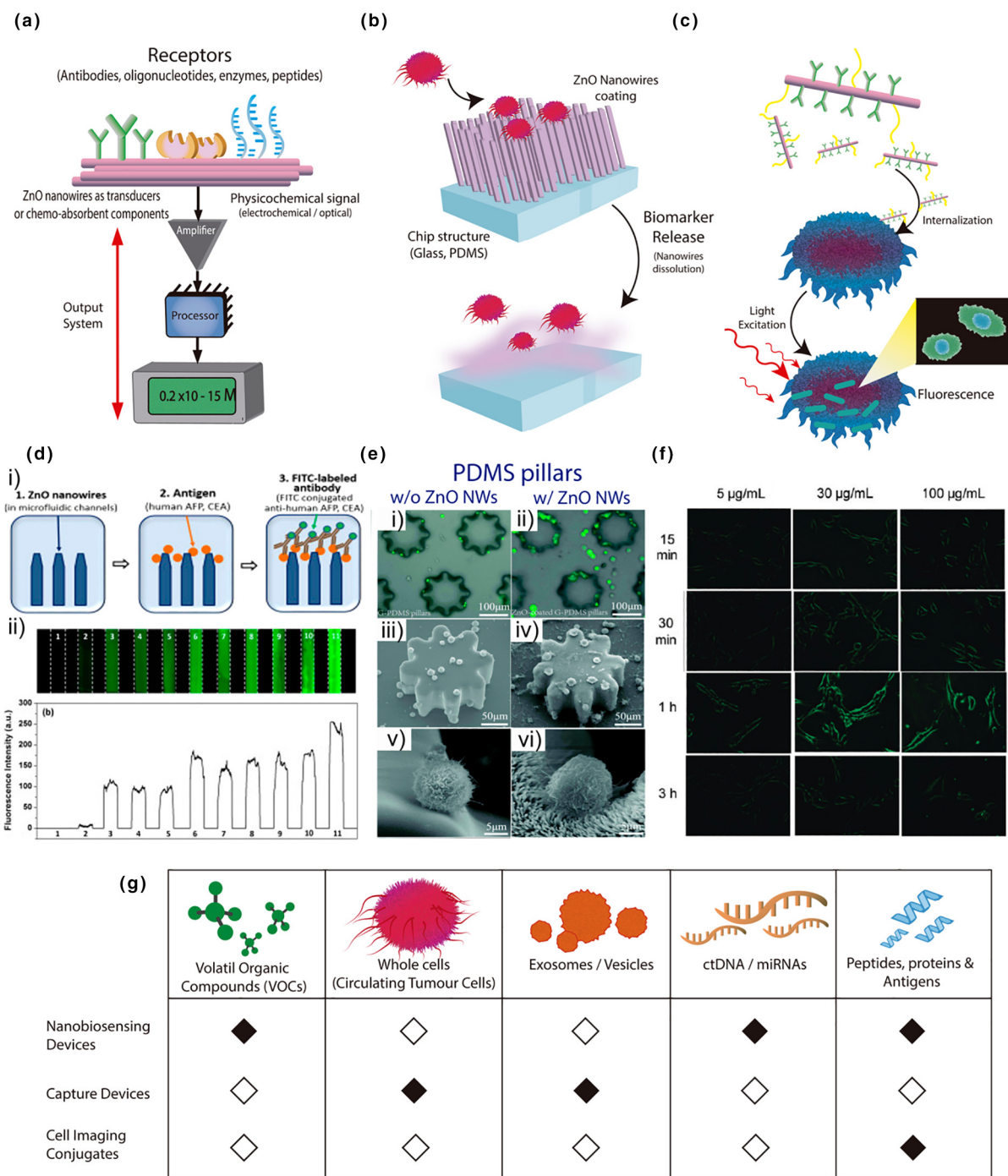
To be on the same track, the application of 1D ZnO NWs for cancer diagnosis has been investigated, although *in vitro* approaches. These analytical diagnostics can be categorised according to their functional nature, such as nano-enabled biosensing devices (Fig. 11 a- if they convert an analyte interaction into quantifiable signals), capture devices (Fig. 11 b- if its function mainly lies in extracting and/or isolating cellular elements), or cell-imaging complexes (Fig. 11). These systems have detected a wide range of biomarkers such as proteins, nucleic acids, organic compounds, exosomes, and whole cells that have been successfully detected, extracted, or imaged with highly critical analytical parameters [72,309,487].

Relationship between the aspect ratio and toxicity

In contrast to their 0D counterparts, it is expected that the intrinsic morphology of 1D nanomaterials would play a considerably different role to produce toxicity. Thus, it is crucial to know in detail about the fate of any nanomaterial in the body, including its participation in the molecular mechanisms that might trigger post-injection/administration toxicity as a function of time. Since cellular uptake mechanisms such as phagocytosis, pinocytosis, and endocytosis are affected by the morphology and surface properties (charge, pH responsiveness, and alternation in properties on external stimulation) of the nanomaterial. It is a point of concern that nanostructures with very high aspect ratios

**FIGURE 10**

Interaction of ZnO NWs with drug daunorubicin (DNR) and their toxicity effect. (a) A strategy of combined ZnO NRs with anti-cancer drug daunorubicin (DNR) in photodynamic therapy (PDT) in human hepatocarcinoma SMMC-7721 cells is shown. In inset (i) SMMC-7721 cells were treated with free DNR; (ii) ZnO NRs were loaded with DNR for the drug delivery system to enhance its anti-tumor efficiency. (b) Fluorescence intensity curves corresponding to samples represented earlier in this figure. (c) Proposed mechanism for the photodynamic activity of ZnO NRs to increase cancer cell injury through the production of ROS [441]. Copyright 2011 Elsevier. (d) Bio-application of ZnO NPs in PDT, combining the nano ZnO with DNR. ZnO NPs with different concentrations were injected into the DNR drug system, and the electrode impedance is observed to decrease in SMMC-7721 cells apparently; (i) negative control ZnO NP-free; (ii) DNR; (iii) 2.5 µg/mL of ZnO NPs and DNR and (iv) 5 µg/mL of ZnO NPs and DNR. (e) PDT process improved the cytotoxicity of ZnO NPs. Moreover, this activity was upgraded with the addition of DNR [442]. Copyright 2010 Springer Open. (f) Role of ZnO NPs as nanocarriers showing a synergistic effect in the anticancer activity targeting both cancer cells and their tumor microenvironment [443]. Copyright 2017 ACS.

**FIGURE 11**

ZnO NWs applications for cancer diagnosis and monitoring. (a) General design of a ZnO-based nanobiosensor. (b) General concept of capture devices based on the dissolution of NWs for the release of biomarkers. (c) Macromolecular conjugates for the specific visualization of cancer cells and tissues. (d) ZnO-based microfluidic immunoassay. Schematic diagram of the antigen-antibody interaction in the ZnO NW array inside de PDMS microfluidic channels (i). Enhanced fluorescent signals linearly correlated to antigen concentration, achieving LODs up to 100 fg/mL for certain cancer biomarkers (ii) Copyright 2018 Elsevier [487]. (e) SEM micrographs of Gear-shaped PDMS pillar capturing microchip without (i, iii, v) and with (ii, iv, vi) ZnO NW coating at different magnifications. Micrograph of single CTC is attached to the pillar (v & vi) Copyright 2020 Royal Society of Chemistry [309]. (f) Serial fluorescence imaging of integrin Rvβ3 on U87MG human glioblastoma cell lines, using diverse concentrations of PEGylated and RGD peptide-conjugated NWs Copyright 2011 American Chemistry Society [72]. (g) Field of application for ZnO NWs of the different types of devices, based on the biomarkers that have been able to detect/capture/target in the literature.

may express difficulties while internalizing within cells. In this scenario, the role of ZnO nanostructures could be estimated *a priori* as higher cytotoxicity for smaller aspect ratios due to the

greater ease for cell uptake and their mechanisms. Theodorou et al., showed in their experiments that ZnO NWs pre-incubated with pulmonary surfactant increased their toxicity

when cell uptake was also increased, indicating a dependence on internalization [488]. Similarly, Müller et al., presented a similar statement about the dependence of high aspect ratio of ZnO NWs in internalization and the macrophage lysosomal in high acidic pH conditions [285]. Shukla et al., performed testing tobacco mosaic virus nano-assemblies and hydroxylated-multi walled carbon nanotubes, respectively, finding nanostructures with lower aspect ratios had higher levels of permeabilization and cytotoxicity [489,490]. On the contrary, Adili et al., exhibited considerably opposite results testing Si and Ni NWs, respectively, after being compared against NP and salt presentations [491,492]. However, these findings are not enough to claim whether a specific aspect ratio-dependent mechanism plays a role or not in terms of the proportional aspect ratio/toxicity relationship. Nonetheless, there may be anatomical and physiological *in vivo* cases where the accumulation of high aspect ratio nanostructures would be associated with higher toxicity levels, with a few cases in the literature illustrating the latter for long aspect ratio materials [493,494]. For instance, the endothelial or epithelial barriers with acidic microenvironments (e.g., the lung lining fluids) may promote the extracellular accumulation and dissolution of ZnO nanostructures, yielding the liberation of high amounts of Zn²⁺ and causing consequent tissue and organic damage. Ultimately, comprehensive knowledge about the morphology and biological interfaces needs to be explored with reference to 1D ZnO applications. In this direction, biocompatible and potentially non-toxic diagnostic and therapeutic systems could be engineered for various biomedical applications.

Nano-enabled biosensing prototypes

Biosensors are analytical devices composed of a recognition surface with biological receptors (antibodies, oligonucleotides, among others), a transducer that converts the interaction into measurable signals, and an output system that amplifies and converts the signals obtained into readable data [495–497]. The introduction of nanostructures in fabricating a biosensing prototype is known to improve analytical performance parameters such as detection at the single-molecule level [498–500]. The primary role of nano-enabled biosensors in cancer is to detect and quantify specific biomarkers of clinical interest for rapid and effective diagnosis [499,501,502]. Niepelt et al., reported ZnO NWs and organic species biofunctionalization via a covalent bond on their surface, taking advantage of the negative charge of DNA molecules for their working as an efficient biosensor [503].

For prostate-specific antigen (PSA) detection, an immunoassay was performed using PSA-specific antibodies immobilized onto Au NPs where an LSPR signal was recorded as a function of PSA concentrations. This sensor exhibited a LOD of 0.51 pg/mL for PSA and showed sensitivity compared to other similar optical nanodevices reported earlier [165,504–507]. Guo, L. et al., developed a fluorescent-based nano biosensing chip where ZnO NW are grown inside a microfluidic channel. Authors claimed to detect various biomarkers related to early-stage cancer stages (such as α -fetoprotein and carcinoembryonic antigen) through an ultra-sensitive detection system. This chips backbone consists of a polydimethylsiloxane (PDMS) structure with microfluidic channels built through soft lithography. Analogous to an ELISA

assay, the PBS and bovine serum albumin (BSA) solutions were utilized, and a solution with FITC-conjugated antibodies was infused and allowed to incubate, Fig. 11 d(i). Ultimately, fluorescent signals were recorded using fluorescence microscopy and latterly quantified, Fig. 11 d (ii). A LOD was standardized as low as 1 pg/mL for the human α -fetoprotein and as low as 100 fg/mL for carcinoembryonic antigen [487]. Other nanobiosensing approaches utilizing ZnO NWs are summarized in Table 4 [72,85,165,309,487,503,508–513].

Capture devices

Capture devices can be described as biomarker collection or isolation systems with research or diagnostic value (the majority working through microfluidics) [514–516]. In contrast to nano-enabled biosensors, these devices generally do not have a transducing mechanism or signal output systems. Detection and quantification of analytes are usually carried out with external equipment to the capture system. Additionally, the capturing efficiency stands out as the most crucial analytical parameter compared to the LOD of nano-enabled biosensors [515–517]. Moreover, these systems are usually designed to separate more abundant biological elements such as whole cells or exosomes. The use of NWs has allowed the creation of an exciting series of chips, which do not necessarily require a microfluidics architecture for effective separation. Even though the scientific literature describes Lab-on-a-Chips that can both actively capture and detect specific biological elements. However, a state-of-the-art Takao Yasui et al., developed a ZnO NW-array system for the separation of extracellular vesicles with valuable miRNAs from cancer patients. The engineered capture device proved to exhibit a higher efficiency for *in situ* extraction of urine extracellular vesicles than ultracentrifugation, which is the most adopted technique for this purpose. This work offered an avenue for determining the markers linked with non-urologic cancers, although further trials are needed [508].

Similarly, a 3D PDMS chip covered with free-standing ZnO NWs to capture exosomes was shown in Fig. 11 (e, f). The porous 3D structure was manufactured according to previous work methodology, in which they used a Ni foam slide that served as a scaffold for the PDMS [518]. The coated scaffold was integrated into a microfluidic chip using the sacrificing template method to obtain the complete ZnO-chip device. Then, a biotin-labeled mouse anti-human CD63 monoclonal antibody was introduced into the chip. For the analysis of exomes, serum or plasma was pumped into the device and then detected by a colorimetric ELISA. The method showed reliable results in analyzing exosomes in plasma and demonstrated a compelling methodology to effectively capture, detect, and recover exosomes from clinical samples [512].

Furthermore, Katwal, G. et al., reported a ZnO NT-NW hybrid structure capable of detecting volatile organic compounds (VOCs) related to breast cancer, using the chemo receptivity of these structures Fig. 11(g) [85]. The structures showed chemo receptivity to 4 different VOCs previously related in the literature as potential cancer biomarkers: 2-propanol, heptanal, 1-phenylethanone, and isopropyl myristate (IPM). A response from the chemoreceptor hybrid structure was found at a concentration

TABLE 4

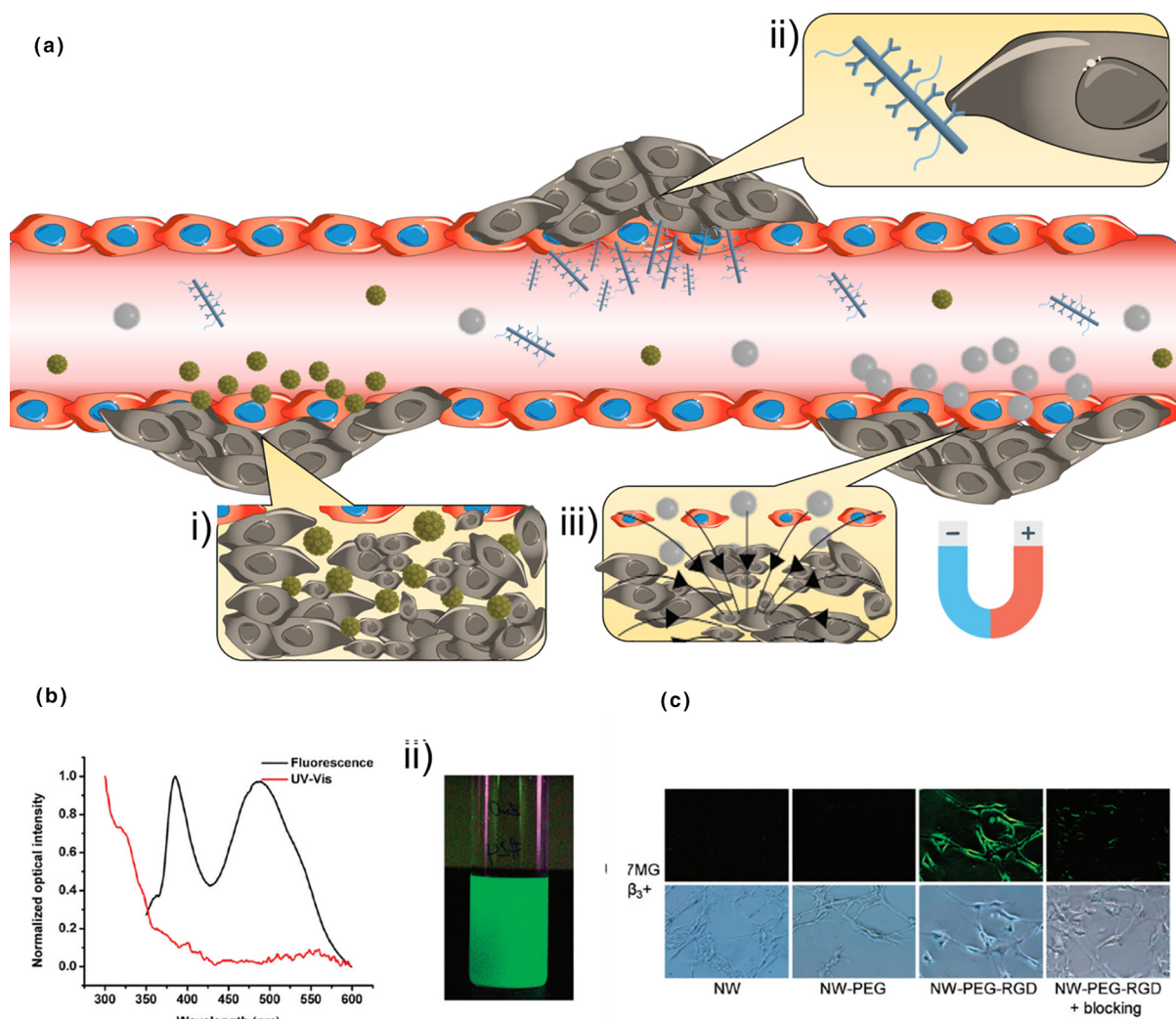
ZnO nanowires applications for cancer diagnosis and monitoring.

Archetype	Presentation	Fundament of Detection	Cancer/ Cell Line Type	Analyte	Synthesis Method	LOD*/Capturing Efficiency**	Used in clinical samples	[Ref]
ZnO NWs with covalently functionalized DNA	Nanobiosensing device	Electrochemical	Not specified	DNA oligonucleotides	Vapor phase synthesis	Not specified	No	[503]
ZnO NWs with EGFR antibodies/TiO ₂ NWs with vimentin antibodies nanocomposite	Cell-imaging	Optical/Fluorescence	Squamous cell carcinoma	Epidermal growth factor	Hydrothermal synthesis	3840 cells/cm ² (in cell count plate) *	No	[510]
ZnO NW-PEG-RGD peptide conjugate	Cell-imaging	Optical/Fluorescent	Theorized for solid tumors (Melanoma, late-stage Glioblastoma, Breast, Prostate, & Ovarian Cancers), Studied with U87MG & MCF-7 cell lines	Integrin \propto v β 3	Vapor phase synthesis	Not specified	No	[72]
ZnO NWs array chip	Nanobiosensing device	Electrochemical	Breast Cancer	Heptanal, Acetophenone, Isopropyl Myristate & 2-Propanol	Electrochemical Synthesis	8.982 ppm (Heptanal)* 798 ppb (Acetophenone) * 134 ppm (Myristate) * 29.5 ppm (2-Propanol) *	No	[511]
PDMS-ZnO NW porous chip with exome-specific antibodies	Capturing device	Optical/ Spectrophotometry (By UV-vis spectrometry after extraction)	MCF-7 Breast cancer Cells	Exosomes (possible cancer miRNA carriers)	Hydrothermal synthesis	2.2 \times 104 particles/ μ L*	Yes	[512]
microfluidic device with ZnO NWs in the channels	Nanobiosensing device	Optical/Fluorescence	Theorized for different cancer types. Studied in cancer biomarkers.	Human α -Fetoprotein & Carcinoembryonic antigen	Hydrothermal synthesis	1 pg/mL* (human α -Fetoprotein) 100 fg/mL* (carcinoembryonic antigen)	No	[487]
3D Optical fiber device with a ZnO NW/Au NPs composite	Nanobiosensing device	Optical /LSPR	Prostate cancer	Prostate-specific antigen	Hydrothermal synthesis	0.51 pg/mL*	No	[165]
MWCNTs/ZnO nanofiber biosensor platform	Nanobiosensing device	Electrochemical	Ovarian cancer	Carcinoma Antigen-125	Electrospinning	0.00113 U/mL*	No	[513]

(continued on next page)

TABLE 4 (CONTINUED)

Archetype	Presentation	Fundament of Detection	Cancer/ Cell Line Type	Analyte	Synthesis Method	LOD*/Capturing Efficiency**	Used in clinical samples	[Ref]
NW-embedded PDMS substrate device	Capturing device	Optical/Fluorescence (By fluorometer after extraction)	Lung, Pancreas, Liver, Bladder, & Prostate Cancers	Extracellular vesicle microRNA from urine samples	Electrochemical synthesis	0.194 ng/µL**	Yes	[508]
ZnO NW FET	Nanobiosensing device	Electrochemical	Theorized for different cancer types. Studied in regularly used molecular linkers.	Biotin-Streptavidin Binding System	Vapor Phase Synthesis	< 2.5 nM*	No	[509]
ZnO NW-coated PDMS chip	Capturing device	Optical/Fluorescence (By flow cytometry after extraction)	MCF7 Breast Cancer & SW480 Colorectal Cell lines. Circulating tumor cells.	EpCAM positive Circulating tumor cells	Hydrothermal synthesis	≥ 93.9% of total cells (for EpCam positive cells only)**	Yes	[309]
ZnO NWs – ZnO nanotubes array sensor	Nanobiosensing device	Electrochemical	Breast cancer	Heptanal, Acetophenone, Isopropyl Myristate & 2-Propanol	Electrochemical Synthesis	100 ppm (2-Propanol, Heptanal & Acetophenone)* 100 parts per billion (Isopropyl Myristate)*	No	[85]

**FIGURE 12**

Targeting mechanisms for imaging and drug delivery of nanomaterials. (a) Passive targeting of cancer cells, owing to the enhanced permeability and retention effect. NPs are diffused into the tumor tissue due to their ease of concentration in the fenestrae (i). Active targeting is aided by using a ligand, such as an antibody or aptamer (ii and iii). External magnetic fields aid magnetic targeting to enhance ferromagnetic and superparamagnetic nanoparticle accumulation into the tumor [529]. (b) UV–Vis absorbance & fluorescence spectra of ZnO NWs in solution (i). ZnO NW fluorescence in ethanol, under UV excitation (ii). Copyright 2011 American Chemistry Society. (c) Fluorescence imaging of integrin α v β 3 positive cells (U87MG glioblastoma cell line) with ZnO NWs, PEGylated-ZnO NWs, Arginine-Glycine-Aspartate-conjugated PEG-ZnO NWs & RGD-PEG-ZnO NWs + c(RGDyK) “blocking” α v β 3 integrin inhibitor. (B–c) Copyright 2011 American Chemistry Society [72].

of 100 parts per billion in the case of the IPM and 100 parts per million for the other substances [85].

Cui et al., created a valuable and low-cost chip for circulating tumor cells (CTCs) detection, with high capturing and releasing yields. The pillars were enriched with ZnO NWs on their surface via a hydrothermal reaction to improve cancer cell adhesion by providing a rough surface. Subsequent addition of anti-EpCAM antibodies for EpCAM positive cancer cells was realized to enhance the capturing yield of cancer cells in the structure. Three different cancer cell lines and peripheral blood samples of clinical breast cancer patients were used for testing. The ZnO coated chip showed a capturing efficiency above 75% at different concentrations of spiked cells and healthy blood, showing notable linearity between the spiked and the captured cells. Moreover, the ZnO NWs degradation via the use of sodium citrate showed release efficiencies above 90%. Finally, the microchip demon-

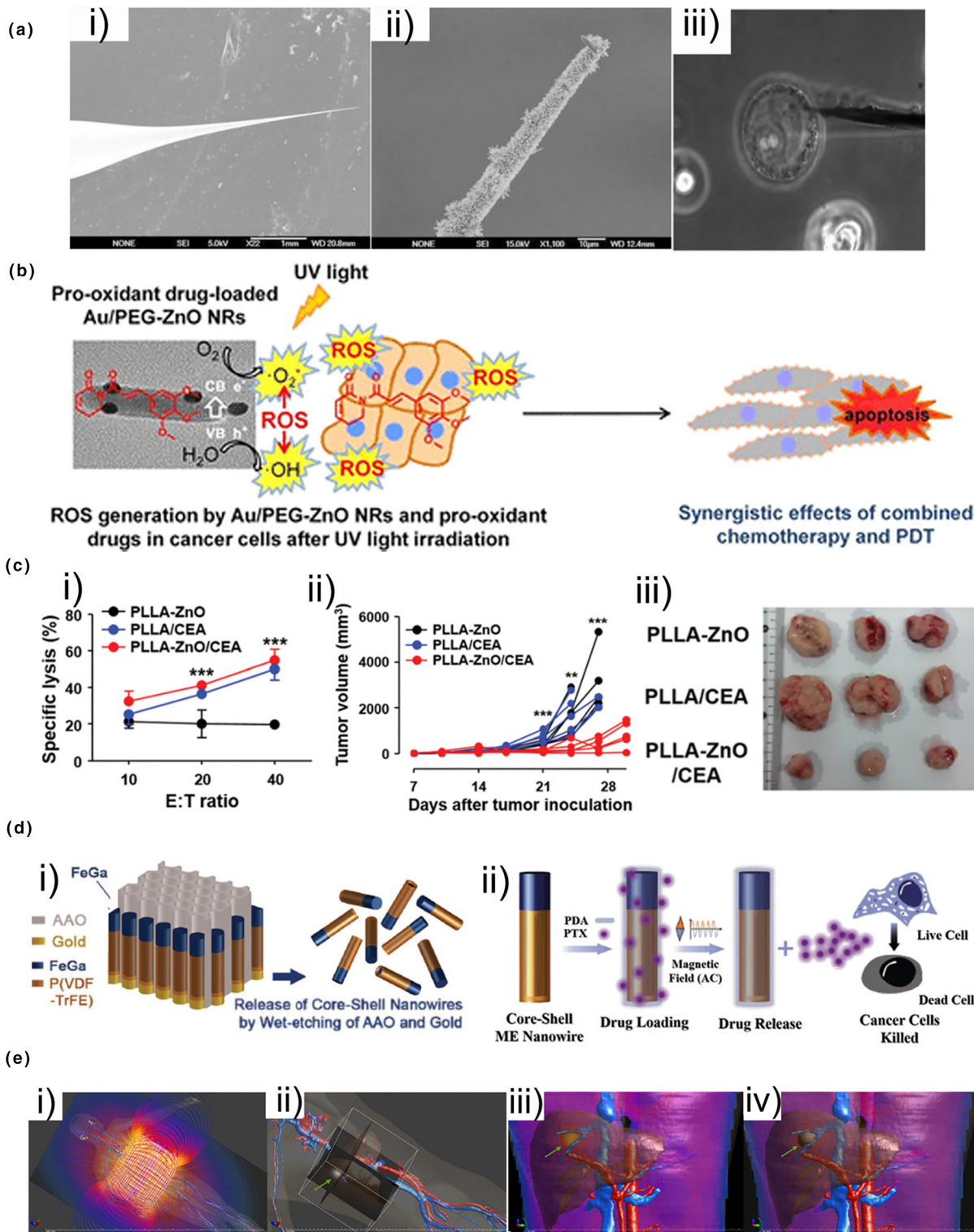
strated a potential utility in detecting and quantifying CTCs in clinical patients [309].

Cell imaging molecular systems

Cell imaging nanoconjugates are macromolecular complexes used to visualize certain types of cells or tissues. For this type of device, the fluorescence and photoluminescence of both the nanostructures and integrated fluorophores play a significant role in cell and tissue imaging. These systems stand out due to their potential to be used both *in vitro* and *in vivo*. They may play a fundamental role in the diagnostics of tumors *in situ* and theragnostic applications [519–528]. The targeting process of the molecular nanoconjugates can either be passive (where the irregular fenestrae of the tumor tissue favors the extravasation of some nanometric complexes) or active (added to the EPR effect, a recognition element such as an antibody or aptamer is added

to the nanoconjugate [529], Fig. 12 (a). An example of this kind of system is the work of Viter et al., who integrated a conjugate of photoluminescent NRs and anti-SSEA-4 monoclonal antibodies to detect cancer cells with the expression of this carbohydrate antigen. ZnO NRs were bound to anti-SSEA-4 and IgG3 antibody and were tested on HeLa cell lines and in both patient-derived primary carcinoma and healthy, skin-derived samples. The nanoconjugate demonstrated a higher binding selectively and photoluminescent signal for CRC1 and BC1, the former being a primary colorectal cancer cell sample and the latter a prior

ies and were tested on HeLa cell lines and in both patient-derived primary carcinoma and healthy, skin-derived samples. The nanoconjugate demonstrated a higher binding selectively and photoluminescent signal for CRC1 and BC1, the former being a primary colorectal cancer cell sample and the latter a prior



breast cancer cell sample. The detection limit of this photoluminescent system was set as 20% plus the baseline signal (constituted by the ZnO NR-IgG3 isotype control system) [530].

Similarly, Yang et al., proposed another system composed of ZnO NRs and anti-epidermal growth factor receptor (EGFR) antibodies to detect squamous cell carcinoma (SCC) as an alternative to fluorescence-based systems. EGFR antibodies were bound to the NRs to compile the light-emitting nanoprobes and were consequently tested in SCC due to their high EGFR expression. In this research, the photoluminescence spectrum of SCC cells treated with ZnO/EGFR nanoprobes showed a strong emission at 377 nm [221]. Hao Hong et al., used functionalized ZnO NWs with an arginine-glycine-aspartic acid (RGD) peptide for the optical imaging of positive cells to integrin α V β 3. For the functionalization of the ZnO NWs, the structures were suspended in ethanol and eventually suspended in dichloromethane, Fig. 12 (b). The complete molecular conjugate was tested on the U87MG (integrin α V β 3 positive) and the MCF-7 (integrin α V β 3 negative) cell lines, finding a specific fluorescent response to cells that express the integrin, Fig. 12 (c). Finally, the team conducted a pilot study with Balb/c mice strain, using a 64 Cu-labeled nanowire-PEG-DOTA conjugate and PET imaging to study the biodistribution of the macromolecular structure *in vivo*; finding most of the concentration in the liver [72]. A further approach is presented by Wei-Jen Li and collaborators, who developed a dichromatic probe based on ZnO and TiO₂ NWs. Both NW structures were synthesized using hydrothermal methods, generating systems with micrometric lengths and diameters between 50 and 100 nm. For the specific detection of cancer cells, the ZnO NWs were functionalized with EGFR antibodies, in contrast with TiO₂ NWs that were treated with Vimentin antibodies. In this research, the utilized squamous cell carcinoma is expressed with EGFR high expression, and Hs68 fibroblast cells are expressed with Vimentin expression. The LOD of cells in the surface for the ZnO/EGFR complex was 3840/cm² of SCC and 3800/cm² in the case TiO/Vimentin internalized in Hs68 cells [72,510,529].

Given their versatility and inherent properties such as intrinsic fluorescence, high surface area, and pH-dependent solubility, ZnO NWs are starting to create a noticeable niche within the field of diagnosis and monitoring, with a relatively extended field of application among different types of biomarkers. This versatil-

ity has allowed them to diversify their uses to create different kinds of devices, nanocomposites, and molecular complexes with a surfeit of applications. Regarding its use in fabricating biosensors, ZnO NWs have demonstrated a very significant role, for example, the desired LOD useful for early diagnostics. The ZnO NWs have also been useful as substrates for collecting cells and vesicular particles from biological matrices, with considerable capturing capacities. Therefore, its use in maintaining cellular elements for biomedical practices could provide relevant progress in the future. Lastly, despite the natural limitations of NWs internalization due to their selective cytotoxicity, a few signs of improvement have been made in creating molecular imaging systems. This opens the possibility for future technologies with embedded NWs that could detect *in vivo* tumors.

Phototherapies

The 1D ZnO nanostructures for developing potential cancer therapies are recent ongoing investigations. Considerable progress is arranged as latent phototherapies, immunotherapies, and a collection of other promising frontiers yet to explore. Considering the capability of ZnO NWs as efficient optical materials, it sets the stage for developing specific oncological treatments in synergy with their structural and chemical properties. Kishwar et al., studied the potential use of ZnO NRs to develop photodynamic therapy against skin cancer. In this work, the growth of ZnO NRs was performed in borosilicate capillaries with sub-micrometric diameters, and those were subsequently loaded with protoporphyrin dimethyl ester as a photosensitizer. Single breast cancer cells from the T-47D cell line were penetrated with the tip, and cell necrosis was witnessed in those after light exposure [531], Fig. 13 (a). A second PDT approach is set up by Hong et al., who created a PEGylated Au/ZnO hybrid nanosystem complexed with piperlongumine to generate a cancer-specific, chemo-photodynamic therapy. The nanostructure proved efficient in developing ROS upon UV radiation in MCF-7 human breast cancer cells, in contrast with PEGylated ZnO NRs alone. This nanosystem can achieve a primarily toxic-specific effect on cancer cells associated with the specific anti-cancer properties of piperlongumine [532], Fig. 13 (b). Similarly, Firdous et al., reported the possible use of ZnO NRs as photosensitizers in HeLa cells after observing them in the carcinogenic line through the

FIGURE 13

Approaches of ZnO NWs uses for potential cancer treatments. (a) SEM micrographs of a borosilicate glass capillary with a 0.5 μ m tip (i) ZnO NWs growing in the sub-micrometer tip at different magnifications (ii and iii). Copyright 2010 Springer Nature [531]. (b) Schematic of a combined chemo-photodynamic cancer therapy proposal, using piperlongumine-loaded, PEGylated Au/ZnO nanorods. Reactive oxygen species are generated by UV light irradiation of the hybrid nanostructure, and piperlongumine triggers apoptosis in cancer cells. Copyright 2019 American Chemistry Society [532]. (c) Cytotoxic T lymphocyte activity (CTL) of splenocytes harvested from immunized mice after 2 weeks of a second vaccination, using crystal violet absorbance assay. CTL was generated by stimulating splenocytes with purified Carcinoembryonic antigen (CEA) for 16 h, followed by incubation with MC38/CEA cells. Measurements for poly-L-lactic acid (PLLA)/ZnO NWs, PLLA/CEA, and PLLA/ZnO NWs/CEA vaccine samples were realized (i). Tumor volume of mice (5 mice per group) was injected with MC38/CEA cells after being immunized with the vaccine samples at 7, 14, and 21 days after tumor cell injection (ii). Representative images of tumors were collected from the sacrificed mice (iii). Copyright 2019 Royal Society of Chemistry [455]. (d) Exemplification of an NW application for a magnetic-based therapy. Schematic of the release process of a FeGa@P(VDF-TrFE) wire-structured magnetoelectric nanorobot system for targeted drug delivery via wet etching of anodic aluminum oxide and gold template. (i) Drug loading and release are assisted by a magnetic field (ii). Copyright 2017 John Wiley & Sons [538]. (e) Exemplification of a model for a magnetic nanoparticle-based hyperthermia potential therapy. Simulation of a magnetic field generated by a coil applicator (i), image-based particle density in the liver (ii), induced tissue temperature distribution considering perfusion and major vasculature (iii), resulting ablation as determined using CEM43 thermal dose model (iv). The targeted tumor location is indicated with an arrow. Copyright 2016 Elsevier [539].

use of laser scanning confocal microscopy [533]. Ultimately, another benefit of light for potential therapies is explained by Maijenburg et al., where an NW consisting of a series of deposited metals was designed. The multifunctional and multisegmented nanosystem makes use of a ZnO segment as a photoanode for hydrogen generation (catalysis property Section 4 and 5). Given the overall magnetic properties and its capability to use methanol as a fuel, it is proposed as a possible nanorobot with a surfeit of uses for *in situ* treatments [534].

Immunotherapy

Being one of the most promising fields for creating new cancer therapies, nano-scaled ZnO efficacy as an immune adjuvant has been investigated. The outcomes suggest that ZnO affects Th2 response on toll-like receptors, and Src signaling pathway [20,461,535,536], tetrapods [149,537], and 1D nanostructures. Prashant Sharma et al., highlighted it as an immune-based treatment using ZnO NWs, and the team engineered a 3D nanostructured composite formed by radially grown ZnO NWs in Poly-L-Lactic acid microfibers, with a tumor antigen destined to antigen-presenting dendritic cells. The nanocomposite could cause a cellular immunity against an *in vitro* tumor model by stimulating cytokines expression, activating diverse surface markers, reducing immune suppressive T_{reg} cells, and by enhancing the infiltration of T cells into the tumors; positioning itself as a potential cancer vaccine, Fig. 13 (c) [455,531,532,538,539].

Hyperthermia therapy

Apart from the above-mentioned properties of ZnO NWs and NRs, there are other exciting and attractive characteristics worthwhile to be explored for the cancer treatment approach. For instance, magnetic-based therapies make up an attractive area to explore 1D nanomaterials due to the new magnetization reversal modes. In the case of 1D ZnO structures, the possibility of inducing the ferromagnetic properties by introducing Zn vacancies opens an aperture of opportunities to explore magnetism-based therapies such as magnetic drug delivery based hyperthermia (HT) treatments [538,539], Fig. 13 (d, e). Since Zn vacancies can be inherently inserted into ZnO NWs, the omission of other transition metals can be achieved [186].

Summary and outlook

This review discusses the opportunity to study and manipulate macromolecules in real-time and during the earliest cancer progression stages using nanomaterials. Additionally, this could consequently generate entirely novel and highly effective therapeutic agents based on nanotechnology. Besides, it is shown the ZnO NWs role on the enhanced adsorption, reactivity, and high surface-volume ratio are within the must seek properties of nanostructured materials for their use in cancer biosensing and treatment applications. In the case of NWs, electronic transport in the axial direction of the structure is highly efficient. It is the main reason by which they are incorporated into electrochemical biosensing platforms. In addition, the isoelectric point of the ZnO nanostructures also makes the functionalization of diverse biological analytes possible. It is also shown beyond being harmful, the ZnO NWs cytotoxicity can be used to develop new strategies for treating cancer. This versatility has allowed

them to diversify their uses to create different kinds of devices, nanocomposites, and molecular complexes with a surfeit of applications. Detecting cancer at early stages by employing ZnO NWs could be vital for the treatment, hence, controlling this deadly disease.

Although the development of ZnO NW-based cancer therapies has not been as prolific as other fields, these structures have shown an exciting synergy with other devices. Since their synthesis is usually performed on a substrate, in contrast to the synthesis of nanoparticles typically in solution form, they open up the possibility that NWs would be embedded more frequently in medical devices with micrometer sub-micron dimensions. Moreover, due to their high surface volume ratios and growth tunability, the NWs could become carriers of important drugs and biomolecules for different types of cancer-related therapies. It is noteworthy to mention that though adequate research has been done with nanotechnology in cancer, it is still essential to focus on the challenge of implementing the clinical trials. Additionally, investigation regarding the advantageous properties of nanomaterials like ZnO is necessary for their final implementation in sensing/treatment devices.

Challenges and future prospects

Due to the inherent limitations of traditional cancer treatments, numerous nanotechnologies for more effective and safer cancer therapy are developed and used. Although significant technological advancements exhibit in this field, the primary impediments to nanomedicine becoming a new paradigm in cancer therapy are the complexity and heterogeneity of tumor biology, an incomplete understanding of nano-bio interactions, and the chemistry, manufacturing, and control challenges associated with clinical implications and marketization.

There is a growing interest in artificial intelligence implications to improve effective treatments and oncological care. One of the most recent tools is the convolutional neural network (CNN), which may have implications for radiotherapy treatment planning [540], showing achievement in foreseeing complete response to neoadjuvant chemoradiation with 80% precision [541]. Besides, Deep Learning is nowadays emerging as a rapid way to predict possibilities to develop precision medicine [542,543]. It has been observed that improving the prediction response to treatment is based on imaging findings, and it can also predict the toxicity induced due to cancer treatment [544], predicting toxicity effect by drug-drug interaction after radiotherapy [545]. Additionally, all can also be linked with top-notch portable health interfaces, such as smartphones and wearable devices, to develop “digital biomarkers” that can describe, influence, and forecast clinical results. Systemic and local cancer therapy, at present, continues to be an essential cost burden on the health system because of the high cost of drugs, expensive laboratory tests, prolonged hospital stays, and living expenses through treatment. Besides that, during and post-treatment procedures generate many toxics, collateral effects, and complications for patients, including damage of distal organs, nausea and vomiting, hair loss, anxiety problems, infection predisposition, peripheral neuropathy, pain, and cognitive issues. Meanwhile, the palliative treatments offer other procedures

simultaneously to the primary formal medical indication, for example, hyperthermia, dietary supplements, biosimilar drugs, and inclusion in clinical trials.

The use of diverse nanomaterials with desired qualities and recent breakthroughs in the field of drug administration has revealed substantial cancer therapeutic and management issues. Nanomaterials are expected to modify the whole healthcare system based on the dramatic gains achieved in the drug delivery business over the previous several decades. However, generating effective cancer nanotherapeutics remains challenging, with just a few pharmacologically relevant nano-formulations having reached clinical trials. Only a few cases of nanotechnology-based cancer diagnosis have progressed to clinical trials, despite of much-encouraging success. Many obstacles need to be overcome to facilitate the translation of nanotechnology into clinical applications. The first complication in using nanotechnology to detect cancer is maintaining its accuracy. It is crucial to achieve accurate and quantitative identification data to be used in the clinic. Nonspecific NPs/NWs probe coupling, accumulation, and unfit detection conditions are only a few of the factors that can impair nanomaterial-based detection signals. Signal variations may also be related to the dynamic configurations of body fluids. Until NP-based assays can be used in clinical environments, nanomaterials reliability and reproducibility need to be thoroughly studied in large clinical sample pools. The second issue is finding a cost-effective way to mass-produce nanoprobes that are highly sensitive, reproducible, and have long-term storage stability. Although most of the present nanoprobes are manufactured in labs under strictly regulated settings, generating these probes in batches remains a substantial difficulty. Because of the shape, size, composition, charge, and surface coating of the nanoprobes, the detection findings vary substantially. Reducing batch-to-batch variability, the synthesis stages and nanoprobe functionalization must be condensed. Understanding the cost-effectiveness of building a nanotechnology-based framework is equally critical.

The third challenge is the accumulation or aggregation of nanoprobes at the tumor site and surrounding tumor vasculatures during targeted therapy [546]. To get a better viewpoint on this aspect, we refer to surgical resection of tumors by various clinicians and surgeons. The most frequent treatment approach for solid tumors is surgical excision, either alone or in conjunction with chemotherapy or radiation [547]. Surgeons must properly detect malignant lesions within the surrounding healthy tissue during tumor removal. Because tumors seldom have well-defined borders dividing malignant and healthy tissue, surgeons may not be able to precisely resect all cancer tissue from the patient during surgery [548]. Consequently, the leftover cancer cells may linger at the tumor perimeter and sprout after surgery, resulting in tumor recurrence. Surgeons often remove the part of the healthy tissue around malignant tumors to lessen the likelihood of recurrence after surgery. However, doctors need to weigh the danger of tumor recurrence against the benefit of good tissue around the tumor for patient survival [549]. Injected nanoparticles by intravenous injection interact with a complex environment prior to reaching the tumor target and destroy foreign chemicals. The main barriers to the effective delivery of NPs on tumors include clearance of the mononuclear phagocyte sys-

tem (MPS), and tumor microenvironment heterogeneity, particularly physiological barriers such as the expression of antigen and vascular and tumor permeability [550]. When NPs reach the bloodstream, they often attach to plasma proteins (opsonization) and are taken up by phagocytic cells in the blood, liver, spleen, and bone marrow [551]. The clearance of this MPS presents two challenges: firstly, the efficient removal of nanoparticles from the circulation, which makes it possible for tumor sites to absorb a small fraction, and secondly, long retention periods of potentially toxic nanoparticles or metabolites, which raise concerns over the off-targeting and chronic toxicity.

One study examined the potential use of nanoparticle administration of near-infrared (NIR) dyes to enhance tumor identification during intra-operative imaging. NPs accumulate/aggregate in tumors and in the tumor vasculature after systemic treatment [552,553] because there is an increased penetration and retention (EPR) effect [554]. Tumor fluorescence may be improved via nanoparticle-based systemic delivery for intraoperative imaging. Since nanoparticles are also found in healthy tissues, such as the liver or spleen, they might accumulate [555]. One of the recent examples is the administration of Feraheme (FH) therapies (commonly used nanoprobe with the combination of two FDA-approved chemicals, e.g., Feraheme and indocyanine green (ICG)), where it has been found that iron can be accumulated in the liver of patients for many months. In this systemic delivery, tumor-localized NPs and the NPs within healthy organs both exhibit fluorescence that could be problematic for further analysis. To overcome this issue, novel and innovative approaches are required to boost tumor-localized NIR fluorescence signals while simultaneously quelling the fluorescence of circulating nanoparticles since this may help to reduce tumor recurrence and metastasis after treatment.

The fourth challenge is to develop extremely sensitive, simple-to-use, and cost-effective nano-assisted analytical devices. Most of the available tests are research-based, and many are inappropriate for clinical usage. Such tests were conducted using complex confocal Raman microscopes that are seldom utilized in hospitals or clinical labs. The effective development of point-of-care (POC) equipment based on nanomaterials will considerably simplify the clinical use of nanotechnology in cancer diagnostics. Another point to consider is the possibility of nanomaterial-induced toxicity due to systematic dosage or administration. This problem is all about the scenario of *in vivo* cases where NP/NW-based imaging is a crucial point. Before new probes are employed for *in vivo* imaging, their potential toxicity should be determined. The shape, size, charge, surface chemistry, targeted ligands, and composition of nanomaterials all affect their toxicity. Biodistribution, biodegradability, and pharmacokinetic aspects of nanomaterials should also be considered. The physicochemical features of NPs impacted their biocompatibility and toxicity in biological systems. Consequently, the meticulous synthesis and characterization of nanomaterials for drug administration and delivery are required to avoid nanocarriers causing unexpected toxicity to healthy cells. Additionally, since these nanocarriers interact with biomolecules, they might aggregate and create a protein corona, interfering with the usual function of nanomedicine formulations and rendering them useless in controlling cancer cell development [546].

Along with their physicochemical qualities, the storage and stability of nanomaterials may also exhibit an effect on their medicinal efficacy.

In terms of clinical translations (therapies), it is critical to determine the ideal physicochemical characteristics for the effective creation of therapeutic NPs/NWs. There has been significant progress in understanding the individual variables contributing to efficient immune evasion, tumor extravasation and diffusion, cell targeting and internalization, and controlled drug release [546]. Nonetheless, comprehensive parallel screening of the plethora of NPs/NWs qualities remains challenging due to the difficulty of rapidly synthesizing nanomaterials libraries with diverse attributes [360]. In comparison to bulk techniques, tunable properties of NPs/NWs have recently gained attention for their ability to rapidly self-assemble with a narrower size distribution, tunable physical and chemical properties, and improved batch-to-batch reproducibility. Such advancements might someday aid in identifying NPs/NWs, like how high-throughput screening of small molecules aided in the identification of drugs.

Fifty-one products based on nanotechnology are currently in clinical practice in the modern clinical nanotechnology scenario [556,557]. Notably, these nanomedications are mainly developed for drugs that are low in the water and highly toxic and often reduce toxicity by increasing the pharmacokinetic properties of the medicinal product concerned. According to Caster et al., although the FDA has regulated few nanomedicines, numerous initiatives are underway with clinical trials indicating that a large number of new medications based on nanotechnology can soon enter the market [558]. Among these nanomaterials, 18 for chemotherapy; 15 for antimicrobial agents; 28 for different medical and psychological applications, autoimmune conditions, and numerous additional diseases and 30 for nuclear acid therapy [559]. Nano-assisted theranostic is currently in the early phases of research (preclinical stage), but they have the potential to be used for real-time imaging of malignancies while a patient is undergoing therapy. Monitoring early therapeutic response indicators may allow treatment regimens to be altered and tailored based on therapeutic responses. Industries and biotechnology-driven investment companies are eager to invest in theranostic compounds because of their potential to become innovative and effective cancer treatment agents. While image-guided and tailored drug-delivery agents have solid scientific explanations and pressing clinical requirements, their complexity makes regulatory approval more challenging than ever.

Another challenge in drug distribution is ensuring human health safety when nanomaterial-related consequences do not manifest immediately. Due to the fact that nanocarriers are utilized to treat cancer, they have the potential to produce unintentional harm as a result of undesired interactions with biological entities. On the other hand, nanoformulations are challenging to mass manufacture on a large scale due to their batch-to-batch variation in physicochemical attributes. Additionally, the sophisticated multistage processing processes required for nanotherapeutics, along with the high cost of raw ingredients, make these nanotherapeutics a costly option. Therefore, well-considered and well-designed manufacturing procedures are required, as is a therapeutic value sufficient to offset production expenses.

Lastly, a significant concern is obtaining regulatory clearance for nanomedicines/nanomaterials used to study cancer-specific detection and treatments, as the FDA has not developed any formal standards for products containing nanomaterials. The measures currently in use are specifically adapted from bulk product guidance. Regulatory decisions on nano-formulated products are focused on an individual calculation of paybacks and risks, making assessments time-consuming and slows commercialization. In addition, as multifunctional nanoplates become more common, approval problems may likely become more challenging. Thus, before nanomaterial-based therapeutic agents for cancer therapy are used in medicine for improved treatment and human survival, design and growth techniques must be used to minimize the issues associated with them. Understanding the complexities of cancer cell physiology and the tumor microenvironment and drug and carrier pharmacokinetics is critical for creating novel cancer therapeutics that are effective. In addition, case-by-case research is expected to realize the enormous potential of cancer nanotherapeutics fully. A robust set of regulatory approval criteria is desperately required to speed up the assessment and acceptance of cancer nanotherapeutics.

Declaration of Competing Interest

The authors declare that they have no known competing financial interests or personal relationships that could have appeared to influence the work reported in this paper.

Acknowledgments

AGM acknowledges CONACyT Scholarship CVU 860916. G.S. gratefully acknowledges the CONACyT project PN 4797 and IG100320. A.D. thanks the DGAPA project PAPIIT IA101321. PKP would like to mention the financial support from the Swedish Research Council (VR grant no. 2016-06014). The authors are also grateful to Belem Solis Izeta and Marco Rodrigo Aguilar Ortiz (M.D.) for their technical assistance. YKM thanks funding by Interreg Deutschland–Denmark with money from the European Regional Development Fund, project number 096-1.1-18 (Access and Acceleration). The graphical abstract was created with BioRender.com.

Conflicts of interest

The authors declare no conflict of interest.

Appendix A. Supplementary data

Supplementary data to this article can be found online at <https://doi.org/10.1016/j.mattod.2021.07.025>.

References

- [1] NIH National Cancer, CA. *Cancer J. Clin.* Atlanta (2020) 1–76.
- [2] C.B. Blackadar, *World J. Clin. Oncol.* 7 (2016) 54–86.
- [3] T.B. Üstün, *Int. Encycl. Public Heal.*, Elsevier, 2017, pp. 304–311.
- [4] F. Bray et al., *CA. Cancer J. Clin.* 68 (2018) 394–424.
- [5] J. Ferlay et al., *Int. J. Cancer* 144 (2019) 1941–1953.
- [6] H. Sung et al., *CA. Cancer J. Clin.* 71 (2021) 209–249.
- [7] J. Ferlay et al., *Int. Agency Res. Cancer* (2020).
- [8] M.W. Costa, N. Rosenthal, in: Abeloff's Clin. Oncol. Fifth Ed., Content Repository Only!, 2013, pp. 2-21.e1.
- [9] Y. Xue, W.R. Wilcox, *Cancer Biol. Med.* 13 (2016) 12–18.
- [10] J. Jin et al., *Front. Oncol.* 9 (2019) 263.

- [11] T. Dorai, B.B. Aggarwal, *Cancer Lett.* 215 (2004) 129–140.
- [12] Y. Zhang et al., *J. Hematol. Oncol.* 12 (2019) 137.
- [13] Y. Zhang et al., *Adv. Mater.* 31 (2019) 1970155.
- [14] S. Tran et al., *Clin. Transl. Med.* 6 (2017) 44.
- [15] D. Bobo et al., *Pharm. Res.* 33 (2016) 2373–2387.
- [16] A. Gautam et al., *Med. Devices Sensors* 3 (2020) e10122.
- [17] R. Kumar et al., *J. Mater. Chem. B* 8 (2020) 8992–9027.
- [18] G. Rathee et al., *Adv. NanoBiomed Res.* (2021) 2100039.
- [19] F. Diao, Y. Wang, *J. Mater. Sci.* 53 (2018) 4334–4359.
- [20] N.H. Cho et al., *Nat. Nanotechnol.* 6 (2011) 675–682.
- [21] J. Jin, Z.M. Bhujwalla, *Front. Oncol.* 9 (2020) 1560.
- [22] E.Y. Lukianova-Hleb et al., *Nat. Nanotechnol.* 11 (2016) 525–532.
- [23] A. Maitra, *Nature* 567 (2019) 181–182.
- [24] J. Massagué, A.C. Obenauf, *Nature* 529 (2016) 298–306.
- [25] L. Sercombe et al., *Front. Pharmacol.* 6 (2015) 286.
- [26] M.F. Attia et al., *J. Pharm. Pharmacol.* 71 (2019) 1185–1198.
- [27] A.S. Sevastre et al., *Coatings* 9 (2019) 628.
- [28] Y.H. Choi, H.K. Han, *J. Pharm. Investig.* 48 (2018) 43–60.
- [29] Y. Shi et al., *Theranostics* 10 (2020) 7921–7924.
- [30] U. Chitgupi, Y. Qin, J.F. Lovell, *NanoTheranostics* 1 (2017) 38–58.
- [31] R. Di Corato et al., *ACS Nano* 9 (2015) 2904–2916.
- [32] X. Huang et al., *J. Mater. Chem. B* 4 (2016) 6258–6270.
- [33] D. Kagan et al., *Small* 6 (2010) 2741–2747.
- [34] Y. Wen, C.L. Schreiber, B.D. Smith, *Bioconjug. Chem.* 31 (2020) 474–482.
- [35] R. Bardhan et al., *Acc. Chem. Res.* 44 (2011) 936–946.
- [36] A. Quarta et al., *Nanoscale* 7 (2015) 2336–2351.
- [37] O. Grauer et al., *J. Neurooncol.* 141 (2019) 83–94.
- [38] A. Espinosa et al., *ACS Nano* 10 (2016) 2436–2446.
- [39] F. Soetaert et al., *Adv. Drug Deliv. Rev.* 163–164 (2020) 65–83.
- [40] M. Auerbach et al., *Transfusion* 48 (2008) 988–1000.
- [41] A.C. Anselmo, S. Mitragotri, *AAPS J.* 17 (2015) 1041–1054.
- [42] E. Andronescu et al., *J. Mater. Sci. Mater. Med.* 21 (2010) 2237–2242.
- [43] A. Caraceni et al., *J. Pain Symptom Manage.* 29 (2005) 507–519.
- [44] S. Hu et al., *Front. Pharmacol.* 9 (2018) 790.
- [45] M.A. Doucey, S. Carrara, *Trends Biotechnol.* 37 (2019) 86–99.
- [46] Q. Cui et al., *Small* 5 (2009) 1246–1257.
- [47] P. Amborkar et al., *Micromachines* 9 (2018) 1–19.
- [48] L. Mu et al., *IEEE Access* 3 (2015) 287–302.
- [49] P. Xie et al., *Nat. Nanotechnol.* 7 (2012) 119–125.
- [50] X.M. Cao, Z.B. Han, *Chem. Commun.* 55 (2019) 1746–1749.
- [51] M. Ghorbani, M.R. Golobostanfar, H. Abdizadeh, *Appl. Surf. Sci.* 419 (2017) 277–285.
- [52] M. Shekofteh-Gohari et al., *Crit. Rev. Environ. Sci. Technol.* 48 (2018) 806–857.
- [53] S. He et al., *J. Power Sources* 434 (2019) 226701.
- [54] C. Huang et al., *Nanoscale* 11 (2019) 10114–10128.
- [55] Y. Wang et al., *ChemistrySelect* 3 (2018) 550–565.
- [56] A. Das, R.R. Wary, R.G. Nair, *Solid State Sci.* 104 (2020) 106290.
- [57] K.A. Bhatti et al., *Mater. Res. Express* 6 (2019) 075902.
- [58] B. Boro et al., *Renew. Sustain. Energy Rev.* 81 (2018) 2264–2270.
- [59] Z.H. Bakr et al., *Ind. Eng. Chem. Res.* 58 (2019) 643–653.
- [60] D. Wang et al., *Nanomaterials* 9 (2019) 1–15.
- [61] K. Sun et al., *Microelectron. Eng.* 153 (2016) 96–100.
- [62] N.R. Shanmugam, S. Muthukumar, S. Prasad, *Futur. Sci. OA* 3 (2017) FSO196.
- [63] S. Agarwal et al., *Sensors Actuators B Chem.* 292 (2019) 24–31.
- [64] R. Kumar et al., *Nano-Micro Lett.* 7 (2015) 97–120.
- [65] Y.K. Mishra et al., *ACS Appl. Mater. Interfaces* 7 (2015) 14303–14316.
- [66] M. González-Garnica et al., *Sensors Actuators, B Chem.* 337 (2021) 129765.
- [67] S. Rackauskas et al., *Nanomaterials* 7 (2017) 381.
- [68] A. Galdámez-Martínez et al., *Nanomaterials* 10 (2020) 857.
- [69] A. Galdámez et al., *Mater. Lett.* 235 (2019) 250–253.
- [70] M. Samadi et al., *Thin Solid Films* 605 (2016) 2–19.
- [71] A. Galdámez-Martínez et al., *Int. J. Hydrogen Energy* 45 (2020) 31942–31951.
- [72] H. Hong et al., *Nano Lett.* 11 (2011) 3744–3750.
- [73] P. Rauwel et al., *J. Nanomater.* 2016 (2016) 5320625.
- [74] V. Parihar, M. Raja, R. Paulose, *Rev. Adv. Mater. Sci.* 53 (2018) 119–130.
- [75] G. Chen, P.-S. Wang, *Chinese Phys. Lett.* 35 (2018) 127701.
- [76] X. Wang et al., *ACS Nano* 11 (2017) 8339–8345.
- [77] R.E. Marotti et al., *Sol. Energy Mater. Sol. Cells* (2004) 85–103.
- [78] J.F. Muth et al., *Appl. Phys. Lett.* 71 (1997) 2572–2574.
- [79] N.M.J. Ditshego, *J. Nano Res.* 55 (2018) 66–74.
- [80] N.P. Shetti et al., *Biosens. Bioelectron.* 141 (2019) 111417.
- [81] H. Morkoç, Ü. Özgür, *Zinc Oxide: Fundamentals, Materials and Device Technology*, Wiley, 2009.
- [82] C. Jagadish, S. Pearton, *Zinc Oxide Bulk, Thin Films and Nanostructures*, Elsevier Science, 2006.
- [83] O. Dulub, L.A. Boatner, U. Diebold, *Surf. Sci.* 519 (2002) 201–217.
- [84] N.A. Mansor et al., *Open J. Appl. Biosens.* 03 (2014) 9–17.
- [85] G. Katwal et al., *Nano Lett.* 16 (2016) 3014–3021.
- [86] J. Park et al., *Sensors Actuators B Chem.* 200 (2014) 173–180.
- [87] J.H. Han et al., *Sensors Actuators B Chem.* 228 (2016) 36–42.
- [88] Z. Kang et al., *Biosens. Bioelectron.* 64 (2015) 499–504.
- [89] Y. Cao et al., *Langmuir* 28 (2012) 7947–7951.
- [90] C.-H. Sang et al., *Biosens. Bioelectron.* 75 (2016) 285–292.
- [91] Y. Wang et al., *Surf. Interface Anal.* 47 (2015) 245–252.
- [92] W. Lin et al., *Cryst. Growth Des.* 9 (2009) 4378–4383.
- [93] L. Guo et al., *Appl. Phys. Lett.* 76 (2000) 2901–2903.
- [94] S. Bagga, J. Akhtar, S. Mishra, in: *AIP Conf. Proc.*, 2018, p. 020004.
- [95] J.-J. Wu et al., *Appl. Phys. Lett.* 81 (2002) 1312–1314.
- [96] L. Vayssières, *Adv. Mater.* 15 (2003) 464–466.
- [97] I. Crupi et al., *Thin Solid Films* 520 (2012) 4432–4435.
- [98] W.L. Hughes, Z.L. Wang, *Appl. Phys. Lett.* 86 (2005) 2003–2006.
- [99] Y.B. Li et al., *Appl. Phys. Lett.* 81 (2002) 144–146.
- [100] P.X. Gao, Y. Ding, Z.L. Wang, *Nano Lett.* 9 (2009) 137–143.
- [101] Y. Wang et al., *Sep. Purif. Technol.* 62 (2008) 727–732.
- [102] H. Zeng et al., *J. Phys. Chem. C* 112 (2008) 19620–19624.
- [103] H. Yim, S. Seo, K. Na, *J. Nanomat.* 2011 (2011) 747196.
- [104] R. Lahri et al., *Med. Phys.* 45 (2018) 3820–3830.
- [105] Z. Li et al., *J. Phys. Chem. C* 112 (2008) 20114–20117.
- [106] L. He et al., *AIPI Adv.* 9 (2019) 125026.
- [107] Z.-Y. Zhang, H.-M. Xiong, *Materials (Basel.)* 8 (2015) 3101–3127.
- [108] M. Martínez-Carmona, Y. Gun'Ko, M. Vallet-Regí, *Nanomaterials* 8 (2018) 1–27.
- [109] M. Alavi, A. Nokhodchi, *Carbohydr. Polym.* 227 (2020) 115349.
- [110] Z. Lu et al., *Carbohydr. Polym.* 156 (2017) 460–469.
- [111] M. Kaushik et al., *Appl. Surf. Sci.* 479 (2019) 1169–1177.
- [112] A. Garcia-Guerra, T.L. Dunwell, S. Trigueros, *Curr. Med. Chem.* 25 (2018) 2448–2464.
- [113] S.H. Moon et al., *Toxicol. Reports* 3 (2016) 430–438.
- [114] M. Esmaeilou et al., *Environ. Toxicol. Pharmacol.* 35 (2013) 67–71.
- [115] G. Micali et al., *J. Am. Acad. Dermatol.* 70 (965) (2014) e1–965.e12.
- [116] K. Memarzadeh et al., *J. Biomed. Mater. Res. - Part A* 103 (2015) 981–989.
- [117] A. Tereshchenko et al., *Sensors Actuators B Chem.* 229 (2016) 664–677.
- [118] P. Chauhan, S. Mahajan, G.B.K.S. Prasad, *J. Drug Deliv. Sci. Technol.* 52 (2019) 738–747.
- [119] L. Siebert et al., *Adv. Funct. Mater.* 31 (2021) 2007555.
- [120] D. Medina Cruz et al., *J. Phys. Mater.* 3 (2020) 034005.
- [121] S. Ahmed et al., *Photochem. Photobiol. B Biol.* 166 (2017) 272–284.
- [122] P. Basnet et al., *J. Photochem. Photobiol. B Biol.* 183 (2018) 201–221.
- [123] A. Yadav et al., *Biotechnol. Lett.* 37 (2015) 2099–2120.
- [124] N. Jain et al., *Appl. Microbiol. Biotechnol.* 97 (2013) 859–869.
- [125] S.-N. Bai, S.-C. Wu, *J. Mater. Sci. Mater. Electron.* 22 (2011) 339–344.
- [126] S. Ma, A.H. Kitai, *J. Mater. Sci.* 52 (2017) 9324–9334.
- [127] L.C. Campos et al., *Adv. Mater.* 20 (2008) 1499–1504.
- [128] N.S. Ramgir et al., *J. Phys. Chem. C* 114 (2010) 10323–10329.
- [129] R.K. Goyal, *Nanomaterials and Nanocomposites*, Wiley-VCH Verlag GmbH & Co. KGaA, Weinheim, Germany, 2016.
- [130] J. Cui, U. Gibson, *Nanotechnology* 18 (2007).
- [131] J. Cui, *Mater. Charact.* 64 (2012) 43–52.
- [132] X. Yan et al., *Cryst. Growth Des.* 8 (2008) 2406–2410.
- [133] H. Simon et al., *Cryst. Growth Des.* 13 (2013) 572–580.
- [134] P. Petkov, et al., in: *Nanosci. Adv. CBRN Agents Detect. Inf. Energy Secur.*, 2015, pp. 3–13.
- [135] S. Xu, Z.L. Wang, *Nano Res.* 4 (2011) 1013–1098.
- [136] J.H. Kim et al., *Adv. Funct. Mater.* 17 (2007) 463–471.
- [137] N.M.J. Ditshego, *J. Nano Res.* 60 (2019) 94–112.
- [138] J. Wang, L. Gao, *Solid State Commun.* 132 (2004) 269–271.
- [139] J. Elias et al., *Electrochim. Acta* 110 (2013) 387–392.
- [140] H. Zhang et al., *Cryst. Growth Des.* 5 (2005) 547–550.
- [141] M.J. Zheng et al., *Chem. Phys. Lett.* 363 (2002) 123–128.
- [142] A.A. Ameer et al., *J. Phys. Conf. Ser.* (2019) 012005.
- [143] N.A. Alshehri et al., *J. Saudi Chem. Soc.* 22 (2018) 538–545.
- [144] P. Rai, W.K. Kwak, Y.T. Yu, *ACS Appl. Mater. Interfaces* 5 (2013) 3026–3032.
- [145] J.-S. Lee et al., *J. Cryst. Growth* 249 (2003) 201–207.
- [146] S. Ma, A.H. Kitai, *Mater. Res. Express* 4 (2017) 065012.

- [147] I. Isakov et al., *Phys. Status Solidi Curr. Top. Solid State Phys.* 10 (2013) 1308–1313.
- [148] W.I. Park et al., *Appl. Phys. Lett.* 80 (2002) 4232–4234.
- [149] A. Agelidis et al., *Front. Immunol.* 10 (2019) 500.
- [150] Y.K. Mishra, R. Adelung, *Mater. Today* 21 (2018) 631–651.
- [151] M. Condello et al., *Toxicol. Vitr.* 35 (2016) 169–179.
- [152] J. Jiang, J. Pi, J. Cai, *Bioinorg. Chem. Appl.* 2018 (2018) 1062562.
- [153] C. Hanley et al., *Nanoscale Res. Lett.* 4 (2009) 1409–1420.
- [154] J.W. Rasmussen et al., *Expert Opin. Drug Deliv.* 7 (2010) 1063–1077.
- [155] H. Wang et al., *J. Nanosci. Nanotechnol.* (2011) 1117–1122.
- [156] A. Wei, L. Pan, W. Huang, *Mater. Sci. Eng. B Solid-State Mater. Adv. Technol.* 176 (2011) 1409–1421.
- [157] S.M. Sultan et al., *Nanoscale Res. Lett.* 9 (2014) 517.
- [158] F.A. Sabah, N.M. Ahmed, Z. Hassan, *J. Phys. Conf. Ser.* (2018).
- [159] N.M.J. Ditshego et al., *Microelectron. Eng.* 145 (2015) 91–95.
- [160] A. Menzel et al., *Adv. Funct. Mater.* 21 (2011) 4342–4348.
- [161] J. Yoon et al., *Materials (Basel.)* 13 (2020) 268.
- [162] E.M. Kaidashev et al., *Appl. Phys. Lett.* 82 (2003) 3901–3903.
- [163] G. Gasparotto et al., *Mater. Sci. Eng. C* 76 (2017) 1240–1247.
- [164] M.L.M. Napi et al., *Materials (Basel.)* 12 (2019) 2985.
- [165] H.-M.M. Kim, J.-H.H. Park, S.-K.K. Lee, *Sci. Rep.* 9 (2019) 1–9.
- [166] J.K. Yoon et al., *Adv. Funct. Mater.* 27 (2017) 1–15.
- [167] J. Kazmi, et al., *RSC Adv.* 10 (2020) 23297–23311.
- [168] N. Novak et al., *Acta Mater.* 162 (2019) 277–283.
- [169] H. Yang et al., *Road Mater. Pavement Des.* 18 (2017) 180–189.
- [170] M. Ghosh, M.G. Rao, *Mater. Express* 3 (2013) 319–327.
- [171] M.H. Zhao, Z.L. Wang, S.X. Mao, *Nano Lett.* 4 (2004) 587–590.
- [172] A. Mitrushchenkov, R. Linguerri, G. Chambaud, *J. Phys. Chem. C* 113 (2009) 6883–6886.
- [173] R. Chowdhury, S. Adhikari, F. Scarpa, *Phys. E Low-Dimensional Syst. Nanostructures* 42 (2010) 2036–2040.
- [174] E. Broitman et al., *Phys. Chem. Chem. Phys.* 15 (2013) 11113–11118.
- [175] S.H. Shin et al., *ACS Nano* 8 (2014) 10844–10850.
- [176] S.H. Bhang et al., *Adv. Funct. Mater.* 27 (2017) 1603497.
- [177] R. Augustine et al., *Nano Res.* 10 (2017) 3358–3376.
- [178] K. Kapat et al., *Adv. Funct. Mater.* 30 (2020) 1909045.
- [179] A. Marino, G. Ciofani, *Adv. Mater. Lett.* 10 (2019) 303–304.
- [180] A. Mukhtar et al., *Nanotechnology* 31 (2020) 433001.
- [181] S.Y. Sokovniin, V.G. Il'v'es, *Tech. Phys. Lett.* 35 (2009) 1026–1028.
- [182] R. Podila et al., *Nano Lett.* 10 (2010) 1383–1386.
- [183] N.H. Hong, J. Sakai, V. Brizé, *J. Phys. Condens. Matter* 19 (2007) 036219.
- [184] A. Sundaresan et al., *Phys. Rev. B - Condens. Matter Mater. Phys.* 74 (2006) 1–4.
- [185] M.A. Garcia et al., *Nano Lett.* 7 (2007) 1489–1494.
- [186] Q. Wang et al., *Phys. Rev. B* 77 (2008) 205411.
- [187] G.Z. Xing et al., *Adv. Mater.* 20 (2008) 3521–3527.
- [188] J. Cui, Q. Zeng, U.J. Gibson, *J. Appl. Phys.* 99 (2006) 2004–2007.
- [189] I. Lorigo et al., *Appl. Phys. Lett.* 109 (2016) 012401.
- [190] S. Deka, P.A. Joy, *Solid State Commun.* 142 (2007) 190–194.
- [191] H. He et al., *J. Am. Chem. Soc.* 127 (2005) 16376–16377.
- [192] S. Farhat, M. Rekaby, R. Awad, *J. Supercond. Nov. Magn.* 31 (2018) 3051–3061.
- [193] X. Ma, *Thin Solid Films* 520 (2012) 5752–5755.
- [194] N. Aggarwal et al., *J. Supercond. Nov. Magn.* 32 (2019) 685–691.
- [195] A. Ramirez-Canon et al., *Phys. Chem. Chem. Phys.* 20 (2018) 6648–6656.
- [196] M. Singh et al., *Nanoscale* 10 (2018) 6039–6050.
- [197] W. Zhen et al., *Appl. Catal. B Environ.* 221 (2018) 243–257.
- [198] C.N.C. Hitam, A.A. Jalil, *J. Environ. Manage.* 258 (2020) 110050.
- [199] P. Wen et al., *CrystEngComm* 22 (2019) 105–112.
- [200] M. Ge et al., *Adv. Sci.* 4 (2017) 1–31.
- [201] S. Ghasabian, M. Atai, M. Imani, *Mater. Res. Express* 4 (2017) 035010.
- [202] A. Rokade et al., *J. Solid State Electrochem.* 21 (2017) 2639–2648.
- [203] M. Samadi et al., *Res. Chem. Intermed.* 45 (2019) 2197–2254.
- [204] J. He et al., *Environ. Int.* 132 (2019) 105105.
- [205] S. Das et al., *Int. J. Environ. Res. Public Health* 15 (2018) 1–11.
- [206] M. Fazilat, *Desalin. WATER Treat.* 169 (2019) 222–231.
- [207] Z. Wang et al., *Phys. Chem. Chem. Phys.* 16 (2014) 2758–2774.
- [208] M. Pirhashemi et al., *J. Ind. Eng. Chem.* 62 (2018) 1–25.
- [209] X. Chen et al., *Chem. Rev.* 110 (2010) 6503–6570.
- [210] Y.S. Seo, S.G. Oh, *Korean J. Chem. Eng.* 36 (2019) 2118–2124.
- [211] G.L. Chiarello, M.V. Dozzi, E. Sell, *J. Energy Chem.* 26 (2017) 250–258.
- [212] N. Yahya et al., *J. Nano Res.* 11 (2010) 25–34.
- [213] D. Guo et al., *J. Photochem. Photobiol. B Biol.* 93 (2008) 119–126.
- [214] A.W. Maijenburg et al., *J. Vis. Exp.* 87 (2014) 51547.
- [215] S.P. Singh, *J. Biomed. Nanotechnol.* 7 (2011) 95–97.
- [216] Y. Liu et al., *Biomaterials* 32 (2011) 1185–1192.
- [217] H. Wang et al., *J. Mater. Sci. Mater. Med.* 20 (2009) 11–22.
- [218] C. Hanley et al., *Nanotechnology* 19 (2008) 295103.
- [219] N. Lewinski, V. Colvin, R. Drezek, *Small* 4 (2008) 26–49.
- [220] K.M. Reddy, et al., *Appl. Phys. Lett.* 90 (2007) 213902–1.
- [221] S.C. Yang et al., *Nanotechnology* 23 (2012) 55202.
- [222] Y.J. Li et al., *Int. J. Pharm.* 489 (2015) 83–90.
- [223] R.S. Mulik et al., *Int. J. Pharm.* 398 (2010) 190–203.
- [224] A. Kumar et al., *ACS Nano* 8 (2014) 4205–4220.
- [225] Y. Ren et al., *J. Control. Release* 228 (2016) 74–86.
- [226] J. Qiu et al., *Nanomaterials* 8 (2018) 131.
- [227] J.H. Lee et al., *Nat. Med.* 13 (2007) 95–99.
- [228] H. Chen et al., *PDA J. Pharm. Sci. Technol.* 61 (2007) 303–313.
- [229] R. Nandi et al., *J. Mater. Chem. B* 5 (2017) 3927–3939.
- [230] S. Wu et al., *Nanoscale Res. Lett.* 14 (2019) 228.
- [231] J. Panda et al., *J. Magn. Magn. Mater.* 485 (2019) 165–173.
- [232] R. Lin et al., *Colloids Surfaces B Biointerfaces* 150 (2017) 261–270.
- [233] M. Patitsa et al., *Sci. Rep.* 7 (2017) 775.
- [234] P. Liu et al., *Oncol. Targets. Ther.* 9 (2016) 5049–5059.
- [235] W. Xue et al., *J. Mater. Chem. B* 6 (2018) 2289–2303.
- [236] W.H. Chen et al., *Biomaterials* 76 (2016) 87–101.
- [237] X. Chen et al., *Microporous Mesoporous Mater.* 217 (2015) 46–53.
- [238] X. Liu et al., *ACS Nano* 10 (2016) 2702–2715.
- [239] R. Prasad et al., *Nanoscale* 8 (2016) 4537–4546.
- [240] S. Yang et al., *Small* 12 (2016) 360–370.
- [241] T. Ramasamy et al., *NPG Asia Mater.* 10 (2018) 197–216.
- [242] H. Wang et al., *ACS Appl. Mater. Interfaces* 9 (2017) 18639–18649.
- [243] W. Wang et al., *Sci. Rep.* 7 (2017) 43036.
- [244] X. Zhuang et al., *J. Control. Release* 228 (2016) 26–37.
- [245] H. Yang, *Nanomed. Nanotechnol. Biol. Med.* 12 (2016) 309–316.
- [246] M.R. Carvalho, R.L. Reis, J.M. Oliveira, *J. Mater. Chem. B* 8 (2020) 1128–1138.
- [247] K. Li et al., *Int. J. Nanomedicine* 8 (2013) 2589–2600.
- [248] F. Zhou et al., *Theranostics* 6 (2016) 679–687.
- [249] D. Kim, Y.Y. Jeong, S. Jon, *ACS Nano* 4 (2010) 3689–3696.
- [250] R.M. Penner, *Annu. Rev. Anal. Chem.* 5 (2012) 461–485.
- [251] A. Dorfman et al., *J. Nanosci. Nanotechnol.* 8 (2008) 410–415.
- [252] K. Kavithaa et al., *Karbala Int. J. Mod. Sci.* 2 (2016) 46–55.
- [253] J. Politi et al., *Sensors Actuators B Chem.* 220 (2015) 705–711.
- [254] J. Zhou, N.S. Xu, Z.L. Wang, *Adv. Mater.* 18 (2006) 2432–2435.
- [255] R.J. Vandebriel, W.H. De Jong, *Nanotechnol. Sci. Appl.* 5 (2012) 61–71.
- [256] J. Liu et al., *Crit. Rev. Toxicol.* 46 (2016) 348–384.
- [257] A. Król et al., *Adv. Colloid Interface Sci.* 249 (2017) 37–52.
- [258] B. Wang et al., *J. Nanoparticle Res.* 10 (2008) 263–276.
- [259] Y.-N.N. Chang et al., *Materials (Basel.)* 5 (2012) 2850–2871.
- [260] T. Kang et al., *Nanoscale Res. Lett.* 8 (2013) 496.
- [261] N. Santo et al., *Water Res.* 53 (2014) 339–350.
- [262] L. Xiang et al., *Environ. Sci. Pollut. Res.* 22 (2015) 10452–10462.
- [263] T.D. Zaveri et al., *Biomaterials* 31 (2010) 2999–3007.
- [264] X. Peng et al., *Aquat. Toxicol.* 102 (2011) 186–196.
- [265] Y. Yin et al., *Nanoscale Res. Lett.* 7 (2012) 439.
- [266] M. Ćepin et al., *Mater. Sci. Eng. C* 52 (2015) 204–211.
- [267] X. Zhu et al., *J. Environ. Sci. Heal Part A Toxic/Hazardous Subst Environ. Eng.* 43 (2008) 278–284.
- [268] T.-K.K. Hong et al., *J. Mater. Chem. B* 1 (2013) 2985–2992.
- [269] V. Valdiglesias et al., *Environ. Int.* 55 (2013) 92–100.
- [270] N.R. Jacobsen et al., *Food Chem. Toxicol.* 85 (2015) 84–95.
- [271] P. Mishra et al., *Drug Discov. Today* 22 (2017) 1825–1834.
- [272] D.M. Berube, *J. Nanoparticle Res.* 10 (2008) 23–37.
- [273] S. Amara et al., *Hum. Exp. Toxicol.* 33 (2014) 1150–1157.
- [274] S.A. James et al., *ACS Nano* 7 (2013) 10621–10635.
- [275] H. Papavassopoulos et al., *PLoS One* 9 (2014) e84983–e84983.
- [276] S.J. Choi, J.H. Choy, *Int. J. Nanomed.* 9 (2014) 261–269.
- [277] M. Baek et al., *Int. J. Nanomed.* 7 (2012) 3081–3097.
- [278] J. Choi et al., *J. Toxicol. Environ. Heal. - Part A Curr. Issues* 78 (2015) 226–243.
- [279] T.-K. Yeh et al., *Nanotechnology* 23 (2012) 085102.
- [280] R. Shrivastava et al., *Drug Chem. Toxicol.* 37 (2014) 336–347.
- [281] R. Roy, M. Das, P.D. Dwivedi, *Mol. Immunol.* 63 (2015) 184–192.
- [282] B.M. Johnson et al., *Nanotoxicology* 9 (2015) 737–748.
- [283] C. Shen et al., *Toxicol. Sci.* 136 (2013) 120–130.
- [284] W. Lin et al., *J. Nanoparticle Res.* 11 (2009) 25–39.
- [285] K.H. Müller et al., *ACS Nano* 4 (2010) 6767–6779.
- [286] C. Jiang, H. Hsu-Kim, *Environ. Sci. Process. Impacts* 16 (2014) 2536–2544.

- [287] L. García-Hevia et al., *Nanoscale* 8 (2016) 10963–10973.
- [288] M. Chevallet et al., *Nanoscale* 8 (2016) 18495–18506.
- [289] J. Nriagu, *Encycl. Environ. Heal.*, Elsevier, 2011, pp. 801–807.
- [290] C.-C. Huang et al., *Toxicol. Vitr.* 24 (2010) 45–55.
- [291] N. Li et al., *Environ. Health Perspect.* 111 (2003) 455–460.
- [292] A. Scherzad et al., *Materials (Basel)* 10 (2017) 1427.
- [293] J. Heim et al., *Nanoscale* 7 (2015) 8931–8938.
- [294] V.A. Senapati et al., *Food Chem. Toxicol.* 85 (2015) 61–70.
- [295] S. Hackenberg et al., *Toxicol. Vitr.* 25 (2011) 657–663.
- [296] S.R. Choudhury et al., *Toxicol. Sci.* 156 (2017) 261–274.
- [297] P. Rossner et al., *Toxicol. Sci.* 168 (2019) 190–200.
- [298] A. Adamcakova-Dodd et al., *Part. Fibre Toxicol.* 11 (2014) 15.
- [299] S. Pasupuleti et al., *Toxicol. Ind. Health* 28 (2012) 675–686.
- [300] J. Liu et al., *Int. J. Nanomed.* 12 (2017) 8085–8099.
- [301] A. Yaqub et al., *Appl. Nanosci.* 10 (2020) 177–185.
- [302] N.A. Abdell Baky et al., *Drug Res. (Stuttgart)* 63 (2013) 228–236.
- [303] A.R. Pinho et al., *Cells* 9 (2020) 1081.
- [304] N.A. Monteiro-Rivière et al., *Toxicol. Sci.* 123 (2011) 264–280.
- [305] Y.H. Mohammed et al., *J. Invest. Dermatol.* 139 (2019) 308–315.
- [306] Y. Wang et al., *Nanomaterials* 7 (2017) 80.
- [307] R. Ning et al., *Small* 10 (2014) 4113–4117.
- [308] R. Wahab et al., *RSC Adv.* 6 (2016) 26111–26120.
- [309] H. Cui et al., *Nanoscale* 12 (2020) 1455–1463.
- [310] G. Appierot et al., *Adv. Funct. Mater.* 19 (2009) 842–852.
- [311] T.J. Brunner et al., *Environ. Sci. Technol.* 40 (2006) 4374–4381.
- [312] P.L. Kool, M.D. Ortiz, C.A.M. Van Gestel, *Environ. Pollut.* 159 (2011) 2713–2719.
- [313] M. Ho et al., *Inhal. Toxicol.* 23 (2011) 947–956.
- [314] G. Oberdörster, E. Oberdörster, J. Oberdörster, *Environ. Health Perspect.* 113 (2005) 823–839.
- [315] E. Ferrone et al., *Nanomaterials* 9 (2019) 1449.
- [316] C. Wang et al., *Biomed. Res. Int.* 2015 (2015) 423287.
- [317] K. Girigoswami et al., *Mater. Sci. Eng. C* 56 (2015) 501–510.
- [318] V. Sravan Bolu et al., *J. Evol. Med. Dent. Sci.* 5 (2016) 6186–6192.
- [319] H. Ma et al., *Environ. Pollut.* 193 (2014) 165–172.
- [320] H. Moratin et al., *Environ. Mol. Mutagen.* 59 (2018) 247–259.
- [321] B.C. Heng et al., *Food Chem. Toxicol.* 48 (2010) 1762–1766.
- [322] M.T. Khorasani et al., *Int. J. Biol. Macromol.* 114 (2018) 1203–1215.
- [323] M. Zhai et al., *J. Photochem. Photobiol. B Biol.* 180 (2018) 253–258.
- [324] S. Kantipudi et al., *IET Nanobiotechnol.* 12 (2018) 473–478.
- [325] H. Chhabra et al., *RSC Adv.* 6 (2016) 1428–1439.
- [326] R. Balen et al., *Appl. Surf. Sci.* 385 (2016) 257–267.
- [327] H. Yin, P.S. Casey, M.J. McCall, *J. Nanosci. Nanotechnol.* (2010) 7565–7570.
- [328] I.L. Hsiao, Y.J. Huang, *J. Nanoparticle Res.* 15 (2013) 1829.
- [329] M. Wolska-Pietkiewicz et al., *Chem. - A Eur. J.* 24 (2018) 4033–4042.
- [330] M. Canta, V. Cauda, *Biomater. Sci.* 8 (2020) 6157–6174.
- [331] E. Ho, *J. Nutr. Biochem.* 15 (2004) 572–578.
- [332] L. Racca et al., *Smart Nanoparticles Biomed.*, Elsevier (2018) 171–187.
- [333] C.T. Chasapis et al., *Arch. Toxicol.* 86 (2012) 521–534.
- [334] G. Bisht, S. Rayamajhi, *Nanobiomedicine* 3 (2016) 9.
- [335] K.W. Ng et al., *Biomaterials* 32 (2011) 8218–8225.
- [336] T.W. Turney et al., *Chem. Res. Toxicol.* 25 (2012) 2057–2066.
- [337] L.C. Costello et al., *Cancer Causes Control* 16 (2005) 901–915.
- [338] W. Song et al., *Toxicol. Lett.* 199 (2010) 389–397.
- [339] J. Bogdan, J. Pławińska-Czarnak, J. Zarzyńska, *Nanoscale Res. Lett.* 12 (2017) 225.
- [340] P. Kumari et al., *Sci. Rep.* 7 (2017) 16284.
- [341] S.K. Verma et al., *Nanomedicine* 13 (2018) 43–68.
- [342] P. Paul et al., *Artif. Cells, Nanomed. Biotechnol.* 46 (2018) S572–S584.
- [343] P. Kumari et al., *Nanomedicine* 13 (2018) 2415–2433.
- [344] B.K. Das et al., *Chem. Biol. Interact.* 297 (2019) 141–154.
- [345] S.K. Verma et al., *Artif. Cells, Nanomedicine Biotechnol.* 46 (2018) S671–S684.
- [346] S.K. Verma et al., *Adv. Nanostructured Mater. Environ. Remediat.*, Springer, Cham, 2019, pp. 145–171.
- [347] S. Kumari et al., *Environ. Nanotechnology, Monit. Manag.* 11 (2019) 100201.
- [348] H. Makkar et al., *Chem. Res. Toxicol.* 31 (2018) 914–923.
- [349] P. Patel et al., *Ecotoxicol. Environ. Saf.* 192 (2020) 110321.
- [350] R. Sheel et al., *Environ. Pollut.* 267 (2020) 115482.
- [351] P. Paul et al., *Green Methods Wastewater Treat.*, Springer, Cham, 2020, pp. 73–86.
- [352] S.K. Verma et al., *Sci. Rep.* 7 (2017) 13909.
- [353] S.K. Verma et al., *RSC Adv.* 7 (2017) 40034–40045.
- [354] S.K. Verma et al., *Toxicol. Sci.* 161 (2018) 125–138.
- [355] S.K. Verma et al., *Toxicol. Res. (Camb.)* 7 (2018) 244–257.
- [356] S.K. Verma et al., *Mater. Sci. Eng. C* 92 (2018) 807–818.
- [357] T. Arun et al., *Mater. Sci. Eng. C* 104 (2019) 109932.
- [358] S.K. Verma et al., *Sci. Total Environ.* 713 (2020) 136521.
- [359] B. Sarkar et al., *Chemosphere* 206 (2018) 560–567.
- [360] A.E. Nel et al., *Nat. Mater.* 8 (2009) 543–557.
- [361] Y. Min et al., *Nat. Mater.* 7 (2008) 527–538.
- [362] T.L. Moore et al., *Chem. Soc. Rev.* 44 (2015) 6287–6305.
- [363] S. Ritz et al., *Biomacromolecules* 16 (2015) 1311–1321.
- [364] B. Dumontel et al., *J. Mater. Chem. B* 5 (2017) 8799–8813.
- [365] J.E. Eixenberger et al., *Chem. Res. Toxicol.* 30 (2017) 1641–1651.
- [366] M. Ramani et al., *J. Phys. Chem. C* 121 (2017) 15702–15710.
- [367] S.E. Krown et al., *J. Biol. Response Mod.* 4 (1985) 640–649.
- [368] S. Saha, P. Sarkar, *Phys. Chem. Chem. Phys.* 16 (2014) 15355–15366.
- [369] P. Khare et al., *J. Biomed. Nanotechnol.* 7 (2011) 116–117.
- [370] A.A. Mazur et al., *Russ. J. Mar. Biol.* 46 (2020) 49–55.
- [371] X. Liu et al., *J. Nanoparticle Res.* 17 (2015) 175.
- [372] C.W. Huang et al., *Environ. Pollut.* 220 (2017) 1456–1464.
- [373] E.R. Carmona et al., *Toxicol. Ind. Health* 32 (2016) 1987–2001.
- [374] D. Singh, A. Kumar, *Bull. Environ. Contam. Toxicol.* 97 (2016) 548–553.
- [375] S.-W. Li, C.-W. Huang, V.H.-C. Liao, *Environ. Pollut.* 256 (2020) 113382.
- [376] A.J. Miao et al., *Environ. Toxicol. Chem.* 29 (2010) 2814–2822.
- [377] R.B. Reed et al., *Environ. Toxicol. Chem.* 31 (2012) 93–99.
- [378] M.M.N. Yung et al., *Sci. Rep.* 7 (2017) 3662.
- [379] Y.C. Jiang et al., *Mater. Sci. Eng. C* 71 (2017) 901–908.
- [380] F. Santoro et al., *ACS Appl. Mater. Interfaces* 9 (2017) 39116–39121.
- [381] E. Malikmammadov et al., *J. Biomater. Sci. Polym. Ed.* 29 (2018) 863–893.
- [382] P. Kielbik et al., *Nanoscale Res. Lett.* 14 (2019) 1–13.
- [383] L. Durand et al., *Int. J. Cosmet. Sci.* 31 (2009) 279–292.
- [384] V.R. Leite-Silva et al., *Eur. J. Pharm. Biopharm.* 104 (2016) 140–147.
- [385] A.O. Gamer, E. Leibold, B. Van Ravenzwaay, *Toxicol. Vitr.* 20 (2006) 301–307.
- [386] C.-C. Lee et al., *Int. J. Environ. Res. Public Health* 17 (2020) 6088.
- [387] S.S.A. An et al., *Int. J. Nanomedicine* 9 (2014) 137.
- [388] G. Rath et al., *Mater. Sci. Eng. C* 58 (2016) 242–253.
- [389] R. Ahmed et al., *Int. J. Biol. Macromol.* 120 (2018) 385–393.
- [390] D. Sahu et al., *ISRN Toxicol.* 2013 (2013) 1–8.
- [391] Y. Morimoto et al., *Int. J. Mol. Sci.* 17 (2016) 1241.
- [392] H. Attia, H. Nounou, M. Shalaby, *Toxics* 6 (2018) 29.
- [393] Z. Han et al., *Int. J. Nanomed.* 11 (2016) 5187–5203.
- [394] H.S. Chun et al., *Ecotoxicol. Environ. Saf.* 137 (2017) 103–112.
- [395] J.K. Park et al., *Adv. Mater.* 22 (2010) 4857–4861.
- [396] D. Shalini, S. Senthilkumar, P. Rajaguru, *Toxicol. Mech. Methods* 28 (2018) 87–94.
- [397] Y. Li, L. Sun, T.J. Webster, *J. Biomed. Nanotechnol.* 14 (2018) 536–545.
- [398] F. Asghari et al., *Artif. Cells, Nanomed.cine Biotechnol.* 45 (2017) 185–192.
- [399] P.C. Nagajyothi et al., *J. Photochem. Photobiol. B Biol.* 146 (2015) 10–17.
- [400] A.A. Shadmehri et al., *Int. J. Nano Dimens.* 10 (2019) 350–358.
- [401] C.O. Tettey, H.M. Shin, *Sci. African* 6 (2019) e00157.
- [402] H. Umar, D. Kavaz, N. Rizamer, *Int. J. Nanomedicine* 14 (2019) 87–100.
- [403] E. Yadav et al., *RSC Adv.* 8 (2018) 21621–21635.
- [404] E. Mobarez et al., *SVU-Int. J. Vet. Sci.* 1 (2018) 25–54.
- [405] M. Rangeela et al., *Drug Invent. Today* 11 (2019) 2358–2361.
- [406] G. Rahimi Kalateh Shah Mohammad et al., *J. Biosci.* 44 (2019) 30.
- [407] S. Yao et al., *Nanotechnology* 29 (2018) 244003.
- [408] C. Abinaya et al., *J. Mayandi, Nano Express* 1 (2020) 010029.
- [409] M. Azizi-Lalabadi et al., *Sci. Rep.* 9 (2019) 1–10.
- [410] R. Dadi et al., *Mater. Sci. Eng. C* 104 (2019) 109968.
- [411] R.C. De Souza et al., *Brazilian J. Chem. Eng.* 36 (2019) 885–893.
- [412] Z. Emami-Karvani, *African J. Microbiol. Res.* 5 (2012) 1368–1373.
- [413] M. Mirhosseini, F.B. Firouzabadi, *Int. J. Dairy Technol.* 66 (2013) 291–295.
- [414] V. Tiwari et al., *Front. Microbiol.* 9 (2018) 1218.
- [415] Y. Xie et al., *Appl. Environ. Microbiol.* 77 (2011) 2325–2331.
- [416] Q. Yuan, S. Hein, R.D.K. Misra, *Acta Biomater.* 6 (2010) 2732–2739.
- [417] M. Fakhar-E-Alam et al., *Laser Phys. Lett.* 11 (2014) 025601.
- [418] Y. Wang et al., *Polymers (Basel)*. 10 (2018) 1272.
- [419] X. Yang et al., *Mater. Sci. Eng. C* 95 (2019) 104–113.
- [420] R.M. El-Gharbawy, A.M. Emara, S.E.S. Abu-Risha, *Biomed. Pharmacother.* 84 (2016) 810–820.
- [421] A. Bayrami et al., *Artif. Cells, Nanomed. Biotechnol.* 46 (2018) 730–739.
- [422] E.I. El-behey et al., *Acta Histochem.* 121 (2019) 84–93.
- [423] M.P. Vinardell, M. Mitjans, *Nanomaterials* 5 (2015) 1004–1021.
- [424] J. Bai Aswathanarayan, R. Rai Vittal, U. Muddegowda, *Artif. Cells, Nanomed. Biotechnol.* 46 (2018) 1444–1451.

- [425] Z. Sanaeimehr, I. Javadi, F. Namvar, *Cancer Nanotechnol.* 9 (2018) 3.
- [426] R. Tanino et al., *Mol. Cancer Ther.* 19 (2020) 502–512.
- [427] A. Nabil et al., *Oxid. Med. Cell. Longev.* 2020 (2020) 1–11.
- [428] N. Wiesmann et al., *J. Trace Elem. Med. Biol.* 51 (2019) 226–234.
- [429] K.C. Barick, S. Nigam, D. Bahadur, *J. Mater. Chem.* 20 (2010) 6446–6452.
- [430] Y.A. Selim et al., *Sci. Rep.* 10 (2020) 3445.
- [431] J.L. Wike-Hooley, J. Haveman, H.S. Reinhold, *Radiother. Oncol.* 2 (1984) 343–366.
- [432] I.F. Tannock, D. Rotin, *Cancer Res.* 49 (1989) 4373–4384.
- [433] M. Damaghi, J.W. Wojtkowiak, R.J. Gillies, *Front. Physiol.* 4 (2013).
- [434] R.A.S. Jagadeesan et al., *Mater. Sci. Eng. C* 81 (2017) 551–560.
- [435] E.J. Ambrose, A.M. James, J.H.B. Lowick, *Nature* 177 (1956) 576–577.
- [436] W. Le et al., *Biophys. Reports* 5 (2019) 10–18.
- [437] J. Zhang et al., *Adv. Mater.* 24 (2012) 1232–1237.
- [438] D.X. Ye et al., *ACS Nano* 10 (2016) 4294–4300.
- [439] I.M.M. Paine et al., *ACS Appl. Mater. Interfaces* 8 (2016) 32699–32705.
- [440] R. Wahab, Q. Saquib, M. Faisal, *Process Biochem.* 98 (2020) 83–92.
- [441] H. Zhang et al., *Biomaterials* 32 (2011) 1906–1914.
- [442] J. Li et al., *Nanoscale Res. Lett.* 5 (2010) 1063–1071.
- [443] J. Wang et al., *ACS Appl. Mater. Interfaces* 9 (2017) 39971–39984.
- [444] Y. Guo, Z. Sun, *J. Exp. Nanosci.* 15 (2020) 390–405.
- [445] K. Patel et al., *Colloids Surfaces B Biointerfaces* 150 (2017) 317–325.
- [446] K. Vimala et al., *J. Colloid Interface Sci.* 488 (2017) 92–108.
- [447] S. Kim, S.Y. Lee, H.J. Cho, *Biochem. Biophys. Res. Commun.* 501 (2018) 765–770.
- [448] A. Ancona et al., *Nanomaterials* 8 (2018).
- [449] P. Sengar et al., *J. Colloid Interface Sci.* 536 (2019) 586–597.
- [450] Y. Li et al., *Inorg. Chem.* 57 (2018) 8012–8018.
- [451] Q. Cai et al., *J. Mater. Chem. B* 6 (2018) 8148–8162.
- [452] N. Zhou et al., *J. Phys. Chem. C* 122 (2018) 7824–7830.
- [453] S. Iqbal et al., *Micromachines* 10 (2019) 60.
- [454] K. Vasuki, R. Manimekalai, *Heliyon* 5 (2019) e02729.
- [455] P. Sharma et al., *Nanoscale* 11 (2019) 4591–4600.
- [456] M. Nilavukkarasi, S. Vijayakumar, S. Prathipkumar, *Mater. Sci. Energy Technol.* 3 (2020) 335–343.
- [457] S. Salari et al., *Appl. Organomet. Chem.* 34 (2020) 1–8.
- [458] A. Hussain et al., *RSC Adv.* 9 (2019) 15357–15369.
- [459] V. Pouresmaeil et al., *Anticancer Agents Med. Chem.* 21 (2020) 316–326.
- [460] P. Bhattacharya et al., *Adv. Nano Res.* 3 (2020) 15–27.
- [461] M. Ramani et al., *Mol. Pharm.* 14 (2017) 614–625.
- [462] M.D. Jayappa et al., *Appl. Nanosci.* 10 (2020) 3057–3074.
- [463] H. Wu, J. Zhang, *Saudi Pharm. J.* 26 (2018) 205–210.
- [464] P. Ruenraroengsak et al., *Nanoscale* 11 (2019) 12858–12870.
- [465] B. Dumontel et al., *Nanomedicine* 14 (2019) 2815–2833.
- [466] P. Sadhukhan et al., *Mater. Sci. Eng. C* 100 (2019) 129–140.
- [467] H. Afzal et al., *Mater. Res. Express* 7 (2019) 015405.
- [468] N. Meghanani et al., *Arch. Pharm. Res.* 43 (2020) 503–513.
- [469] D. Cao et al., *Nano Converg.* 7 (2020).
- [470] W. Yuan et al., *Nanotechnology* 24 (2013) 045605.
- [471] A. Marino et al., *Sci. Rep.* 8 (2018) 6257.
- [472] A. Marino et al., *J. Colloid Interface Sci.* 538 (2019) 449–461.
- [473] S. Bae et al., *ACS Appl. Mater. Interfaces* 7 (2015) 27554–27561.
- [474] U. Hashim et al., in: P. Andrea (Ed.), 2008 Int. Conf. Electron. Des., IEEE, 2008, pp. 1–5.
- [475] G. Zheng, C.M. Lieber, *Methods Mol. Biol.* 790 (2011) 223–237.
- [476] S.K. Lee et al., *Biosens. Bioelectron.* 54 (2014) 181–188.
- [477] J. Li et al., *ACS Appl. Mater. Interfaces* 8 (2016) 2511–2516.
- [478] R. Janissen et al., *Nano Lett.* 17 (2017) 5938–5949.
- [479] A.A. Leonardi et al., *ACS Sensors* 3 (2018) 1690–1697.
- [480] Y.S. Jeon et al., *ACS Appl. Mater. Interfaces* 11 (2019) 23901–23908.
- [481] S. Li et al., *Int. J. Electrochem. Sci.* 15 (2020) 505–514.
- [482] Y. Xia et al., *Adv. Mater.* 15 (2003) 353–389.
- [483] L.A. Bauer, N.S. Birenbaum, G.J. Meyer, *J. Mater. Chem.* 14 (2004) 517–526.
- [484] A. Gao et al., *Sci. Rep.* 6 (2016) 22554.
- [485] R. Smith, S.M. Geary, A.K. Salem, *ACS Appl. Nano Mater.* 3 (2020) 8522–8536.
- [486] A. Gao et al., *Biosens. Bioelectron.* 91 (2017) 482–488.
- [487] L. Guo et al., *Biosens. Bioelectron.* 99 (2018) 368–374.
- [488] I.G. Theodorou et al., *Nanotoxicology* 10 (2016) 1351–1362.
- [489] H.-J. Eom, J.-S. Jeong, J. Choi, *Environ. Health Toxicol.* 30 (2015) e2015001.
- [490] S. Shukla et al., *Adv. Healthc. Mater.* 4 (2015) 874–882.
- [491] A. Adili et al., *Nanotoxicology* 2 (2008) 1–8.
- [492] L.P. Felix et al., *Toxicol. Reports* 3 (2016) 373–380.
- [493] H. Meng et al., *Biomaterials* 174 (2018) 41–53.
- [494] S. Lin et al., *ACS Nano* 8 (2014) 4450–4464.
- [495] N. Bhalla et al., *Essays Biochem.* 60 (2016) 1–8.
- [496] S. Ajami, F. Teimouri, *J. Res. Med. Sci.* 20 (2015) 1208–1215.
- [497] M. Asal et al., *Sensors (Switzerland)* 18 (2018) 1924.
- [498] L.M. Bellan, D. Wu, R.S. Langer, *Wiley Interdiscip. Rev. Nanomed. Nanobiotechnol.* 3 (2011) 229–246.
- [499] A. Gdowski et al., *Adv. Exp. Med. Biol.* 807 (2014) 33–58.
- [500] A. Chamorro-Garcia, A. Merkoçi, *Nanobiomedicine* 3 (2016) 184954351666357.
- [501] R. Shandilya et al., *Biosens. Bioelectron.* 130 (2019) 147–165.
- [502] M. Sharifi et al., *Biosens. Bioelectron.* 126 (2019) 773–784.
- [503] R. Niepelt et al., *Nanoscale Res. Lett.* 6 (2011) 1–7.
- [504] K. Yang et al., *Biosens. Bioelectron.* 94 (2017) 286–291.
- [505] N. Xia et al., *Int. J. Nanomed.* 13 (2018) 2521–2530.
- [506] G. Ertürk et al., *Sensors Actuators B Chem.* 224 (2016) 823–832.
- [507] R.M. Kong et al., *Anal. Bioanal. Chem.* 407 (2015) 369–377.
- [508] T. Yasui et al., *Sci. Adv.* 3 (2017) e1701133.
- [509] A. Choi et al., *Sensors Actuators B Chem.* 148 (2010) 577–582.
- [510] W.J. Li et al., *J. Biophotonics* 10 (2017) 92–97.
- [511] Y. Xu et al., *J. Biomed. Nanotechnol.* 9 (2013) 1164–1172.
- [512] Z. Chen et al., *Biosens. Bioelectron.* 122 (2018) 211–216.
- [513] K.B. Paul et al., *Biosens. Bioelectron.* 88 (2017) 144–152.
- [514] E.D. Pratt et al., *Chem. Eng. Sci.* 66 (2011) 1508–1522.
- [515] B. Zhu, B.D. Plouffe, S.K. Murthy, *Microfluid. Cell Cult. Syst.*, Elsevier, 2012, pp. 325–340.
- [516] T.W. Lo et al., *Lab Chip* 20 (2020) 1762–1770.
- [517] R. Riahi et al., *Int. J. Oncol.* 45 (2014) 1870–1878.
- [518] S.B. Cheng et al., *Anal. Chem.* 88 (2016) 6773–6780.
- [519] K.T. Thurn et al., *Nanoscale Res. Lett.* 2 (2007) 430–441.
- [520] D.P. Cormode et al., *Arterioscler. Thromb. Vasc. Biol.* 29 (2009) 992–1000.
- [521] M. Nowostawska et al., *J. Nanobiotechnol.* 9 (2011) 13.
- [522] Y. He et al., *Angew. Chem. - Int. Ed.* 50 (2011) 3080–3083.
- [523] J.C. Chang et al., *Wiley Interdiscip. Rev. Nanomed. Nanobiotechnol.* 4 (2012) 605–619.
- [524] D.C. Ferreira Soares, *J. Mol. Pharm. Org. Process Res.* 02 (2014) e113.
- [525] H. Hong et al., *ACS Appl. Mater. Interfaces* 7 (2015) 3373–3381.
- [526] X. Qin et al., *Anal. Chem.* 91 (2019) 4529–4536.
- [527] S.S. Sekhon et al., *Mol. Cell. Toxicol.* 14 (2018) 361–368.
- [528] Z. Shahroosvand et al., *Appl. Nanosci.* 10 (2020) 1441–1452.
- [529] T.D. Clemons et al., *Langmuir* 34 (2018) 15343–15349.
- [530] R. Viter et al., *Nanotechnology* 27 (2016) 465101.
- [531] S. Kishwar et al., *Nanoscale Res. Lett.* 5 (2010) 1669–1674.
- [532] E.J. Hong et al., *ACS Biomater. Sci. Eng.* 5 (2019) 5209–5217.
- [533] S. Firdous, *Laser Phys. Lett.* 15 (2018) 095604.
- [534] A.W. Maijenburg et al., *Small* 7 (2011) 2709–2713.
- [535] N.-Y. Ha et al., *J. Nanobiotechnol.* 14 (2016) 76.
- [536] S. Afroz et al., *Nanoscale* 9 (2017) 14641–14653.
- [537] T.E. Antoine et al., *J. Immunol.* (2016).
- [538] X.-Z. Chen et al., *Adv. Mater.* 29 (2017) 1605458.
- [539] N.R. Datta et al., *Cancer Treat. Rev.* 50 (2016) 217–227.
- [540] S. Wang et al., *2017 39th Annu. Int. Conf. IEEE Eng. Med. Biol. Soc.*, IEEE, 2017, pp. 1752–1755.
- [541] J.-E. Bibault et al., *Sci. Rep.* 8 (2018) 12611.
- [542] H. Fröhlich et al., *BMC Med.* 16 (2018) 150.
- [543] M.Q. Ding et al., *Mol. Cancer Res.* 16 (2018) 269–278.
- [544] M. Zitnik, M. Agrawal, J. Leskovec, *Bioinformatics*, Oxford University Press, 2018, pp. i457–i466.
- [545] B. Ibragimov et al., *Med. Phys.* 45 (2018) 4763–4774.
- [546] J. Shi et al., *Nat. Rev. Cancer* 17 (2017) 20–37.
- [547] K.D. Miller et al., *CA. Cancer J. Clin.* 66 (2016) 271–289.
- [548] L. Zhang et al., *World J. Surg. Oncol.* 16 (2018) 124.
- [549] D. Reichel et al., *Nanotheranostics* 3 (2019) 196–211.
- [550] S.D. Li, L. Huang, in: *Mol. Pharm.*, United States, 2008, pp. 496–504.
- [551] R.K. Jain, *Annu. Rev. Biomed. Eng.* 1 (1999) 241–263.
- [552] Z. Song et al., *Adv. Mater.* 28 (2016) 7249–7256.
- [553] R. Thiruppathi et al., *Adv. Sci.* 4 (2017) 1600279.
- [554] H. Maeda, H. Nakamura, J. Fang, *Adv. Drug Deliv. Rev.* 65 (2013) 71–79.
- [555] E. Blanco, H. Shen, M. Ferrari, *Nat. Biotechnol.* 33 (2015) 941–951.
- [556] V. Sainz et al., *Biochem. Biophys. Res. Commun.* 468 (2015) 504–510.

- [557] C.L. Ventola, P T 42 (2017) 742–755.
- [558] J.M. Caster et al., Wiley Interdiscip. Rev. Nanomed. Nanobiotechnol. 9 (2017) e1416.
- [559] J.K. Patra et al., J. Nanobiotechnology 16 (2018) 71.
- [560] Z. Gu et al., Pharmaceutics 12 (2020) 1–25.
- [561] A.K. Rengan et al., Nanoscale 6 (2014) 916–923.
- [562] L. Wang et al., Nanoscale 10 (2018) 13673–13683.
- [563] V.S. Kalambur, E.K. Longmire, J.C. Bischof, Langmuir 23 (2007) 12329–12336.